D-Branes in Anti-de-Sitter Space

Peter Byungho Lee

peter@theory.caltech.edu

B.S. (University of California, Berkeley) 1998

M.S. (California Institute of Technology) 2000

In Partial Fulfillment of the Requirements for the Degree of

Doctor of Philosophy

California Institute of Technology 452-48, Pasadena, CA 91125

Committee in charge:

Professor Hirosi Ooguri, Chair

Professor Marc Kamionkowski

Professor John H. Schwarz

Professor Mark B. Wise

submitted year 2003

(Defended March 05, 2003)

Abstract

We investigate the role of Dp-branes, which are $p+1$ dimensional membranes where open strings end, in two different types of anti-de-Sitter backgrounds: $AdS_3 \times S_3 \times M^4$ and $AdS_5 \times S^5$, where M^4 is a compact four-dimensional manifold such as the four-torus T^4 or the $K3$ surface.

In the spirit of the AdS/CFT correspondence, D-brane physics on an anti-de-Sitter space should be captured by a dual conformal field theory defined on the boundary of AdS. Recently, Karch and Randall and DeWolfe, Freedman and Ooguri proposed in [9, 10, 11] that the presence of a single $D5$-brane in $AdS_5 \times S^5$ is dual to a defect conformal field theory in which the usual $\mathcal{N} = 4$ bulk SYM theory is coupled to a $2+1$ dimensional conformal defect field theory. Extending their result, we take the Penrose limit of a single $D5$-brane embedded in $AdS_5 \times S^5$ and propose a correspondence between open string states ending on the $D5$-brane and gauge-invariant operators living on the dual defect conformal field theory. Furthermore, we check this proposal by verifying that the anomalous dimension of the gauge theory operators matches the light-cone Hamiltonian of open strings ending on the $D5$-brane.

Maldacena has proposed that type IIB string theory compactified on $AdS_3 \times S^3 \times M^4$ is dual to a $1 + 1$ conformal field theory defined on the conformal boundary of AdS_3 [12]. In this thesis, we restrict our attention to the study of a D-brane embedded in $AdS_3 \times S^3 \times M^4$ backgrounds and leave the explicit construction of the AdS/CFT correspondence of this setup for future work by others. First, we investigate the spectrum of open strings on AdS_2 branes in AdS_3 in an NS-NS background using the $SL(2, R)$ WZW model. Then, we construct boundary states for the AdS_2 branes in the Euclideanized AdS_3 background and compute the one-loop free energy of open strings stretched between the branes.

Acknowledgment

There are many people to whom I owe an immense amount of gratitude. Professor Hirosi Ooguri has patiently guided me through his many creative insights and played a major role in all aspects of my academic progress for the past three years. I would also like to thank many other teachers who not only taught me physics but also showed me what an exciting and sometimes greatly rewarding field that physics is. These mentors include the late Mr. Squatrito and the late Prof. David Judd, Prof. John Schwarz, and Prof. Edward Witten.

I would also like to thank the people in the Caltech theory group for providing a friendly and carefree atmosphere to conduct research in. I would especially like to acknowledge Helen Tuck and Carol Silberstein for all their help.

I have been fortunate enough to collaborate with many admirable colleagues whose company was greatly appreciated. Calin Ciocarlie, Jaume Gomis, Sanefumi Moriyama, Jonathan Tannenhauser, and especially Jongwon Park all played an important role. I appreciate many debates about physics and life that I enjoyed with Jongwon Park and wish him much success in the future. I have also benefited from many interesting discussions with Christopher Lee, Yi Li, Yuji Okawa, Arkadas Ozakin, Harlan Robins, Paul Skerritt, and Soojin Son.

I owe much gratitude to Prof. Mark Wise for all his encouragement and aid in my recent flirtation with finance. I have enjoyed many conversations with Kashif Alvi in this field as well. Last but not least, I thank Jisun Kim and my parents for their warm support and encouragement.

This research was supported in part by DOE grant DE-FG03-92-ER40701 and an NSF fellowship.

Contents

Chapter 1

Introduction

String theory is a leading candidate for the theory of quantum gravity. It starts on the premise that elementary particles are derived from one-dimensional objects, strings, rather than point-like objects as assumed in the usual quantum field theories such as the $SU(3) \times SU(2) \times U(1)$ standard model. All known string theories carry spin-two, massless objects in its mass spectrum which are identified as gravitons. Not only does string theory give rise to a consistent theory of quantum gravity, it leads to other favorable outcomes such as gauge groups large enough to construct grand unified theories (GUT's). It turns out that the structure of string theory is highly constrained by requiring self-consistency. As a consequence, it is well appreciated that flat space string theory exists only in ten dimensions when one includes fermionic excitations for supersymmetry.[1]

One of the major triumphs of string theory in recent years is the concrete realization of the link between gauge theories and string theories. Initial hints of a link were already presented by 't Hooft in the early 70's when he proposed a procedure to perturbatively quantize $SU(N)$ gauge theories in the large N limit [1]. It turns out we can interpret the gauge theory in this limit as a string theory in which the string coupling constant scales as $1/N$. It was only recently in 1997 that Maldacena proposed a concrete realization of this interpretation by relating string theory on an

[1] One can also define flat "bosonic" string theory without fermions in twenty-six dimensions. However, the theory contains tachyons which signals an instability [13].

anti-de-Sitter (AdS) space background to a conformal field theory (CFT) defined on the boundary of AdS. Many non-trivial checks of the AdS/CFT correspondence have appeared in the literature[2].

Despite this success, most of the checks on the string theory side were done in the supergravity approximation due to the difficulty of including Ramond-Ramond (RR) fields in string theory computations. Recently, it has been shown that string theory can be fully solved in the PP-wave background, which can be obtained by taking the Penrose limit of AdS, even in the presence of RR flux [5, 6]. Shortly after this development, Berenstein et al. [7] have put forward an exciting proposal that successfully tests the AdS/CFT correspondence beyond the supergravity approximation. The success of the AdS/CFT correspondence naturally gives a strong motivation to study string theory on general anti-de-Sitter backgrounds. In this thesis, we explore some aspects of Dp-branes living in anti-de-Sitter backgrounds and explain their relevance in the context of the AdS/CFT correspondence.

We investigate the role of Dp-branes, which are $p+1$ dimensional membranes that couple to RR fluxes, in two different types of anti-de-Sitter backgrounds: $AdS_5 \times S^5$ and $AdS_3 \times S_3 \times M^4$ where M^4 denotes a compact four-dimensional manifold such as the four-torus T^4 or the $K3$ surface. String theory on $AdS_5 \times S^5$ can be obtained by taking the near-horizon limit of a stack of D3 branes in type IIB string theory [8]. Likewise, string theory on $AdS_3 \times S^3 \times M^4$ is obtained by taking the near horizon limit of D1-D5 brane setup compactified on $R^6 \times M^4$. In this thesis, we are interested in the S-dual of this setup so that one is left with a NS-NS background, and the string theory becomes exactly solvable as a $SL(2, R)$ WZW model.

In the spirit of the AdS/CFT correspondence, D-brane physics on an anti-de-Sitter space should be captured by a dual conformal field theory defined on the boundary of AdS. Recently, Karch and Randall and DeWolfe, Freedman and Ooguri proposed in [9, 10, 11] that the presence of a single D5-brane in $AdS_5 \times S^5$ is dual to a defect conformal field theory in which the usual $\mathcal{N} = 4$ bulk SYM theory is coupled to a $2+1$ dimensional conformal defect. Extending their result, we take the Penrose limit

[2]For a comprehensive review of the AdS/CFT correspondence, see [2, 3, 4] and references therein.

of a single $D5$-brane embedded in $AdS_5 \times S^5$ and propose a correspondence between open string states ending on the $D5$-brane and gauge-invariant operators living on the dual defect conformal field theory. Furthermore, we check this proposal by verifying that the anomalous dimension of the gauge theory operators matches the light-cone Hamiltonian of open strings ending on the $D5$-brane.

It has been proposed that type IIB string theory compactified on $AdS_3 \times S^3 \times M^4$ is dual to a two-dimensional conformal field theory defined on the conformal boundary of AdS_3 [12]. More specifically, the low energy dynamics is given by a 1+1 dimensional sigma model whose target space is a deformation of the symmetric product of k copies of M^4, where k depends on M^4. In this thesis, we restrict our attention to the study of a D-brane defined on $AdS_3 \times S^3 \times M^4$ backgrounds. The explicit construction of the AdS/CFT correspondence for this setup deserves further study. First, we investigate the spectrum of open strings on AdS_2 branes in AdS_3 in an NS-NS background using the $SL(2,R)$ WZW model. Then, we construct boundary states for the AdS_2 branes in the Euclideanized AdS_3 background and compute one-loop free energy of open strings stretched between the branes. One hopes that our analysis will eventually lead to a verification of the AdS/CFT correspondence beyond the supergravity approximation since string theory on AdS_3 carries only NS-NS fields and can be fully solved using the $SL(2,R)$ WZW model.

The main goal of this thesis is two-fold. First is to study the role of open strings in the context of the AdS/CFT correspondence, and the second is to test it beyond the supergravity approximation by restricting to space-time backgrounds, such as the PP-wave background and the AdS_3 space, in which string theory can be entirely solved.

Chapter 2

D-Branes in AdS_5 and PP-Wave Background

2.1 Introduction

The AdS/CFT correspondence has led to deep understandings of string theory and field theory. However, until recently, much of the progress in this direction has been limited to supergravity approximations due to the difficulty when one has Ramond-Ramond background. Recently, it has been shown that string theory can be fully solved in the pp-wave background even in the presence of RR flux [5, 6] in the light-cone Green-Schwarz formalism. Shortly after this development, Berenstein et al. [7] have put forward an exciting proposal that tests AdS/CFT correspondence beyond the supergravity approximation. More specifically, they have related closed string states in the pp-wave background with operators of the dual $\mathcal{N} = 4$ SYM with large R-charge $J \sim \sqrt{N}$ and finite $\Delta - J$.

In this chapter, we extend the results of [7] to the case of open strings ending on a D5-brane in the pp-wave background. We consider a large number of D3-branes and a single D5-brane in the near-horizon limit. The resulting system is $AdS_5 \times S^5$ with the D5-brane spanning $AdS_4 \times S^2$. Recently, extending the idea of [9, 10], De Wolfe et al. [11] have proposed that its dual field theory is a defect conformal field theory in which the usual $\mathcal{N} = 4$ bulk SYM theory is coupled to a

three-dimensional conformal defect. This defect field theory has been further studied by [14], demonstrating quantum conformal invariance for the non-Abelian case. By taking the Penrose limit [15, 16] of this setup, one obtains a D5-brane in the pp-wave background. We construct a complete list of gauge invariant operators in the defect conformal field theory which is dual to the open string states ending on the D5-brane. Interestingly, particular boundary conditions of open stings on the D5-brane are encoded in symmetry breaking pattern induced by the defect and a specific form of defect couplings in the dual field theory.

This chapter is organized as follows. In Section 2, we give a brief review of the D-brane setup and the field content of the defect conformal field theory. In Section 3, we discuss the Penrose limit of this background and obtain the open string spectrum. In the last section, we propose a list of gauge invariant operators dual to the open string states. Finally in Appendix A, we explicitly check that the anomalous dimension of the chiral primary operators vanishes up to order g_{YM}^2. D-branes in PP-wave background were also considered by many other works[1]. This chapter is based on the published article [20].

2.2 Review of defect conformal field theory

In this section, we briefly review the D3-D5 brane setup of [9] and the field content of its dual defect conformal field theory discussed in [11]. The interested reader can find further details in the aforementioned papers. We start with the coordinate system in which the world-volume of a stack of N D3-branes span the directions (x^0, x^1, x^2, x^9) and a single D5-brane spans the directions $(x^0, x^1, x^2, x^3, x^4, x^5)$. The D-branes sit at the origin of their transverse coordinates. The setup is summarized in the following table:

[1]Some representative samples include [17, 18, 19].

	0	1	2	3	4	5	6	7	8	9
D3	x	x	x							x
D5	x	x	x	x	x	x				

The presence of the D5-brane breaks 16 space-time supersymmetries to 8 supersymmetries and reduces the global symmetry group $SO(6)$ to $SO(3) \times SO(3)$, where each $SO(3)$ acts on the 345 and 678 coordinates, respectively. In AdS/CFT correspondence, one is interested in taking the near horizon limit, where the string coupling $g \to 0$ and $N \to \infty$ with the product gN fixed. In this limit, we have the D5-brane spanning $AdS_4 \times S^2$ subspace of $AdS_5 \times S^5$. The dual conformal field theory of type IIB string theory in this background is $\mathcal{N} = 4$ SYM theory [8] that lives on the boundary of AdS_5 parameterized by (x^0, x^1, x^2, x^9). The D5-brane introduces a codimension one conformal defect on this boundary located at $x^9 = 0$. An analogous model can be considered for the $AdS_3 \times S^3$ case, where an AdS_2 brane introduces a one-dimensional defect in the dual CFT [52]. Such a reasoning has been used by [21, 22] to construct boundary states for the AdS_2 branes.

It has been argued by DeWolfe et al. [11] that type IIB string theory in $AdS_5 \times S^5$ with a $AdS_4 \times S^2$ brane is dual to a *defect conformal field theory*, wherein a subset of fields of $d = 4$, $\mathcal{N} = 4$ SYM couples to a $d = 3$, $\mathcal{N} = 4$ $SU(N)$ fundamental hypermultiplet on the defect preserving $SO(3, 2)$ conformal invariance and 8 supercharges. Let us summarize the field content of the defect conformal field theory relevant for our purposes. Denote the $SU(2)$ acting on the 345 directions as $SU(2)_H$ and the one acting on the 678 directions as $SU(2)_V$. Then we have the usual bulk $d = 4$, $\mathcal{N} = 4$ vector multiplet which decomposes into a $d = 3$, $\mathcal{N} = 4$ vector multiplet and a $d = 3$, $\mathcal{N} = 4$ adjoint hypermultiplet. The bosonic components of the vector multiplet are $A_\mu (\mu = 0, 1, 2), X^6, X^7, X^8$, with the scalars transforming as a **3** of $SU(2)_V$, while those of hypermultiplet are A_9, X^3, X^4, X^5, with the scalars as a **3** of $SU(2)_H$. The derivatives of X^3, X^4, X^5 along the 9-direction, which is normal to the defect, are also a part of the vector multiplet. The four adjoint $d = 4$ Majorana spinors of $\mathcal{N} = 4$ SYM transform as a (**2**,**2**) of $SU(2)_H \times SU(2)_V$, which is denoted as λ^{im}. Under the

dimensional reduction to $d = 3$, they decompose into pairs of 2-component $d = 3$ Majorana spinors, λ_1^{im} and λ_2^{im}, where the former is in the vector multiplet and the latter in the hyper multiplet. We also have a $d = 3$, $\mathcal{N} = 4$ $SU(N)$ fundamental hypermultiplet on the defect. It consists of complex scalars q^m transforming as a **2** of $SU(2)_H$ and $d = 3$ Dirac spinors Ψ^i transforming as a **2** of $SU(2)_V$. They are coupled canonically to three-dimensional gauge fields A_μ. Hence supersymmetry will induce couplings to the rest of the bulk vector multiplet as well, while the bulk hypermultiplet does not couple to the defect hypermultiplet at tree level. This fact will play a crucial role in reproducing the open string spectrum in Section 4. The field content of interest is summarized in the following table.

Field	Spin	$SU(2)_H$	$SU(2)_V$	$SU(N)$	Δ
X^3, X^4, X^5	0	1	0	adjoint	1
X^6, X^7, X^8	0	0	1	adjoint	1
λ^{im}	$\frac{1}{2}$	$\frac{1}{2}$	$\frac{1}{2}$	adjoint	$\frac{3}{2}$
q^m	0	$\frac{1}{2}$	0	N	$\frac{1}{2}$
$\bar{q}^m$	0	$\frac{1}{2}$	0	$\bar{N}$	$\frac{1}{2}$
Ψ^i	$\frac{1}{2}$	0	$\frac{1}{2}$	N	1
$\bar{\Psi}^i$	$\frac{1}{2}$	0	$\frac{1}{2}$	$\bar{N}$	1

Field theory action takes the form

$$S = S_4 + S_3, \tag{2.1}$$

where S_4 is the usual $d = 4$, $\mathcal{N} = 4$ SYM part and S_3 is the $d = 3$ defect CFT action with defect couplings with $d = 4$, $\mathcal{N} = 4$ SYM fields. They are derived in [11] using the preserved $d = 3$, $\mathcal{N} = 4$ supersymmetry and the global symmetries. The authors of [11] convincingly argue that the chiral primary operators in the defect CFT are

$$\bar{q}^m \tilde{\sigma}^{(I_0}_{mn} X_H^{I_1} ... X_H^{I_J)} q^n, \tag{2.2}$$

where we define a *shifted* Pauli matrices $\tilde{\sigma}^I$ $(I = 3, 4, 5)$ as σ^{I-2} and $(...)$ denotes traceless symmetrization. These operators will turn out to be the important building

blocks for open strings ending on the D5-brane in Section 4.

2.3 Open strings in pp-waves

Let us now consider the pp-wave limit of near-horizon limit of D3-D5 brane setup described in the previous section. It is convenient to introduce global coordinates on $AdS_5 \times S^5$ in taking the Penrose limit. The metric takes the form

$$ds^2 = R^2 \left[-dt^2 \cosh^2\rho + d\rho^2 + \sinh^2\rho d\Omega_3^2 + d\psi^2 \cos^2\varphi + d\varphi^2 + \sin^2\varphi d\Omega_3'^2 \right], \quad (2.3)$$

where $R^4 = 4\pi g \alpha'^2 N$. We introduce light-cone coordinates $\tilde{x}^{\pm} = (t \pm \psi)/2$ and take the Penrose limit ($R \to \infty$ with g fixed) after rescaling coordinates as follows

$$\tilde{x}^+ = x^+, \quad \tilde{x}^- = \frac{x^-}{R^2}, \quad \rho = \frac{r}{R}, \quad \theta = \frac{y}{R}. \quad (2.4)$$

After rescaling $x^{\pm}$ to introduce a mass scale, μ, the metric and the Ramond-Ramond form takes the form

$$ds^2 = -4dx^+dx^- - \mu^2 \vec{z}^{\,2} dx^{+2} + d\vec{z}^{\,2}, \quad (2.5)$$

$$F_{+1234} = F_{+5678} = \mu, \quad (2.6)$$

where $\vec{z} = (z^1, ...z^8)$.[2] The SO(2) generator, $J = -i\partial_\psi$, rotates the 34 plane in the original D3-D5 setup. One finds that

$$2p^- = -p_+ = i\partial_{x^+} = i\partial_{\bar{x}^+} = i(\partial_t + \partial_\psi) = \Delta - J, \quad (2.7)$$

$$2p^+ = -p_- = i\partial_{x^-} = \frac{i}{R^2}\partial_{\bar{x}^-} = \frac{i}{R^2}(\partial_t - \partial_\psi) = \frac{\Delta + J}{R^2}. \quad (2.8)$$

Therefore, the Penrose limit corresponds to restricting to operators with large $J \sim \sqrt{N}$ and finite $\Delta - J$. Notice that we are in the large 't Hooft coupling regime since we keep g fixed.

In the Penrose limit, the string action reduces to the following form in the light-cone gauge

$$S = \frac{1}{2\pi\alpha'} \int d\tau \int_0^{\pi\alpha' p^+} d\sigma \left[\frac{1}{2}\dot{z}^2 - \frac{1}{2}z'^2 - \frac{1}{2}\mu^2 z^2 + i\left(\frac{1}{2}S_1\partial_+ S_1 + \frac{1}{2}S_2\partial_- S_2 - \mu S_1 \Gamma^{1234} S_2 \right) \right], \quad (2.9)$$

[2] We have chosen the null geodesic in the Penrose limit to lie on the D5-brane because in the light-cone gauge, Neumann conditions are automatically imposed on $x^{\pm}$.

where S_i are positive chirality $SO(8)$ spinors. One can readily see that taking the light-cone gauge leads to Neumann boundary conditions for x^+, x^- in the open-string sector since

$$\partial_\sigma x^- = \frac{\partial_\tau z^i \partial_\sigma z^i}{p^+}. \tag{2.10}$$

We identify (z^5, z^6, z^7, z^8) directions with the original (x^5, x^6, x^7, x^8) directions and z^4 with the orthogonal direction to D5 brane in AdS_5. We label the coordinates in the Penrose limit such that the boundary conditions for the D5-brane are given as

+	-	1	2	3	4	5	6	7	8
N	N	N	N	N	D	N	D	D	D

where N and D denote Neumann and Dirichlet boundary conditions, respectively. For S_i, the appropriate boundary condition is [23]

$$S_2 = \Gamma^{1235} S_1. \tag{2.11}$$

The boundary condition for the fermions effectively reduces the degree of freedom by half. Taking the Penrose limit and taking the light-cone gauge break the symmetry group $SO(3,2) \times SU(2)_H \times SU(2)_V$ to $SO(3) \times SU(2)_V$. This point has been clarified in [24]. The full open string spectrum on a D5-brane has recently been computed by [18]. The mode expansions for the bosonic part are

$$z^I_{NN}(\tau,\sigma) = \cos(\mu\tau) z^I_0 + \frac{1}{\mu}\sin(\mu\tau) p^I_0 + i\sum_{n=1}^{\infty} \frac{1}{\sqrt{\omega_n}} e^{-i\omega_n\tau} \cos\left(\frac{n\sigma}{\alpha' p^+}\right) a^I_n + c.c., \tag{2.12}$$

$$z^I_{DD}(\tau,\sigma) = i\sum_{n=1}^{\infty} \frac{1}{\sqrt{\omega_n}} e^{-i\omega_n\tau} \sin\left(\frac{n\sigma}{\alpha' p^+}\right) a^I_n + c.c., \tag{2.13}$$

where we have defined

$$\omega_n = \sqrt{\mu^2 + \frac{n^2}{4(\alpha' p^+)^2}}. \tag{2.14}$$

Important difference between the Neumann and Dirichlet expansions is that the Dirichlet expansion does not have a zero mode. This gives rise to 4 massive bosonic

oscillators. Similarly, eight zero modes coming from fermions form 4 massive fermionic oscillators and their contribution to the zero point energy exactly cancel the contribution from the bosonic zero modes. Due to the mass term, fermionic creation and annihilation operators have $+1/2$ and $-1/2$ eigenvalues with respect to Γ^{45} respectively, and both transform separately as a doublet of $SU(2)_V$. Hence, the light cone open string ground state should be a singlet of $SU(2)_V$ for the fermionic zero modes, thus correctly reproducing D5-brane SYM multiplet.

The light cone Hamiltonian is given as

$$2p^- = -p_+ = H_{lc} = \sum_{n=0}^{\infty} N_n \sqrt{\mu^2 + \frac{n^2}{4(\alpha' p^+)^2}}, \tag{2.15}$$

where N_n denotes the total occupation number of that mode for both bosonic and fermionic oscillators. Rewriting the Hamiltonian in variables better suited for $AdS_5 \times S^5$, one notes that a typical string excitation contributes to $\Delta - J = 2p^-$ with frequency

$$(\Delta - J)_n = \sqrt{1 + \frac{\pi g N n^2}{J^2}}. \tag{2.16}$$

2.4 Open strings from defect conformal field theory

In this section, we construct a list of gauge invariant operators in the defect CFT dual to states in the open string Hilbert space. Recall that J is the generator of rotation on the X^3-X^4 plane. Define

$$Z \equiv \frac{1}{\sqrt{2}}\left(X^3 + iX^4\right), \qquad \sigma^Z \equiv \frac{1}{\sqrt{2}}\left(\tilde{\sigma}^3 + i\tilde{\sigma}^4\right) = \frac{1}{\sqrt{2}}\left(\sigma^1 + i\sigma^2\right), \tag{2.17}$$

Both the operators Z and $\bar{q}^m \sigma^Z_{mn} q^n$ have $\Delta = J = 1$. The fact that Z belongs to the bulk hypermultiplet will be important later. We propose that the open string

light-cone ground state corresponds to

$$|0,p^+\rangle_{l.c.} \longleftrightarrow \frac{1}{N^{J/2}}\sigma^Z_{mn}\bar{q}^m \underbrace{ZZ\cdot\cdot\cdot\cdot\cdot Z}_{J-1} q^n. \tag{2.18}$$

As mentioned above, this is a chiral primary operator with $\Delta = J$ found in [11]. Because it is a chiral primary, $\Delta - J = 0$ in the strong 't Hooft coupling limit. This property agrees with the fact that the light-cone ground state has zero energy. Furthermore, it does not transform under $SU(2)_V$ as one expects from the light-cone ground state.

For excited states, as in the closed string case [7], we insert proper operators with $\Delta - J = 1$ without phases for zero modes and with appropriate phases for nonzero modes. Here we consider Neumann and Dirichlet directions separately since there are several crucial differences.

For the zero mode excitations along the Neumann directions, we have the following correspondence[3]:

$$a^{\dagger 1}_0|0,p^+\rangle_{l.c.} \longleftrightarrow \frac{1}{\sqrt{J}}\sum_{l=0}^{J}\frac{1}{N^{J/2+1}}\sigma^Z_{mn}\bar{q}^m Z^l(D_0Z)Z^{J-l}q^n, \tag{2.19}$$

$$a^{\dagger 2}_0|0,p^+\rangle_{l.c.} \longleftrightarrow \frac{1}{\sqrt{J}}\sum_{l=0}^{J}\frac{1}{N^{J/2+1}}\sigma^Z_{mn}\bar{q}^m Z^l(D_1Z)Z^{J-l}q^n, \tag{2.20}$$

$$a^{\dagger 3}_0|0,p^+\rangle_{l.c.} \longleftrightarrow \frac{1}{\sqrt{J}}\sum_{l=0}^{J}\frac{1}{N^{J/2+1}}\sigma^Z_{mn}\bar{q}^m Z^l(D_2Z)Z^{J-l}q^n, \tag{2.21}$$

$$a^{\dagger 5}_0|0,p^+\rangle_{l.c.} \longleftrightarrow \frac{1}{\sqrt{J}}\sum_{l=0}^{J}\frac{1}{N^{J/2+1}}\sigma^Z_{mn}\bar{q}^m Z^l X^5 Z^{J-l}q^n. \tag{2.22}$$

The above open string states are associated with preserved symmetries of the D5 brane. They are massive however since the symmetries do not commute with the light cone Hamiltonian. Hence, these operators are obtained from the open string

[3]To be rigorous, the directions X^0, X^1, X^2, X^9 are related to the original coordinates by a conformal transformation after wick rotation as in the radial quantization. This transformation leaves the 9 direction orthogonal to the defect.

ground state operator (2.18) by acting corresponding preserved symmetries in the defect conformal field theory. For example, the fourth operator (2.22) is obtained by acting a $SU(2)_H$ rotation on the ground state operator. The rotation also acts on the boundary fields $q^{\bar{m}}$ and q^n giving rise to additional terms such as

$$\tilde{\sigma}^5_{mn}\bar{q}^m Z^{J+1} q^n \,. \tag{2.23}$$

For notational simplicity, we have suppressed this term in the above list. Likewise, the other three operators have additional boundary contributions. In the weak 't Hooft coupling regime, these operators have $\Delta - J = 1$. Since they are in the same multiplet as the chiral primary operator (2.18), their dimensions are also protected by supersymmetry.

For nonzero mode excitations along the Neumann directions, we insert operators with *cosine* phases[4][5]

$$a^{\dagger 1}_n|0,p^+\rangle_{l.c.} \quad\longleftrightarrow\quad \frac{1}{\sqrt{J}}\sum_{l=0}^{J}\frac{\sqrt{2}\cos\left(\frac{\pi nl}{J}\right)}{N^{J/2+1}}\sigma^Z_{mn}\bar{q}^m Z^l(D_0Z)Z^{J-l}q^n, \tag{2.24}$$

$$a^{\dagger 2}_n|0,p^+\rangle_{l.c.} \quad\longleftrightarrow\quad \frac{1}{\sqrt{J}}\sum_{l=0}^{J}\frac{\sqrt{2}\cos\left(\frac{\pi nl}{J}\right)}{N^{J/2+1}}\sigma^Z_{mn}\bar{q}^m Z^l(D_1Z)Z^{J-l}q^n, \tag{2.25}$$

$$a^{\dagger 3}_n|0,p^+\rangle_{l.c.} \quad\longleftrightarrow\quad \frac{1}{\sqrt{J}}\sum_{l=0}^{J}\frac{\sqrt{2}\cos\left(\frac{\pi nl}{J}\right)}{N^{J/2+1}}\sigma^Z_{mn}\bar{q}^m Z^l(D_2Z)Z^{J-l}q^n, \tag{2.26}$$

$$a^{\dagger 5}_n|0,p^+\rangle_{l.c.} \quad\longleftrightarrow\quad \frac{1}{\sqrt{J}}\sum_{l=0}^{J}\frac{\sqrt{2}\cos\left(\frac{\pi nl}{J}\right)}{N^{J/2+1}}\sigma^Z_{mn}\bar{q}^m Z^l X^5 Z^{J-l}q^n. \tag{2.27}$$

The factor of $\sqrt{2}$ is necessary for correct normalization of the free Feynman diagram in the two-point function. Notice that unlike the closed string case, the operators with single insertions are not trivially zero which reflects the fact that there is no level

[4]This point is also noticed in [17].

[5]In principle, we should assign phases including the boundary contributions. Again, for simplicity, we suppress them since it does not affect following calculations.

matching condition for open strings. In addition, the sign of n has no significance, which corresponds to the fact that there is only one set of oscillators instead of both the left and right moving sectors.

We can compute the anomalous dimension of these operators following the closed string case discussed in the appendix of [7]. The only difference from the closed string case is that the exponential phase has been replaced by the cosine phase. For example, let $\mathcal{O}$ be the fourth operator (2.22) above. The contribution from $\frac{1}{2\pi g}\int d^4x 2Tr[X^5 Z X^5 \bar{Z}]$ in the bulk action gives

$$\begin{aligned}
\langle \mathcal{O}(x)\mathcal{O}^*(0)\rangle &= \frac{\mathcal{N}}{|x|^{2\Delta}}\left[1+\frac{1}{J}\sum_{l=0}^{J-1} N(2\pi g) 8\cos\left(\frac{\pi n l}{J}\right)\cos\left(\frac{\pi n(l+1)}{J}\right)\frac{1}{4\pi^2}\log|x|\Lambda\right] \\
&= \frac{\mathcal{N}}{|x|^{2\Delta}}\left[1+\frac{1}{J}\sum_{l=0}^{J-1} N(2\pi g) 4\left\{\cos\left(\frac{\pi n(2l+1)}{J}\right)+\cos\left(\frac{\pi n}{J}\right)\right\}\frac{1}{4\pi^2}\log|x|\Lambda\right] \\
&= \frac{\mathcal{N}}{|x|^{2\Delta}}\left[1+N(2\pi g)4\cos\left(\frac{\pi n}{J}\right)\frac{1}{4\pi^2}\log|x|\Lambda\right], \qquad (2.28)
\end{aligned}$$

where $\mathcal{N}$ is a normalization factor and Λ is the UV cutoff scale. As argued in [7], contributions from other Feynman diagrams cancel this contribution when $n = 0$[6]. Therefore, the full contribution can be taken into account by simply replacing $\cos\left(\frac{\pi n}{J}\right)$ with $\cos\left(\frac{\pi n}{J}\right) - 1$. Finally, we have to the leading order

$$\langle \mathcal{O}(x)\mathcal{O}^*(0)\rangle = \frac{\mathcal{N}}{|x|^{2\Delta}}\left[1-\frac{\pi g N n^2}{J^2}\log|x|\Lambda\right]. \qquad (2.29)$$

Therefore, one gets

$$(\Delta - J)_n = 1 + \frac{\pi g N n^2}{2J^2} = 1 + \frac{n^2}{8(\alpha' p^+)^2}\,. \qquad (2.30)$$

This is exactly the first order expansion of light-cone energy of corresponding string states.

[6]Refer to Appendix A which explicitly shows the anomalous dimension vanishes for the case $n = 0$ since the operators are then chiral primaries.

Now consider the directions with Dirichlet boundary conditions. As mentioned earlier, the associated mode expansions do not have zero modes. For nonzero mode excitations, we insert appropriate operators with *sine* phases as follows

$$a^{\dagger 4}_{\ n}|0,p^+\rangle_{l.c.} \longleftrightarrow \frac{1}{\sqrt{J}}\sum_{l=0}^{J}\frac{\sqrt{2}\sin\left(\frac{\pi nl}{J}\right)}{N^{J/2+1}}\sigma^Z_{mn}\bar{q}^m Z^l(D_9 Z)Z^{J-l}q^n, \tag{2.31}$$

$$a^{\dagger 6}_{\ n}|0,p^+\rangle_{l.c.} \longleftrightarrow \frac{1}{\sqrt{J}}\sum_{l=0}^{J}\frac{\sqrt{2}\sin\left(\frac{\pi nl}{J}\right)}{N^{J/2+1}}\sigma^Z_{mn}\bar{q}^m Z^l X^6 Z^{J-l}q^n, \tag{2.32}$$

$$a^{\dagger 7}_{\ n}|0,p^+\rangle_{l.c.} \longleftrightarrow \frac{1}{\sqrt{J}}\sum_{l=0}^{J}\frac{\sqrt{2}\sin\left(\frac{\pi nl}{J}\right)}{N^{J/2+1}}\sigma^Z_{mn}\bar{q}^m Z^l X^7 Z^{J-l}q^n, \tag{2.33}$$

$$a^{\dagger 8}_{\ n}|0,p^+\rangle_{l.c.} \longleftrightarrow \frac{1}{\sqrt{J}}\sum_{l=0}^{J}\frac{\sqrt{2}\sin\left(\frac{\pi nl}{J}\right)}{N^{J/2+1}}\sigma^Z_{mn}\bar{q}^m Z^l X^8 Z^{J-l}q^n. \tag{2.34}$$

Notice that the sine phases naturally kill the zero modes when $n = 0$. We should ask what is the fate of the operators with insertions along the Dirichlet directions without phase. These operators are obtained by acting on the ground state operator with symmetries broken by the defect[7]. Therefore, their dimensions are not generally protected. In fact, the operators X^6, X^7, X^8 are in the bulk vector multiplet and couple to the defect hyper multiplet via the defect F-term to the leading order. Similarly, the normal derivative $D_9 Z$ couples to the defect hyper multiplet despite the fact that Z itself is in the bulk hyper multiplet[11]. This boundary interaction gives rise to large anomalous dimensions of order $N/J \sim J$ when one inserts operators *without phases*. Hence such operators will disappear in the strong 't Hooft coupling regime as implied by the open string spectrum. Nevertheless, once we include the sine phase, boundary interactions are suppressed by a factor of $\sin^2\left(\frac{\pi n}{J}\right) \sim 1/J^2$, and they can be ignored to the leading order in $1/J$. Therefore, the only contribution to anomalous dimensions comes from the bulk interaction. The computation is essentially the same as above, and the result agrees with the open string spectrum.

[7] As a result, we do not have additional boundary terms unlike the case for Neumann directions.

For fermionic excitations, we insert $J = 1/2$ components of λ^{im}, which is just λ^{1m}.[8] As in the bosonic sector, the number of zero modes is half of that of non-zero modes. Hence, we need a similar mechanism to remove possible gauge theory operators corresponding to the 4 unphysical zero modes. The symmetry breaking pattern and the form of boundary interactions in the defect CFT allow one to do this consistently. Recall that the operators λ_1^{1m} and λ_2^{1m} are in the vector and hyper multiplets respectively. Only λ_1^{1m} couples to the defect hypermultiplet while λ_2^{1m} can be obtained from Z by acting preserved supersymmetries [9]. Therefore, we associate sine and cosine phases with λ_1^{1m} and λ_2^{1m} respectively. As in the bosonic sector, this assignment reproduces the open string spectrum in the fermionic sector. This result is also implied by the 8 preserved supersymmetries.

2.5 Discussion

In this chapter, we have considered a Penrose limit of type IIB string theory on $AdS_5 \times S^5$ with a D5-brane spanning $AdS^4 \times S^2$ whose dual field theory is $\mathcal{N} = 4$ SYM coupled to a three-dimensional conformal defect. The Penrose limit gives rise to a D5-brane in the pp-wave background. The limit corresponds to looking at a subsector of operators in the dual field theory with large $J \sim \sqrt{N}$ and finite $\Delta - J$ in the large 't Hooft coupling regime. We have studied perturbative open string spectrum on this brane and constructed a complete list of gauge invariant operators dual to the open string states from the defect conformal field theory. The peculiar feature of defect couplings, symmetry breaking pattern in the dual field theory and sine-cosine phases are essential to reproduce the proper boundary conditions for the open strings.

One can also consider several M D5-branes. Then the defect hypermultiplet gets an additional $U(M)$ index with q^m and $\bar{q}^n$ transforming as $\mathbf{M}$ and $\bar{\mathbf{M}}$ of $U(M)$ re-

[8] We take i to be the quantum number of J, which is a generator of Cartan subalgebra of $SU(2)_H$.

[9] They also transform q and $\bar{q}$ into Ψ and $\bar{\Psi}$. Therefore, when we insert λ_2^{1m}, we have additional boundary terms with q or $\bar{q}$ replaced by Ψ or $\bar{\Psi}$.

spectively. This naturally induces Chan-Paton factors at the ends of open strings as expected. It would be interesting to construct defect conformal field theories arising from other supersymmetric brane intersections and study their Penrose limits. Then we expect to find specific defect couplings and symmetry breaking patterns which reflect the boundary conditions of the D-branes in this limit.

Lastly in Appendix A, we have explicitly shown that the anomalous dimensions vanish for the chiral primary operators, which correspond to vaccuum states on the string side, as expected. However, a finite piece remained which diverges like N in the Penrose limit but not in the usual 't Hooft limit in which $g_{YM}^2 N$ is kept fixed. It has not been settled whether this subtlety can be overcome by absorbing the finite piece in some regularization scheme or not. If not, a well-defined perturbative gauge theory may not be defined in the Penrose limit and the full nonperturbative effects have to be considered. It would be very interesting to resolve this issue and to see if other open string setups, such as the one considered by [17], also possess a similar problem.

Chapter 3

Open Strings in AdS_3

3.1 Introduction

In the previous chapter, we have considered the spectrum of a single D5-brane in $AdS_5 \times S^5$ and discussed its dual defect conformal field theory proposed in [11]. We then took the Penrose limit of this setup and proposed gauge invariant operators dual to open string states on the string theory side. In this chapter, we consider D-branes in $AdS_3 \times S^3 \times M^4$. For this case, a defect conformal field theory dual to the D-brane setup has not been rigorously constructed in the lines of [11][1]. From this point on, we will be mainly interested in the D-brane setup for its own sake and leave the AdS/CFT correspondence for future work. More specifically, we study the spectrum of open strings confined to live on AdS_2 branes embedded in AdS_3.

The $SL(2,R)$ WZW model is ubiquitous in string theory. It arises in contexts ranging from the Liouville model in two-dimensional gravity [26, 27, 28, 29] to three-dimensional Einstein gravity [30] to two-dimensional black holes [31] to Neveu-Schwarz 5-branes [32] and their relation to singularities in Calabi-Yau spaces [33, 34, 35]. In addition, the $SL(2,R)$ WZW model describes the worldsheet of a string propagating in AdS_3 with a background NS-NS B-field. The application to string theory in AdS_3 is of particular interest, as it opens a window onto the AdS/CFT correspondence be-

[1] A first step towards this goal has been taken by [25].

yond the gravity approximation. For all of these reasons, the $SL(2,R)$ WZW model has been intensively studied for more than a decade.[2]

Recently, a proposal was put forward [37] and checked [36] for the structure of the Hilbert space of the model. The symmetries of the theory require that its Hilbert space decompose as a sum of irreducible representations of the current algebra $\widehat{SL}(2,R)\times\widehat{SL}(2,R)$. But which representations appear, and with what multiplicities? According to the proposal of [37], the Hilbert space contains discrete representations and continuous representations, as well as their images under spectral flow. It was argued in [37] that the discrete representations and their spectral flow images correspond to short strings in AdS_3, and the continuous representations and their images to long strings. In both cases, the integer w indexing the spectral flow was interpreted as the winding number of the strings about the center of AdS_3.

The analysis of [37] determined the spectrum of *closed* strings in AdS_3. We address the corresponding problem for *open* strings. More specifically, our setting is critical open bosonic string theory in $AdS_3 \times \mathcal{M}$, with an NS-NS background, and in the presence of a D-brane whose world-volume fills an AdS_2 subspace of AdS_3 and wraps some subspace of the compact space $\mathcal{M}$. This AdS_2 *brane* preserves one linear combination of the left- and right-moving current algebras. Consequently, the Hilbert space of open strings ending on the AdS_2 brane decomposes as a sum of irreducible representations of a single $\widehat{SL}(2,R)$. Our main task will be to determine which representations appear in the spectrum.

Some intuition may be gained from the $SU(2)$ counterpart of our problem [38, 39, 40, 41, 42, 43, 44, 45, 46]. In the $SU(2)$ case, the D-brane worldvolumes analogous to our AdS_2 branes are S^2 subspaces embedded in the $SU(2)$ group manifold S^3. These S^2 *branes* are quantized: if the level of the WZW model is k, there are $k+1$ possible D-brane configurations, labeled by a quantum number n taking the values $n = -k/2, -k/2+1, \ldots, k/2$. If k is even, the D-brane with quantum number $n = 0$ wraps the equatorial S^2 within S^3. In general, the D-branes associated with increasing $|n|$ wrap smaller and smaller 2-spheres. By the time n reaches $\pm k/2$, the

[2] A representative sample of references is given in [36].

S^2 worldvolumes have degenerated to the north or south pole of S^3.

The Hilbert space $\mathcal{H}_n$ of open strings ending on the S^2 brane with quantum number n decomposes as

$$\mathcal{H}_n = \bigoplus_{j=0}^{k/2-|n|} D_j \,, \tag{3.1}$$

where D_j is the irreducible representation of the current algebra $\widehat{SU}(2)$ whose ground states make up the spin-j representation of $SU(2)$ [41]. It is evident from (3.1) that the Hilbert space "loses" representations as $|n|$ increases. For example, the Hilbert space of open strings ending on an equatorial S^2 brane is $\mathcal{H}_{n=0} = \bigoplus_{j=0}^{k/2} D_j$, which is the holomorphic square root of the Hilbert space of closed strings in $SU(2)$, projected onto integral j. On the other hand, when $n = \pm k/2$ and the D-brane has shrunk to the north pole or the south pole, the Hilbert space is reduced to the single representation $\mathcal{H}_{n=\pm k/2} = D_{j=0}$.

We seek a similarly detailed picture of the Hilbert space of AdS_2 branes in AdS_3. Our method resembles that of [37]: we start by constructing *classical* open string world-sheet solutions, based on which we then conjecture the form of the *quantum* Hilbert space. To test the validity of this approach, and to introduce the tools we will need for $SL(2,R)$ in what may be a more familiar context, we begin in Section 3.2 with a semiclassical treatment of S^2 branes in the $SU(2)$ WZW model. The Hilbert space structure that emerges from our semiclassical methods is identical to that of (3.1), though we cannot see the quantization of the parameter n.[3] Our approach explains naturally in terms of the geometry of S^3 why $\widehat{SU}(2)$ representations are skimmed off the Hilbert space as $|n|$ increases.

We then return to the $SL(2,R)$ model. Following a review in Section 3.3 of the closed string Hilbert space, we take up the subject of AdS_2 branes in Sections 3.4 and 3.5. Like the S^2 branes in $SU(2)$, the AdS_2 branes in $SL(2,R)$ are quantized. The quanutm number they carry is essentially fundamental string charge. In a suitable coordinate system, each AdS_2 brane is located at some fixed value ψ_0 of one of the

[3] A semiclassical argument for the quantization of n was given in [44].

coordinates. The quantization condition is

$$\sinh \psi_0 = g_s Q \,, \tag{3.2}$$

where g_s is the string coupling constant and Q is the fundamental string charge carried by the brane. The condition (3.2) restricts ψ_0 to a discrete (but now, neither finite nor bounded!) set of allowed values. As with the S^2 branes, though, our analysis is insensitive to this quantization.

The simplest case, $\psi_0 = 0$, is treated in Section 3.4. This case is the $SL(2,R)$ analogue of the equatorial S^2 branes in the $SU(2)$ model. An AdS_2 brane with $\psi_0 = 0$ is a "straight" brane cutting through the middle of AdS_3. The Dirichlet boundary condition defining such a straight brane preserves the full spectral flow symmetry of the closed string theory. Semiclassical analysis suggests that the open string Hilbert space is the holomorphic square root of the Hilbert space of closed strings in AdS_3. A one-loop Euclidean partition function calculation, described in Appendix D, confirms this conjecture.

Section 3.5 is devoted to branes with $\psi_0 \neq 0$. Exact quantitative results are unavailable here; nevertheless, we are able to arrive at a qualitative picture of the Hilbert space.

An AdS_2 brane with $\psi_0 \neq 0$ is analogous to an S^2 brane with $n \neq 0$ in the $SU(2)$ model. Varying ψ_0 away from zero curves the brane towards the boundary of AdS_3. Unlike the situation for S^2 branes in S^3, there is no loss of representations as $|\psi_0|$ increases. This difference is traceable to a simple difference in the geometry of the two setups.

Introducing an AdS_2 brane with $\psi_0 \neq 0$ breaks half the spectral flow symmetry: the curved-brane Dirichlet boundary condition is preserved only if the integer w parametrizing the spectral flow is even. Nevertheless, we can construct classical short and long string solutions—and the Hilbert space contains discrete and continuous representations—of both odd and even w. There is an important difference, though, between the short and long string solutions, having to do with the action on AdS_3 of PT, the space-time parity and time-reversal symmetry. When acting on discrete

representations, PT flips the parity of w. Thus it is possible to reach a discrete representation of any given value of w from a discrete representation of any other given w by a sequence of symmetry transformations: even w spectral flow and, if necessary, target space PT. Consequently, the ψ_0 dependence of the density of states of the discrete representations is the same for all w. By contrast, PT maintains the parity of w when acting on continuous representations. Thus the ψ_0 dependence of the density of states of the continuous representations is different for odd and even w. We highlight this difference by examining the contributions of the odd and even w sectors to the divergence structure of the one-loop Euclidean partition function.

In the limit $\psi_0 \to \pm\infty$, the AdS_2 brane approaches the boundary of AdS_3, and the induced electric field on the brane worldvolume approaches its critical value. We therefore conjecture that the $\psi_0 \to \infty$ limit reproduces noncommutative open string (NCOS) theory on AdS_2. At the end of Section 3.5, we show that, in this limit, the WZW Lagrangian takes a form similar to the Lagrangian of noncommutative open strings [47, 48], appropriately modified to account for the AdS_2 background. We also take some preliminary steps towards a computation of the one-loop partition function.

Towards the completion of this work, we received the preprint [49], which contains some overlap with certain of our results. In addition, branes in AdS_3 were recently studied from a different point of view in [50].

3.2 S^2 Branes in the $SU(2)$ WZW model

In this section, we study S^2 branes in the $SU(2)$ WZW model from a semiclassical point of view. Our reasons for doing so are twofold. First, the $SU(2)$ WZW model is in several important ways similar to—and different from—the $SL(2,R)$ model which is our main focus, and it is useful to develop the ideas we will need later on in a more familiar setting. Second, the $SU(2)$ model provides a testing ground for the semiclassical techniques that will eventually help us maneuver through the intricacies of the $SL(2,R)$ model. By examining *classical* open strings ending on S^2 branes in S^3, we will be led to the picture of [41] for the structure of the *quantum* Hilbert space.

Before turning to the analysis of S^2 branes in S^3, let us begin with some remarks on branes in WZW models in general [51, 43]. In free bosonic open string theory with target space coordinates X^a, the standard boundary conditions at the string endpoints may be expressed as

$$\partial_+ X^a = \pm \partial_- X^a \,, \tag{3.3}$$

with the plus sign indicating a Neumann condition and the minus sign a Dirichlet condition. In the free theory, the $\partial_+ X^a$ ($\partial_- X^a$) are (anti-)holomorphically conserved currents. The simplest extension to strings propagating on group manifolds replaces $\partial_+ X^a$ ($\partial_- X^a$) by the (anti)-holomorphically conserved currents J_R^a (J_L^a). In addition, we could generalize (3.3) to the condition

$$\partial_+ X^a = R^a_b \partial_- X^b \,, \tag{3.4}$$

where R^a_b is a constant matrix; which directions are Neumann and which Dirichlet are then determined by the eigenvalues of R^a_b. The corresponding operation in the WZW model involves "twisting" the condition relating the left- and right-moving currents by an automorphism R of the Lie algebra [51, 43],

$$J_R^a + R^a_b J_L^b = 0 \,. \tag{3.5}$$

The statement that R is a Lie algebra automorphism means that, for all Lie group generators T^a and T^b, $[R(T^a), R(T^b)] = R([T^a, T^b])$. The automorphism R is further required to preserve conformal invariance at the worldsheet boundary. In (3.3) we had a choice of sign; choosing the plus sign in (3.5) ensures that the boundary conditions preserve the affine symmetry algebra.[4]

The condition (3.5) is called a *gluing condition*, and implies the boundary conditions satisfied by the target space coordinates. The gluing condition (3.5) defines branes, whose worldvolumes within the group manifold G extend in the directions for which the boundary conditions derived from (3.5) are Neumann. The brane worldvolume containing a fixed element $g \in G$ can be represented as the "twined" conjugacy

[4]We will not consider the more general brane configurations that can be obtained by relaxing this requirement.

class

$$\mathcal{W}_g^r = \{r(h)gh^{-1} : h \in G\}, \tag{3.6}$$

where r is the group automorphism induced near the identity from the Lie algebra automorphism R.[5]

Now let us make this concrete for the case of branes in S^3, the group manifold of $SU(2)$. We write the general $SU(2)$ group element as

$$g = \exp\left(i\vec{\psi}\cdot\vec{\sigma}\right) , \tag{3.7}$$

where

$$\vec{\psi} = \left(\psi - \frac{\pi}{2}\right)(\sin\omega\cos\phi, \sin\omega\sin\phi, \cos\omega) , \tag{3.8}$$

the coordinates (ψ, ω, ϕ) lie in the ranges

$$-\frac{\pi}{2} \le \psi \le \frac{\pi}{2} , \qquad 0 \le \omega \le \pi , \qquad 0 \le \phi \le 2\pi , \tag{3.9}$$

and $\vec{\sigma} = (\sigma_1, \sigma_2, \sigma_3)$ is the vector of Pauli matrices. Explicitly, in this parametrization,

$$g = \begin{pmatrix} \sin\psi - i\cos\omega\cos\psi & -ie^{-i\phi}\cos\psi\sin\omega \\ -ie^{i\phi}\cos\psi\sin\omega & \sin\psi + i\cos\omega\cos\psi \end{pmatrix} . \tag{3.10}$$

The S^3 metric in these coordinates is

$$ds^2 = d\psi^2 + \sin^2\psi\,(d\omega^2 + \sin^2\omega\, d\phi^2) , \tag{3.11}$$

from which it is apparent that the surfaces of constant ψ are 2-spheres embedded in S^3.

Classical string worldsheets in S^3 are given by solutions of the $SU(2)$ WZW model. We take the worldsheet coordinates to be τ and σ. For closed strings, σ is periodic with period 2π; for open strings, $0 \le \sigma \le \pi$. It is also convenient to define the light-cone combinations

$$x^{\pm} = \tau \pm \sigma . \tag{3.12}$$

[5]For X in the Lie algebra and t sufficiently small, $r(e^{tX}) = e^{tR(X)}$.

The WZW theory possesses three right- and left-moving currents, which may be grouped into the matrices

$$J_R = k\,\partial_+ g g^{-1}\,, \qquad J_L = k\,g^{-1}\partial_- g\,; \tag{3.13}$$

here k is the level of the WZW model. The WZW equations of motion state that these currents are conserved, *i.e.*, $\partial_- J_R = \partial_+ J_L = 0$.

Taking the Lie algebra automorphism in (3.5) to be trivial leads to the gluing condition

$$J_L = -J_R\,. \tag{3.14}$$

The worldvolumes of the associated branes are ordinary conjugacy classes of S^3: they are the 2-spheres given by

$$\mathrm{Tr}\, g = 2\sin\psi_0\,, \tag{3.15}$$

for some constant $\psi_0 \in [-\pi/2, \pi/2]$. The worldvolume of the S^2 *brane* with $\psi_0 = 0$ spans the equatorial 2-sphere of S^3; as $|\psi_0| \to \pi/2$, the S^2 branes degenerate to single points at the north or south pole.

It is useful to introduce a second parametrization of the $SU(2)$ group element,

$$g = \begin{pmatrix} \sin r \sin\theta + i\cos r \sin t & -\cos r\cos t - i\cos\theta\sin r \\ \cos r\cos t - i\cos\theta\sin r & \sin r\sin\theta - i\cos r\sin t \end{pmatrix}, \tag{3.16}$$

where the coordinates (r, θ, t) satisfy

$$0 \le r \le \frac{\pi}{2}\,, \qquad 0 \le \theta, t \le 2\pi\,. \tag{3.17}$$

The S^3 metric in these coordinates takes the form

$$ds^2 = \cos^2 r\, dt^2 + dr^2 + \sin^2 r\, d\theta^2\,. \tag{3.18}$$

One simple class of open string configurations satisfying the WZW equations of motion is given by

$$t = a\tau\,, \qquad \theta = a\sigma + \theta_0\,, \qquad r = r_0\,, \tag{3.19}$$

where $0 \leq a < 1$ and $0 \leq \theta_0 \leq \pi/2$.[6] The solutions satisfy the Dirichlet condition defining the S^2 brane, provided

$$\sin\theta_0 = \frac{\sin\psi_0}{\sin r_0} \qquad \text{and} \qquad a = 1 - \frac{2\theta_0}{\pi}\,. \tag{3.20}$$

It follows that

$$a \leq 1 - \frac{2|\psi_0|}{\pi}\,. \tag{3.21}$$

That is, a has an upper bound that decreases with increasing $|\psi_0|$. The geometry of the S^2 branes and their attached open strings is shown in Figure 3.1(a).

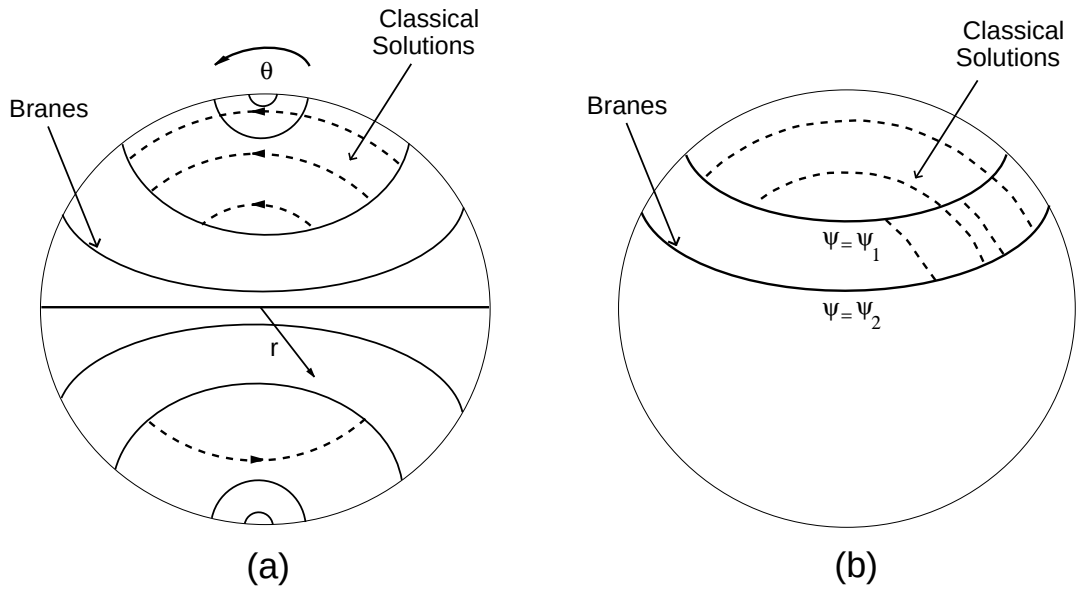

Figure 3.1: (a) A view at fixed t of S^2 branes and open strings ending on them. (b) A view at fixed t of a system of two S^2 branes with open strings.

Let us compare the result of our classical analysis with the known structure of the quantum Hilbert space of open strings ending on S^2 branes. The Hilbert space

[6] This range for θ_0 assumes that $\psi_0 > 0$. If $\psi_0 < 0$, the proper range for θ_0 is $\pi \leq \theta_0 \leq 3\pi/2$. The bound $0 \leq a < 1$ will be explained in greater detail in the analogous $SL(2,R)$ context in Section 3.5.1; essentially, any solution with arbitrary a can be mapped by spectral flow to a solution satisfying the bound. One important difference between the $SL(2,R)$ and $SU(2)$ models, though, is that, in the quantum theory of the $SL(2,R)$ model, spectral flow generates new representations of the current algebra, whereas in the $SU(2)$ model, it does not.

is a sum of representations of $\widehat{SU}(2)$; the spin j of a representation appearing in the sum is related to the parameter a of the associated classical solution by $j = ka/2$. Although the analysis we have just presented is not refined enough to see it, ψ_0 is quantized [44] as $\psi_0 = \frac{\pi n}{k}$, where $n = -k/2, -k/2+1, \ldots, k/2$. Thus, for given ψ_0, the bound (3.21) on a translates into a bound

$$j \leq \frac{k}{2} - |n| \tag{3.22}$$

on the spins of the allowed representations in the Hilbert space. This bound matches the conformal field theory analysis of [41], in which the Hilbert space $\mathcal{H}_n$ of open strings ending on the brane labeled by n was shown to be

$$\mathcal{H}_n = \bigoplus_{j=0}^{k/2} N_{\alpha\alpha}^{j} D_j \,, \tag{3.23}$$

where $\alpha = \frac{1}{2}(n + \frac{k}{2})$, D_j is the irreducible spin-j highest weight representation of $\widehat{SU}(2)$, and the fusion coefficients are given by

$$N_{\alpha\beta}^{j} = \begin{cases} 1 & \text{if } |\alpha-\beta| \leq j \leq \min\{\alpha+\beta, k-\alpha-\beta\} \\ & \text{and } 2(j+\alpha+\beta) \equiv 0 \bmod 2 \\ 0 & \text{otherwise}\,. \end{cases} \tag{3.24}$$

A priori, the sum over j is to be taken in half-integer steps (*i.e.*, $j = 0, 1/2, \ldots, k/2$). However, the fusion coefficient $N_{\alpha\alpha}^{j}$ is nonzero only if j is an integer. The equatorial S^2 brane has $\alpha = k/4$; the branes at the poles have $\alpha = 0$ and $\alpha = k/2$. For all α, the sum cuts off at $\min(2\alpha, k-2\alpha)$, which is readily seen to be equivalent to the cutoff (3.22). Thus (3.23) is identical to (3.1). Our classical methods have reproduced information about the quantum Hilbert space.

The restriction to integral j in the sum (3.23) (or (3.1)) can be simply understood, at least for equatorial S^2 branes. In addition to the stringy solutions (3.19), the equatorial S^2 brane also admits the particle-like geodesic solutions

$$t = a\tau\,, \qquad r = 0\,. \tag{3.25}$$

Let us consider the $k \to \infty$ limit of the theory. In this limit, if we expand around geodesic solutions like (3.25), the WZW model reduces to quantum mechanics on S^2. Its Hilbert space is therefore the space $\mathcal{L}^2(S^2)$ of square-integrable functions on S^2. This space decomposes into spherical harmonics, which correspond to representations of integral spin only.

We conclude this section with a slight generalization. Let us consider a system of two S^2 branes, located at $\psi = \psi_1 = \pi n_1/k$ and $\psi = \psi_2 = \pi n_2/k$; without loss of generality, we may assume that $\psi_1 > 0$ and $|\psi_1| > |\psi_2|$, as shown in Figure 1(b). The conformal field theory analysis of (3.23) and the expression (3.24) for the fusion coefficients tell us that the Hilbert space of strings stretching from the brane at ψ_1 to the brane at ψ_2 has the decomposition

$$\mathcal{H}_{n_1,n_2} = \bigoplus_{j=\frac{1}{2}|n_1-n_2|}^{\frac{1}{2}(k-n_1-n_2)} D_j \,. \tag{3.26}$$

We wish to reproduce the bound on j by semiclassical methods. We consider classical solutions of the form (3.19), subject to the Dirichlet boundary conditions

$$\sin\theta_0 \sin r_0 = \sin\psi_1 \,, \tag{3.27}$$

$$\sin(a\pi + \theta_0) \sin r_0 = \sin\psi_2 \,. \tag{3.28}$$

An argument like the one in the single-brane example shows that now a is bounded both above and below,

$$\frac{|\psi_1 - \psi_2|}{\pi} \leq a \leq 1 - \frac{\psi_1 + \psi_2}{\pi} \,. \tag{3.29}$$

The solutions saturating the inequalities are those with $r_0 = \pi/2$. Since $j = ka/2$, the bound on a translates to

$$\frac{1}{2}|n_1 - n_2| \leq j \leq \frac{1}{2}(k - n_1 - n_2) \,, \tag{3.30}$$

which matches the conformal field theory result.

3.3 Closed strings in AdS_3

Our search in Sections 3.4 and 3.5 for solutions of the $SL(2,R)$ WZW model corresponding to open strings ending on branes will be guided by the known properties of closed string solutions. In this section, we summarize the analysis of [37] of closed bosonic string theory in AdS_3. Our review has two parts. First, we survey the classical closed string solutions of the $SL(2,R)$ WZW model, beginning with simple geodesic solutions and building up more complicated solutions by acting with global isometries and spectral flow. Next, we sketch the structure of the quantum Hilbert space.

3.3.1 Classical solutions

The space AdS_3 is the group manifold of $SL(2,R)$. If we think of AdS_3 (with unit anti-de Sitter radius) as the hyperboloid

$$(X^0)^2 - (X^1)^2 - (X^2)^2 + (X^3)^2 = 1 \tag{3.31}$$

embedded in $\mathbf{R}^{2,2}$, then a point in AdS_3 is given by the $SL(2,R)$ matrix

$$g = \begin{pmatrix} X^0 + X^1 & X^2 + X^3 \\ X^2 - X^3 & X^0 - X^1 \end{pmatrix}. \tag{3.32}$$

Alternatively, we may parametrize g in terms of the global coordinates (ρ, θ, t) defined in Appendix C,

$$g = \begin{pmatrix} \cos t \cosh\rho - \cos\theta \sinh\rho & \sin t \cosh\rho + \sin\theta \sinh\rho \\ -\sin t \cosh\rho + \sin\theta \sinh\rho & \cos t \cosh\rho + \cos\theta \sinh\rho \end{pmatrix}. \tag{3.33}$$

The AdS_3 metric in these coordinates is

$$ds^2 = -\cosh^2\rho\, dt^2 + d\rho^2 + \sinh^2\rho\, d\theta^2 . \tag{3.34}$$

The parametrization (3.33) is the $SL(2,R)$ counterpart of the $SU(2)$ parametrization (3.16).

Like the $SU(2)$ theory, the $SL(2,R)$ theory possesses three conserved right- and left-moving currents,

$$J_R^a(x^+) = k\mathrm{Tr}\left(T^a\partial_+ g g^{-1}\right)\,, \qquad J_L^a(x^-) = k\mathrm{Tr}\left(T^{a*} g^{-1}\partial_- g\right) \qquad (a=+,-,3)\,. \tag{3.35}$$

Here k is again the level of the WZW model, and the T^a, given in terms of the Pauli matrices by

$$T^3 = -\frac{i}{2}\sigma_2\,, \qquad T^\pm = \frac{1}{2}(\sigma_3 \pm i\sigma_1)\,, \tag{3.36}$$

form a basis of the Lie algebra of $SL(2,R)$. Sometimes we write the currents in the matrix form

$$J_R = k\partial_+ g g^{-1}\,, \qquad J_L = k g^{-1}\partial_- g\,. \tag{3.37}$$

The general solution g of the WZW model can be factored as a product of left-moving and right-moving parts,

$$g(\sigma,\tau) = g_+(x^+) g_-(x^-)\,, \tag{3.38}$$

but, as we have said, it is useful to begin by studying geodesic solutions, which depend only on the time coordinate τ.

The simplest timelike geodesic solution is

$$g_0 = \begin{pmatrix} \cos\,\alpha\tau & \sin\,\alpha\tau \\ -\sin\,\alpha\tau & \cos\,\alpha\tau \end{pmatrix}, \tag{3.39}$$

describing a point particle at the center of AdS_3,

$$t = \alpha\tau\,, \qquad \rho = 0\,. \tag{3.40}$$

The most general timelike geodesic can be obtained by acting on (3.39) with the global isometry group $SL(2,R)\times SL(2,R)$ of the WZW model. Such a solution has the form

$$g = U\begin{pmatrix} \cos\,\alpha\tau & \sin\,\alpha\tau \\ -\sin\,\alpha\tau & \cos\,\alpha\tau \end{pmatrix} V, \tag{3.41}$$

where U and V are constant $SL(2,R)$ elements. The parameter α in (3.39) and (3.41) is related through the Virasoro constraints to the conformal weight h of the sigma model on the compact space $\mathcal{M}$. The conserved currents of the solution (3.41) are

$$J^3_L = J^3_R = \frac{k\alpha}{2}\,, \qquad J^\pm_L = J^\pm_R = 0\,, \tag{3.42}$$

and the energy, defined as the sum of the zero modes of J^3_L and J^3_R, is $k\alpha$.

The construction of spacelike geodesics is similar. The simplest spacelike geodesic solution

$$g_0 = \begin{pmatrix} e^{\alpha\tau} & 0 \\ 0 & e^{-\alpha\tau} \end{pmatrix} \tag{3.43}$$

describes a straight line through the spacelike section $t = 0$ of AdS_3. The most general spacelike geodesic solution is

$$g = U g_0 V\,, \tag{3.44}$$

where, again, U and V are constant $SL(2,R)$ isometries. Its currents are

$$J^3_L = J^3_R = 0\,, \qquad J^\pm_L = J^\pm_R = \frac{k\alpha}{2}\,, \tag{3.45}$$

and its energy is zero.

Given a classical solution $\tilde{g}(\sigma,\tau) = \tilde{g}_+(x^+)\tilde{g}_-(x^-)$, we can generate a new solution $g(\sigma,\tau) = g_+(x^+)g_-(x^-)$ by *spectral flow*, which involves setting

$$g_+ = e^{\frac{i}{2}wx^+\sigma^2}\tilde{g}_+\,, \qquad g_- = \tilde{g}_- e^{\frac{i}{2}wx^-\sigma^2}\,, \tag{3.46}$$

for some integer w. Spectral flow acts on the AdS_3 global coordinates by

$$\rho \to \rho\,, \qquad t \to t + w\tau\,, \qquad \theta \to \theta + w\sigma\ , \tag{3.47}$$

and on the $SL(2,R)$ currents by

$$J^3_R = \tilde{J}^3_R + \frac{kw}{2}\,, \qquad J^\pm_R = \tilde{J}^\pm_R e^{\mp iwx^+}\,, \tag{3.48}$$

$$J^3_L = \tilde{J}^3_L + \frac{kw}{2}\,, \qquad J^\pm_L = \tilde{J}^\pm_L e^{\mp iwx^-}\,; \tag{3.49}$$

or in terms of Fourier modes,

$$J^3_{R,L\,n} = \tilde{J}^3_{R,L\,n} + \frac{kw}{2}\delta_{n,0}\,, \qquad J^\pm_{R,L\,n} = \tilde{J}^\pm_{R,L\,n\mp w}\,. \tag{3.50}$$

Timelike geodesics are mapped under spectral flow to short string solutions, which expand and contract periodically in global time and wind w times around the center of AdS_3. Spacelike geodesics are mapped to long string solutions, which start in the infinite global-time past as circular strings of infinite radius wound w times near the boundary of AdS_3, collapse (to a point, if there is no angular momentum) as $t \to 0$, and expand again as $t \to \infty$ to wound circular strings at the boundary. The solutions constructed in this way have energies

$$E = \frac{kw}{2} + \frac{1}{w}\left(\mp\frac{k\alpha^2}{2} + 2h\right)\,, \tag{3.51}$$

where the minus sign corresponds to short strings and the plus sign to long strings.

3.3.2 The quantum Hilbert space

We now recall the structure of the quantum Hilbert space of the $SL(2,R)$ WZW model. The Hilbert space decomposes as the sum of *discrete* representations of the $\widehat{SL}(2,R)$ current algebra, *continuous* representations of the current algebra, and the images of these representations under spectral flow. Let us briefly review what this means.

The zero modes J^a_0 of the generators J^a of the (left- or right-moving) $\widehat{SL}(2,R)$ current algebra form a closed subalgebra, which generates the group $SL(2,R)$. Among the unitary representations of this $SL(2,R)$ are the *principal discrete* highest- and lowest-weight representations, which are realized in the Hilbert space

$$\mathcal{D}^\pm_j = \{|j;m\rangle : m = \pm j, \pm(j+1), \pm(j+2), \ldots\}\,. \tag{3.52}$$

The states $|j;m\rangle$ are simultaneous eigenstates of L_0, the zeroth Virasoro generator obtained from the Sugawara construction, and J^3_0, the $SL(2,R)$ Cartan generator, with eigenvalues $-j(j-1)$ and m. These representations are unitary if $j > 0$. The representations $\hat{\mathcal{D}}^\pm_j$ of the $\widehat{SL}(2,R)$ current algebra are constructed by considering

the states in $\mathcal{D}_j^{\pm}$ as primary states for the action of J_n^a. That is, the states $|j;m\rangle$ are taken to be annihilated by the J_n^a with $n>0$, while the J_n^a with $n<0$ are understood as creation operators, whose repeated action on the states $|j;m\rangle$ yields states that fill out the representations $\hat{\mathcal{D}}_j^{\pm}$.

Another unitary representation of $SL(2,R)$ is the *continuous* representation, realized in the Hilbert space

$$\mathcal{C}_j^{\alpha} = \{|j,\alpha;m\rangle : m = \alpha, \alpha\pm 1, \alpha\pm 2, \ldots\}\,, \tag{3.53}$$

with $0\le\alpha<1$ and $j=1/2+is$, for real s. Again, the states in $|j,\alpha;m\rangle$ are simultaneous eigenstates of L_0 and J_0^3, with eigenvalues $-j(j-1)$ and m. The representation $\mathcal{C}_j^{\alpha}$ of $SL(2,R)$ gives rise to a representation $\hat{\mathcal{C}}_j^{\alpha}$ of the current algebra in the manner described above for the discrete representations.

As we have just noted, the representations $\hat{\mathcal{D}}_j^{\pm}$ and $\hat{\mathcal{C}}_j^{\alpha}$ are described by the action of the current algebra modes J_n^a on their constituent states. Spectral flow by w units alters the modes J_n^a, as noted in (3.50), and so maps the representations $\hat{\mathcal{D}}_j^{\pm}$ and $\hat{\mathcal{C}}_j^{\alpha}$ into new representations $\hat{\mathcal{D}}_j^{\pm,w}$ and $\hat{\mathcal{C}}_j^{\alpha,w}$. The closed string Hilbert space was proposed in [37] to be the direct sum of $\hat{\mathcal{D}}_j^{+,w}\otimes\hat{\mathcal{D}}_j^{+,w}$ and $\hat{\mathcal{C}}_j^{\alpha,w}\otimes\hat{\mathcal{C}}_j^{\alpha,w}$, the two factors in each tensor product accounting for left- and right-moving states. The permissible values of j for the discrete representations are bounded by $\frac{1}{2}<j<\frac{k-1}{2}$; note that, before the physical state conditions are imposed, j may be any real number in this range. The states in $\hat{\mathcal{D}}_j^{+,w}\otimes\hat{\mathcal{D}}_j^{+,w}$ correspond to wound short strings and their excitations,[7] while the states in $\mathcal{C}_j^{\alpha,w}\otimes\mathcal{C}_j^{\alpha,w}$ correspond to wound long strings and their excitations. The spectra of both kinds of states was computed in [37] and was checked by an independent calculation in [36].

It is important to keep clear the distinction between the Hilbert space of the WZW model and the Hilbert space of the physical string theory. The (AdS_3 part of the) latter is the subspace of the former defined by the Virasoro constraints. Spectral flow is a symmetry of the WZW model, but does not commute with the Virasoro

[7] The representations $\hat{\mathcal{D}}_j^{+,w}$ and $\hat{\mathcal{D}}_{\frac{k}{2}-j}^{-,w+1}$, may be identified. This accounts for the exclusion of $\hat{\mathcal{D}}_j^{-,w}$ from the list of allowed representations: it would be redundant to include it.

constraints, and is therefore not realized explicitly in the physical string Hilbert space. While in our analysis of classical solutions above and in subsequent sections, we have freely borrowed and will continue to borrow the intuitions (and language) of strings, we should bear in mind that our conclusions really pertain to the Hilbert space of the WZW model before the imposition of the Virasoro constraints.

3.4 The straight AdS_2 Brane

Having reviewed closed string theory in AdS_3, we now add branes to the game. We said in Section 3.2 that the brane worldvolumes in group manifolds can be thought of as twined conjugacy classes of the form

$$\mathcal{W}_g^r = \{r(h)gh^{-1} : h \in G\}\,, \tag{3.54}$$

where r is a group automorphism. In the case $G = AdS_3$, it was shown by Bachas and Petropoulos [52] that the only physically reasonable branes are those for which r is the nontrivial outer automorphism that acts on a group element h, parametrized as a 2×2 matrix as in (3.33), by

$$r(h) = \omega_0^{-1} h \omega_0\,, \qquad \text{with} \qquad \omega_0 = \begin{pmatrix} 0 & 1 \\ 1 & 0 \end{pmatrix}. \tag{3.55}$$

For this choice of r, the twined conjugacy class $\mathcal{W}_g^r$ is equivalently characterized as the set of $g' \in SL(2,R)$ such that $\mathrm{Tr}\,(\omega_0 g') = \mathrm{Tr}\,(\omega_0 g)$. The worldvolumes of the resulting branes are two-dimensional, since they are parametrized by arbitrary $SL(2,R)$ group elements subject to the single condition

$$\mathrm{Tr}\,(\omega_0 g') = 2\sinh\psi_0\,, \tag{3.56}$$

where $\sinh\psi_0$ is a constant whose physical meaning will become apparent shortly. Upon tracing through the procedure for extracting boundary conditions for coordinates from the gluing conditions for currents, one indeed finds (3.56) as the Dirichlet

condition for the coordinate transverse to the worldvolume. The gluing conditions for the coordinates parallel to the brane worldvolume take the form

$$J_L = -\omega_0 J_R \omega_0 \,, \tag{3.57}$$

and can be shown to be equivalent to the appropriate Neumann conditions for the $SL(2,R)$ WZW model action.

Thinking of AdS_3 as the hyperboloid (3.31) in four-dimensional space, (3.64) becomes the statement $X^2 = \sinh\psi_0$. Subject to this condition, (3.31) becomes

$$(X^0)^2 - (X^1)^2 + (X^3)^2 = 1 + \sinh^2\psi_0 \,, \tag{3.58}$$

which is the equation of two-dimensional anti-de Sitter space. Thus the worldvolume geometry of the physical branes of [52] is that of AdS_2 embedded in AdS_3. Analysis of the Dirac-Born-Infeld action of these AdS_2 *branes* shows that they consist of one D-string bound to some number of fundamental strings. The fundamental string charge Q is proportional to the constant $\sinh\psi_0$; it follows that ψ_0 is quantized. The quantization condition is

$$\sinh\psi_0 = g_s Q \,, \tag{3.59}$$

where g_s is the string coupling constant.

In dealing with AdS_2 branes, it is convenient to switch to a coordinate system in which the Dirichlet condition is simple. The AdS_2 *coordinates* (ψ, ω, t) are defined in terms of the global coordinates by

$$\sinh\psi = \sin\theta \sinh\rho \,, \qquad \cosh\psi \sinh\omega = -\cos\theta \sinh\rho \,, \qquad t = t \,, \tag{3.60}$$

and in terms of the embedding hyperboloid coordinates by

$$X^1 = \cosh\psi \sinh\omega \,, \qquad X^2 = \sinh\psi \,, \qquad X^0 + iX^3 = \cosh\psi \cosh\omega e^{it} \,. \tag{3.61}$$

The AdS_3 metric in AdS_2 coordinates is

$$ds^2 = d\psi^2 + \cosh^2\psi(-\cosh^2\omega dt^2 + d\omega^2) \,. \tag{3.62}$$

The AdS_2 coordinates are the $SL(2,R)$ analogue of the coordinate system given in (3.7) for $SU(2)$. In AdS_2 coordinates, the Dirichlet condition giving the location

of the AdS_2 brane becomes $\psi = \psi_0$. Some AdS_2 branes in AdS_3 are shown in Figure 3.2.

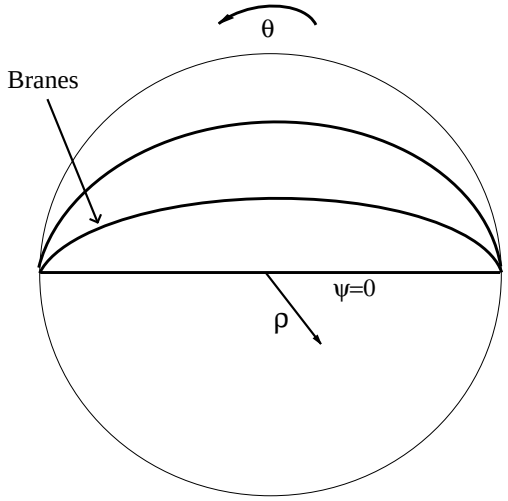

Figure 3.2: AdS_2 branes in AdS_3. The view is of the (ρ, θ) plane at fixed global time t. The branes are surfaces of constant ψ.

In understanding AdS_2 branes and the strings that end on them, there is a crucial distinction to be made between the "straight" branes located at $\psi = \psi_0 = 0$ and the "curved" branes located at $\psi = \psi_0 \neq 0$. In this section, we study straight branes, following the paradigm of Section 3.3. First we construct classical geodesic solutions confined to the brane. Next we investigate how spectral flow generates classical string solutions that satisfy the appropriate boundary conditions. This leads to a proposal for the open string spectrum. We conclude by describing a check of this proposal by an explicit partition function calculation modeled on that of [36].

3.4.1 Classical solutions

Our experience with closed strings suggests that looking at geodesics might be a promising starting point for the study of open string solutions. A σ-independent solution that satisfies the Dirichlet condition necessarily lies entirely within the brane.

The timelike and spacelike geodesics (3.39) and (3.43) obviously satisfy this requirement. In the closed string case, we built the most general timelike and spacelike geodesic solutions from these basic ones by acting with the global isometry group $SL(2,R) \times SL(2,R)$. In the presence of an AdS_2 brane, however, the only permitted isometries are those preserving the gluing conditions

$$J_L = -\omega_0 J_R \omega_0 \tag{3.63}$$

and leaving fixed the brane worldvolume—or equivalently, preserving the Dirichlet condition

$$\mathrm{Tr}\,(\omega_0 g) = 2\sinh\psi_0\,. \tag{3.64}$$

The isometry $g \to UgV$ transforms the currents according to

$$J_R \to U J_R U^{-1}\,, \qquad J_L \to V^{-1} J_L V\,. \tag{3.65}$$

The conditions for this isometry to preserve (3.63) and (3.64) are therefore

$$V^{-1} J_L V = -\omega_0 U J_R U^{-1} \omega_0\,, \tag{3.66}$$

$$\mathrm{Tr}\,(\omega_0 U g V) = \mathrm{Tr}\,(\omega_0 g)\,, \tag{3.67}$$

which are satisfied if and only if $V = \omega_0 U^{-1} \omega_0$. Thus the boundary conditions imposed by the AdS_2 brane break the global isometry group from $SL(2,R) \times SL(2,R)$ to a single $SL(2,R)$. This is natural: the two factors of $SL(2,R)$ in closed string theory correspond to independent transformations of left- and right-moving modes, whereas the left- and right-moving modes of open strings are related by the gluing conditions at the worldsheet boundary. Our choice of gluing conditions guarantees that the $SL(2,R)$ global symmetry is naturally promoted to an affine symmetry, just as in the closed string case.

The preceding analysis of the breaking of the isometry group holds for straight branes and curved branes alike: nothing in the argument depended on the value of ψ_0.[8] One difference between the straight and curved cases is that, as we have

[8] If $\psi_0 = 0$, the most general solution of (3.66) and (3.67) is $V = \pm\omega_0 U^{-1} \omega_0$, but the counting of parameters remains the same.

noted, straight branes contain particle-like solutions such as the ones shown in Figure 3.3. Curved branes, on the other hand, do not. When we generate the open string solutions associated with curved branes, we will need a different starting point. We will explore this in more detail in Section 3.5.

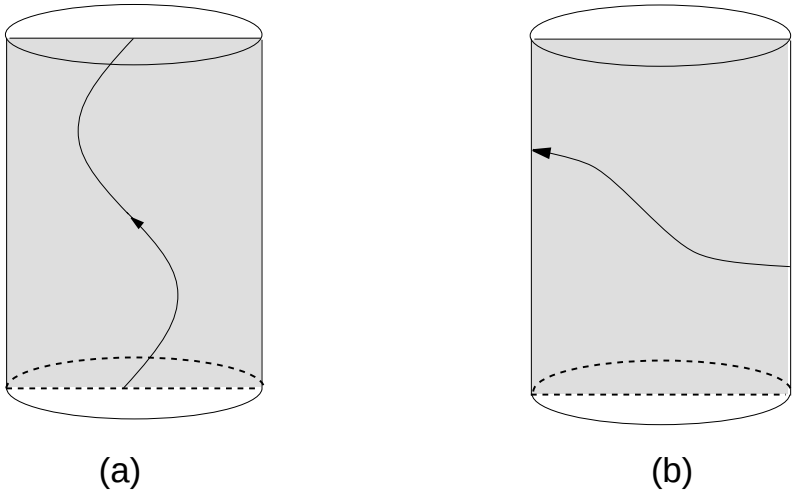

Figure 3.3: (a) A timelike geodesic and (b) a spacelike geodesic confined to the brane at $\psi_0 = 0$.

Spectral flow generates new open string solutions from old ones. In the closed string case, the parameter w was required to be an integer, to maintain the periodicity of the closed strings. In the presence of an AdS_2 brane, w must again be integer, but for a different reason: to ensure compatibility of spectral flow with the gluing conditions (3.63).

Is the Dirichlet condition compatible with spectral flow? Suppose we are given a solution satisfying the boundary condition

$$\sinh\psi \equiv \sin\theta \sinh\rho = \sinh\psi_0 \tag{3.68}$$

at $\sigma = 0$ and $\sigma = \pi$. If we act with w units of spectral flow, we obtain a new solution characterized by

$$\sinh\psi_{\rm new} = \sin\theta \sinh\rho = \sinh\psi_0 \qquad \text{at } \sigma = 0\,,$$

$$\sinh\psi_{\rm new} = \sin(\theta+\pi w)\sin\rho = \pm\sin\theta\sinh\rho = \pm\sinh\psi_0 \qquad \text{at } \sigma=\pi \quad (3.69)$$

where the sign is plus if w is even and minus if w is odd. For a straight AdS_2 brane, $\psi_0 = 0$, and so the Dirichlet condition imposes no added restrictions on w. On the other hand, spectral flow is a symmetry of curved branes only for even w.[9] This is a key difference between straight and curved branes, and much of Section 3.5 will be devoted to its consequences.

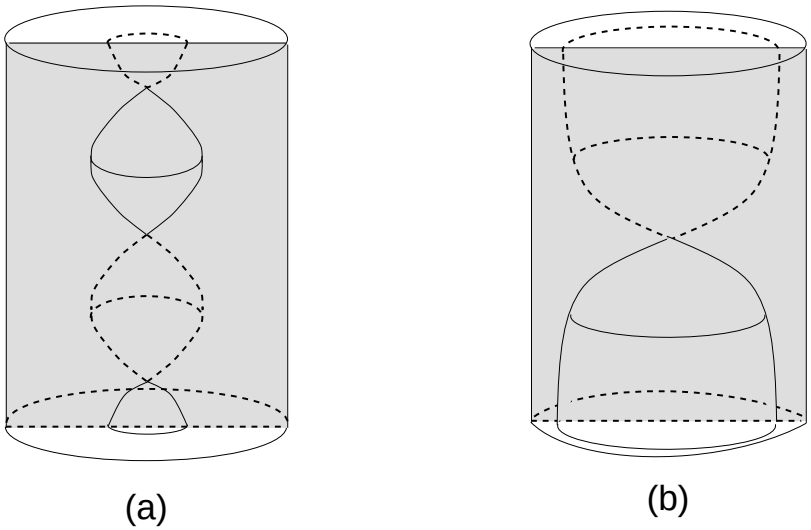

Figure 3.4: (a) An open short string classical solution corresponding to $w = 1$ spectral flowed timelike geodesic solutions. (b) A classical open long string solution corresponding to $w = 1$ spectral flowed spacelike geodesic.

Spectral flow applied to timelike geodesics yields short strings. If w is odd, these are wound open strings that contract and expand periodically in t, and whose endpoints are symmetric with respect to the central axis $\rho = 0$ of AdS_3. If w is even, the string endpoints coincide, giving wound circular strings. Spacelike geodesics are mapped by spectral flow to long strings. Examples of strings of both kinds with $w = 1$ are shown in Figure 3.4. A calculation just like the one sketched in Section 3.3 shows

[9] If w is odd, then a string whose $\sigma = 0$ endpoint lies on a brane at $\psi = \psi_0$ will end up at $\sigma = \pi$ with $\psi = -\psi_0$. This will come in handy in Section 3.5.

the space-time energy of these solutions to be

$$E = J_0^3 = \frac{kw}{4} + \frac{1}{w}\left(\mp\frac{k\alpha^2}{4} + h\right) , \tag{3.70}$$

where the minus sign is for short strings and the plus sign for long strings. The energy of these open strings is precisely half the energy (3.51) of their closed string counterparts.

3.4.2 The quantum Hilbert space

The classical solutions describing short and long strings ending on the straight AdS_2 brane are in a sense "exactly half" of the corresponding closed string solutions: left movers and right movers are related by the gluing conditions, and the energy of the resulting strings is half that of the closed strings. As in the closed string case, discrete representations ought to be associated with short strings and continuous representations with long strings. We therefore propose that the quantum Hilbert space is the direct sum of $\hat{\mathcal{D}}_j^{+,w}$ and $\hat{\mathcal{C}}_j^{\alpha,w}$, summed over all integers w, and with $\frac{1}{2} < j < \frac{k-1}{2}$ for the discrete representations and $j = \frac{1}{2} + is$ with $s \in \mathbf{R}$ for the continuous representations. Our proposed open string spectrum is thus the holomorphic square root of the closed string spectrum found in [37].

In Appendix D, we verify this conjecture by an independent calculation of the spectrum. We compute the finite-temperature partition function in Euclidean AdS_3 and interpret the result in terms of the free energy, summed over string states. This enables us to read off the spectrum of open string states. The result is in exact agreement with the conjecture.

3.5 The curved AdS_2 brane

We now consider open strings constrained to end on a curved AdS_2 brane located at $\psi = \psi_0 \neq 0$; without loss of generality, we may assume $\psi_0 > 0$. Our method is the same as in the closed string and straight brane cases: we begin in Section 3.5.1 with the study of classical solutions and their symmetries, and then in Section

3.5.2 conjecture the structure of the quantum Hilbert space. Several elements of the story are different for curved branes. First, there are no classical geodesic solutions. Second, and more seriously, spectral flow is a symmetry of the AdS_2 brane only if the winding number w is even. Generating solutions with odd winding number thus calls for new tricks, which we describe in detail.

As we explain in Section 3.5.2, the chief consequence of these differences is that, in the Hilbert space of the WZW model, the density of states of the odd winding continuous representations of $\widehat{SL}(2,R)$ behaves differently from the density of states of the even winding continuous representations as a function of the brane position ψ_0. Both kinds of representations are present in the spectrum for all ψ_0, though, as is the entire set of discrete representations. This is to be contrasted with the $SU(2)$ WZW model, whose Hilbert space in the presence of S^2 branes loses representations as ψ_0 increases.

In Section 3.5.3 we present a generalization to a system with two curved AdS_2 branes. In Section 3.5.4 we study the limit $\psi_0 \to \infty$ in which the AdS_2 brane becomes highly curved. In this limit, the WZW model Lagrangian resembles that of noncommutative open string theory in AdS_2.

3.5.1 Classical solutions

The program we followed in the last section began by constructing σ-independent classical solutions lying within the brane. If $\psi_0 > 0$, no such solutions exist. For suppose $g = g(\tau)$ is a (non-constant) solution. It must satisfy the Dirichlet condition $\mathrm{Tr}\,(\omega_0 g) = 2\sinh\psi_0$, as well as the gluing condition (3.63), which for the case at hand reads

$$g^{-1}\partial_\tau g = -\omega_0 \partial_\tau g g^{-1}\omega_0\,, \tag{3.71}$$

as $\partial_+ g = \partial_- g = \frac{1}{2}\partial_\tau g(\tau)$. Multiplying on the right by $(\partial_\tau g)^{-1}$, inverting, and taking the trace gives $\mathrm{Tr}\,(g\omega_0) = -\mathrm{Tr}\,(\omega_0 g)$, and thus $\mathrm{Tr}\,(g\omega_0) = 0$, in contradiction with the Dirichlet condition.

Though there are no particle-like solutions, we are led to simple string solutions by

the following physical argument. Imagine starting with the timelike geodesic (3.40) in a flat AdS_2 brane and then increasing ψ_0 by turning on a background electric field on the brane. The timelike geodesic on the brane can be thought of as an infinitely small string, whose endpoints are equally and oppositely charged with respect to the background electric field. As ψ_0 increases, the string must stretch so that its tension will balance the forces due to the electric field. This picture suggests the basic timelike string solution shown in Figure 3.5(a),

$$t = \alpha\tau\,, \qquad \theta = \alpha\sigma + \theta_0\,, \qquad \rho = \rho_0\,, \tag{3.72}$$

with

$$\theta_0 = \frac{\pi}{2}(1-\alpha)\,, \qquad \sinh\rho_0 = \frac{\sinh\psi_0}{\sin\theta_0}\,, \tag{3.73}$$

and $0 \le \alpha < 1$. At fixed time, this solution describes a string curved in a circular

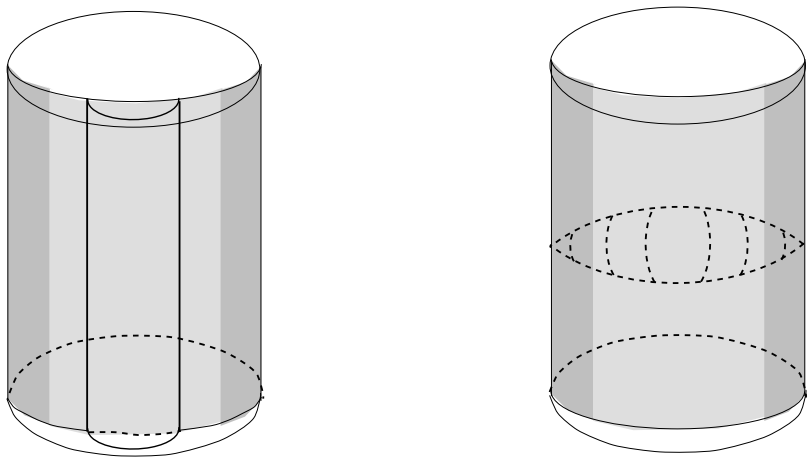

Figure 3.5: The basic (a) "timelike" and (b) "spacelike" string solutions ending on a curved AdS_2 brane.

arc and symmetric about $\theta = \pi/2$. It is easily checked that (3.72) solves the equation of motion. Its currents are the same as those of (3.40), and so it obeys (3.63). The choice of θ_0 and ρ_0 ensure that (3.64) is satisfied as well.[10]

[10]The most trivial solution imaginable is a "pointlike instanton": a solution with t, ρ, and θ all

The solution (3.72) is the $SL(2,R)$ analogue of the $SU(2)$ solution (3.19) for open strings ending on S^2 branes. An important difference between the two is that the range of α in (3.72) is $0 \leq \alpha < 1$, regardless of the value of ψ_0, whereas the corresponding parameter a in the $SU(2)$ case is subject to the upper bound (3.21), which depends on ψ_0. This bound restricts the allowed representations in the $SU(2)$ WZW model Hilbert space. We will argue in Section 3.5.2 that the absence of such a bound for AdS_2 branes implies that there is no similar restriction on the allowed representations in the $SL(2,R)$ model Hilbert space. Our classical analysis reveals this difference between the two models to be entirely geometric: in the $SL(2,R)$ model, every AdS_2 brane stretches from $\theta = 0$ to $\theta = \pi$, while in the $SU(2)$ case, the range of θ, and hence of a, depends on ψ_0.

The basic spacelike solution is given in matrix form as

$$g = \begin{pmatrix} \sqrt{1+\beta^2}\, e^{\alpha\tau} & \beta\, e^{\alpha(\sigma-\frac{\pi}{2})} \\ \beta\, e^{-\alpha(\sigma-\frac{\pi}{2})} & \sqrt{1+\beta^2}\, e^{-\alpha\tau} \end{pmatrix}, \tag{3.74}$$

and in global coordinates as

$$\begin{aligned} \tan t &= \frac{\beta \sinh(\alpha(\sigma-\pi/2))}{\sqrt{1+\beta^2}\cosh\alpha\tau}\,, \\ \tan\theta &= \frac{-\beta\cosh(\alpha(\sigma-\pi/2))}{\sqrt{1+\beta^2}\sinh\alpha\tau}\,, \\ \cosh^2\rho &= (1+\beta^2)\cosh^2\alpha\tau + \beta^2\sinh^2(\alpha(\sigma-\pi/2))\,, \end{aligned} \tag{3.75}$$

where $\beta = \sinh\psi_0/\cosh\frac{\pi}{2}\alpha$.[11] This solution, depicted in Figure 3.5(b), is a stringy generalization of the spacelike geodesic (3.43). It begins in the infinite worldsheet

constant. It is amusing to observe that (3.72) may be obtained as the image under spectral flow by α units of the pointlike instanton solution with $t = 0$, $\theta = \theta_0$, and $\rho = \rho_0$. Of course, α is, in general, fractional, and so the notion of spectral flow here is purely formal.

[11] One way to derive this solution is to assume first that ψ_0 is small and perturb the spacelike geodesic (3.43) accordingly. From the lowest-order corrections to (3.43) it is possible to guess the form of (3.74), and to check that it is a valid solution even if ψ_0 is not small. The basic timelike solution (3.72) may be derived from the timelike geodesic (3.39) by similar methods.

past $\tau = -\infty$ at $t = 0$ and at the edge $\theta = 0$, $\rho = \infty$ of the brane, and arrives in the infinite worldsheet future $\tau = +\infty$ at the other edge $\theta = \pi$, $\rho = \infty$, again at global time $t = 0$. Its excursion from the brane in the worldsheet interim is governed by α. When α is small, the string stays near the brane; as α increases, it strays farther and farther away. A routine calculation shows that the currents of (3.74) are the same as those of (3.43).

Having obtained the basic timelike and spacelike solutions, our next task is to generate new solutions by acting with isometries and spectral flow. As we commented in Section 3.4, the allowed isometries are the same in the presence of curved AdS_2 branes as with straight branes. We have already seen, though, that spectral flow is different. If w is even, spectral flow is still a symmetry of the curved brane, and we can apply it to (3.72) and (3.74) without incident. For example, spectral flow applied to (3.72) gives

$$t = (\alpha + w)\tau\,, \qquad \theta = (\alpha + w)\sigma + \theta_0\,, \qquad \rho = \rho_0\,. \tag{3.76}$$

If w is even, this solution describes a cylindrical worldsheet making $w/2$ (not w!) complete cycles around the center of AdS_3, and whose endpoints coincide with the endpoints of the original solution (3.72).

Applying an even amount of spectral flow to (3.74) gives a long string-like solution. Its properties are most easily seen by replacing $t \to t + w\tau$, $\theta \to \theta + w\sigma$ in the coordinate description (3.75). It begins in the infinite space-time past as a circular string of infinite radius with its endpoints coincident at $\theta = 0$. Next it collapses to finite radius. Its endpoints become separated in t and move in towards the center ($\theta = \pi/2$) of the brane. Finally, the string re-expands towards infinite radius, where its endpoints reconverge at $\theta = \pi$.

How shall we generate solutions with odd w? Our strategy will be different in the timelike and spacelike cases. The construction in the timelike case makes use of the discrete target space symmetry

$$\mathrm{PT} : g \to \omega_0 g \omega_0\,. \tag{3.77}$$

Calling this symmetry PT is justified by its action on the global coordinates,

$$t \to -t\,, \qquad \theta \to \pi - \theta\,, \tag{3.78}$$

which reveals it as the composition of a parity and a time-reversal transformation. The PT symmetry acts on the currents by

$$J_{R,L} \to \omega_0 J_{R,L} \omega_0\,, \tag{3.79}$$

and hence on their modes by

$$J^3_{R,L\,n} \to -J^3_{R,L\,n}\,, \qquad J^\pm_{R,L\,n} \to -J^\mp_{R,L\,n}\,. \tag{3.80}$$

These expressions make it clear that PT is an automorphism of the current algebra and a symmetry of the WZW model. Moreover, it preserves the gluing condition (3.63) and the Dirichlet condition (3.64).

The PT symmetry maps short strings of winding number w to short strings of winding number $-w-1$. To see this in a simple example, consider the closed string or straight brane timelike geodesic (3.40). Acting with w units of spectral flow gives the solution

$$t = (\alpha + w)\tau\,; \tag{3.81}$$

thus, without loss of generality, we may take $0 \le \alpha < 1$ in (3.40), and regard a solution $t = \alpha\tau$ with general α as the image of the solution with $0 \le \alpha < 1$ under a suitable amount of spectral flow. Now if we apply PT to (3.81), we get a solution with

$$t = -(\alpha + w)\tau = (\alpha' + (-w-1))\tau\,, \tag{3.82}$$

where $\alpha' = 1 - \alpha$ satisfies $0 \le \alpha' < 1$. By our previous logic, this is to be thought of as the image of (3.40) with parameter α' under $-w-1$ units of spectral flow.

Our course for finding short string solutions with odd w is now clear: we simply act with PT on a solution with $w = 0$ (*e.g.*, the image under an isometry of the basic timelike solution (3.72)) to reach the $w = -1$ sector, and then act on the result with $w+1$ units of spectral flow, which is a symmetry because $w+1$ is even. As an

example, if we implement this procedure on (3.72), we find the solution

$$t = (1 - \alpha + w)\tau\,, \qquad \theta = (1 - \alpha + w)\sigma + \pi - \theta_0\,, \qquad \rho = \rho_0\,. \tag{3.83}$$

Figure 3.6 shows a more complicated open short string solution with $w = 1$.

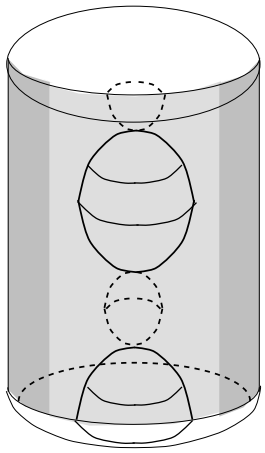

Figure 3.6: A classical open $w = 1$ short string solution.

This trick fails for long string solutions. An argument like the one given above demonstrates that PT maps long string solutions with winding number w to long strings with winding number $-w$, and therefore does not mix odd and even winding sectors. Instead, to construct spacelike solutions with odd w, we recall that spectral flow leaves fixed the $\sigma = 0$ endpoint of a string ending at $\psi = \psi_0$, but maps the $\sigma = \pi$ endpoint to $\psi = -\psi_0$. This prompts us to introduce a second AdS_2 brane located at $\psi = -\psi_0$. If we can find an unwound spacelike string with one endpoint on the brane at ψ_0 and the other endpoint on the brane at $-\psi_0$, then the action of spectral flow with odd w will produce a string with odd winding number, both of whose endpoints lie on the ψ_0 brane.

Given (3.74), it is relatively straightforward to find unwound spacelike strings stretching from the ψ_0 brane to the $-\psi_0$ brane. There are two distinct classes of solutions, depending on the value of α. Let $\beta = \sinh\psi_0/\sinh\frac{\pi}{2}\alpha$. For $|\beta| < 1$, we

have the solution

$$g = \begin{pmatrix} \sqrt{1-\beta^2}\, e^{\alpha\tau} & -\beta\, e^{\alpha(\sigma-\frac{\pi}{2})} \\ \beta\, e^{-\alpha(\sigma-\frac{\pi}{2})} & \sqrt{1-\beta^2}\, e^{-\alpha\tau} \end{pmatrix} . \tag{3.84}$$

For $|\beta| > 1$,

$$g = \begin{pmatrix} \sqrt{\beta^2-1}\, e^{\alpha\tau} & -\beta\, e^{\alpha(\sigma-\frac{\pi}{2})} \\ \beta\, e^{-\alpha(\sigma-\frac{\pi}{2})} & -\sqrt{\beta^2-1}\, e^{-\alpha\tau} \end{pmatrix} . \tag{3.85}$$

What do these solutions look like? The two branes meet at the two lines $\theta = 0$ and $\theta = \pi$ on the boundary $\rho = \infty$ of AdS_3. The solution with $|\beta| < 1$ describes a string that begins in the infinite worldsheet past at the point $t = 0$ on one of these lines ($\theta = \pi$ if β is positive), fills out a spacelike surface between the two branes, and contracts in the infinite worldsheet future to the point $t = 0$ on the other line. The solution with $|\beta| > 1$ describes a string that begins at a point on one of the lines ($\theta = \pi$ if β is positive), fills out a timelike surface between the two branes with minimum radius $\cosh^{-1}\beta$, and returns after an interval π of target space time to a point on the same line. The two cases are sketched in Figure 3.7. The solution in the borderline case $|\beta| = 1$,

$$g = \begin{pmatrix} 0 & -e^{\alpha(\sigma-\frac{\pi}{2})} \\ e^{-\alpha(\sigma-\frac{\pi}{2})} & 0 \end{pmatrix} , \tag{3.86}$$

stretches between the centers $\theta = \pi/2$ of the two branes at global time $t = \pi/2$.

Acting with an odd amount w of spectral flow on these strings gives long string solutions whose endpoints both lie on the brane at $\psi = \psi_0$. The image of (3.84) under spectral flow begins in the infinite space-time past as a string of infinite radius whose two endpoints lie on opposite edges of the brane. With increasing t, the string contracts until, at $t = 0$, the endpoints cross at the center $\theta = \pi/2$ of the brane. Afterwards, the string expands until $t = \infty$, when the endpoints again reach opposite edges of the brane. At $t = \infty$, each endpoint is at the edge opposite to the edge at

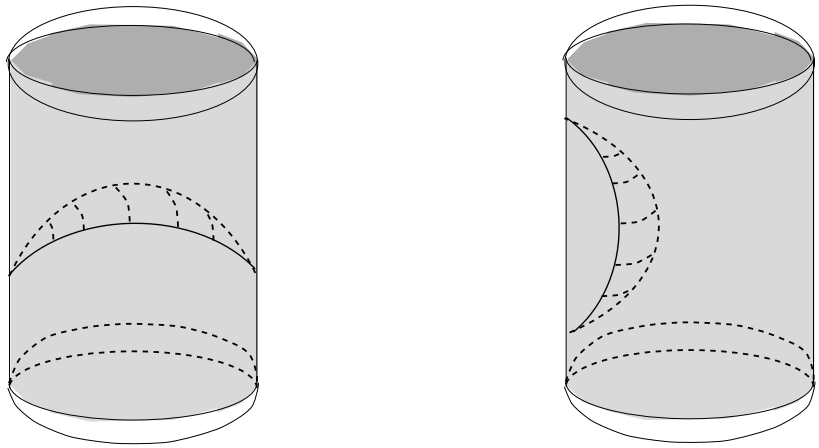

Figure 3.7: Strings stretched between the branes at $\psi = +\psi_0$ and $\psi = -\psi_0$, with (a) $|\beta| < 1$ and (b) $|\beta| > 1$.

which it began at $t = -\infty$. By contrast, in the flowed solution with $|\beta| > 1$, the endpoints do not have enough energy to reach the center of the AdS_2 brane, and return at $t = \infty$ to the edge at which they began. Figure 3.8 depicts the long strings.

To summarize, we have constructed classical solutions for open strings ending on a curved AdS_2 brane. We began with simple timelike and spacelike string solutions akin to the closed string and straight brane geodesics considered in Sections 3.3 and 3.4. Acting with the isometry group $SL(2, R)$ generated more unwound solutions. As in the straight brane case, spectral flow with even w gave us new winding solutions, but unlike the straight brane case, spectral flow with odd w was no longer a symmetry. Short string and long string solutions in odd winding sectors do exist, but to reach them, we required new techniques: target-space PT symmetry for short strings and the introduction of a brane at $\psi = -\psi_0$ for long strings.

3.5.2 The quantum Hilbert space

In Section 3.4.2 we described the structure of the Hilbert space of the $SL(2, R)$ WZW model in the presence of an AdS_2 brane at $\psi_0 = 0$. Now, drawing on what we have

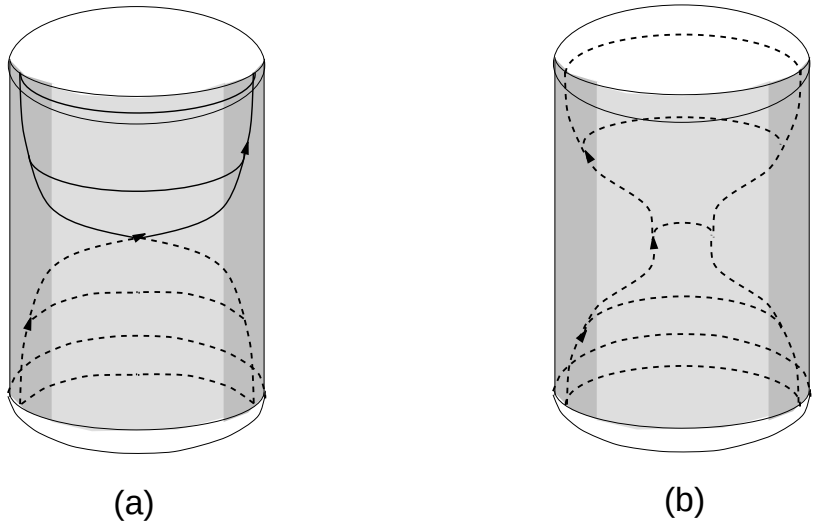

Figure 3.8: A long classical string solution corresponding to $w = 1$ sector for (a) $|\beta| < 1$ and (b) $|\beta| > 1$.

learned about classical open strings ending on curved branes, we sketch how the Hilbert space changes as ψ_0 is increased above zero.

The WZW model Hilbert space at $\psi_0 = 0$ contained discrete representations $\hat{\mathcal{D}}_j^{+,w}$, for $w \in \mathbf{Z}$ and $\frac{1}{2} < j < \frac{k-1}{2}$. We propose that all of these representations persist in the $\psi_0 > 0$ Hilbert space. "Discrete" is something of a misnomer in the context of the WZW model of (the universal cover of) $SL(2,R)$, since the discreteness of j is enforced only by the Virasoro constraints. At the level of the WZW model Hilbert space, before the Virasoro constraints are imposed, j is not quantized, and it is meaningful to speak of the density of states defined by a measure in j-space. In the presence of a curved brane at $\psi = \psi_0$, this measure depends on ψ_0. We conjecture that the ψ_0 dependence is the same in all winding sectors.

As in the straight brane case, the WZW model Hilbert space at nonzero ψ_0 contains continuous representations $\hat{\mathcal{C}}_{\frac{1}{2}+is}^{\alpha,w}$, for all $\alpha \in [0,1)$, $w \in \mathbf{Z}$, and $s \in \mathbf{R}$. Once again, the density of states of these representations now depends on ψ_0. We conjecture that the ψ_0 dependence is the same in all even winding sectors and in all odd winding sectors, but that the dependence in the even winding sectors is different from

the dependence in the odd winding sectors.

In support of our conjectures, we note first that, for all ψ_0, we were able to construct classical short string solutions for α satisfying $0 \leq \alpha < 1$, which is the semiclassical version of the range $\frac{1}{2} < j < \frac{k-1}{2}$. This, we observed, is unlike the situation in the $SU(2)$ WZW model, where the range of j for which classical solutions exist is bounded in terms of ψ_0. In the $SU(2)$ WZW model, the truncation of classical solutions as ψ_0 increased manifested itself in the quantum theory as a loss of representations in the Hilbert space. In the $SL(2,R)$ WZW model, there is no truncation classically, which leads us to believe that in the quantum theory, representations spanning the entire range of j are likewise present.[12] The measure in the space of j may depend on ψ_0, but this is the only possible ψ_0 dependence in the structure of the discrete sector of the Hilbert space.

Spectral flow by an even amount is a symmetry of the theory. It follows that the ψ_0 dependence of the density of representations must be the same in all even winding sectors and in all odd winding sectors. In addition, target space PT symmetry links even and odd winding short string sectors. Consequently, the ψ_0 dependence of the density of discrete representations must in fact be the same in all winding sectors.

The existence of classical long string solutions is strong evidence that the WZW model Hilbert space contains continuous representations. Spectral flow by an even amount is a symmetry of the long string solutions, but target space PT symmetry does not mix even and odd long string winding sectors. Therefore, the ψ_0 dependence of the density of states of the continuous representations is the same in all even winding sectors and in all odd winding sectors, but the dependence in the even sectors is, in general, different from the dependence in the odd sectors.

We will presently provide further evidence that this is so by studying a certain family of *physical* short string solutions in the even and odd winding sectors. We compute the energy E of these solutions as a function of their size R. In both the odd and even winding sectors, $E(R)$ increases monotonically at large R to a value whose functional form as a function of w is the same in all sectors. However, the

[12] A more computational argument in support of this claim is presented in Section 3.5.4.

dependence of E on R—and on ψ_0—is different in the two types of sectors. The existence of an upper bound for $E(R)$ in the short string sectors implies that, above this bound, a continuous representation appears. The ψ_0 dependence of $E(R)$ at large R is different for odd and even w. This implies that the ψ_0 dependence of the density of states of the emergent continuous representations is likewise different for odd and even w.

The short string solutions under consideration belong to the physical Hilbert space. To apply our conclusions to the WZW model Hilbert space, we reason *a fortiori*: since the (AdS_3 part of the) physical string Hilbert space is the WZW model Hilbert space after the imposition of the Virasoro constraints, if continuous representations exist in the physical Hilbert space, surely they must exist in the WZW model Hilbert space.

We now fill in the details of this argument. To construct the even winding solutions, we begin with the basic unwound timelike solution

$$t = \alpha\tau\,, \qquad \theta = \alpha\sigma + \theta_0\,, \qquad \rho = \rho_0\,, \tag{3.87}$$

with $0 \leq \alpha < 1$, $\theta_0 = \frac{\pi}{2}(1-\alpha)$, and

$$\sinh\rho_0 = \frac{\sinh\psi_0}{\cos\frac{\pi\alpha}{2}}\,. \tag{3.88}$$

We then act with the isometry given by $U = e^{\frac{1}{2}\rho_1\sigma_3}$ and $V = \omega_0 U^{-1}\omega_0 = U$, where ρ_1 is a constant. Finally, we perform an even amount w of spectral flow. The currents of the resulting solution are

$$J^3_R = \frac{k}{2}(\alpha\cosh\rho_1 + w)\,, \tag{3.89}$$

$$J^\pm_R = \pm\frac{ik}{2}(\alpha\sinh\rho_1\, e^{\mp iwx^+})\,, \tag{3.90}$$

and similarly for J^a_L.

To construct the odd winding solutions, we once again introduce a second AdS_2 brane at $\psi = -\psi_0$, and consider the unwound short string

$$t = \alpha\tau\,, \qquad \theta = \alpha\sigma + \theta_0\,, \qquad \rho = \rho_0\,, \tag{3.91}$$

with $0 \leq \alpha < 1$, $\theta_0 = \pi(1 - \frac{\alpha}{2})$, and

$$\sinh \rho_0 = \frac{\sinh \psi_0}{\sin \frac{\pi\alpha}{2}} \,. \tag{3.92}$$

This is a string stretching between the two branes. Again, we act with the isometry given by $U = e^{\frac{1}{2}\rho_1\sigma_3}$ and $V = \omega_0 U^{-1}\omega_0 = U$, and perform w units of spectral flow on the result. Since w now is odd, both endpoints of the resulting solution lie on the brane at $\psi = \psi_0$. The currents of this solution, too, are given by (3.89) and (3.90).

To obtain physical string solutions in $AdS_3 \times \mathcal{M}$, we must impose the Virasoro constraints $T^{AdS}_{\pm\pm} + h = 0$, where T^{AdS} is the energy-momentum tensor for the AdS_3 modes of the string, and h is the energy-momentum tensor for $\mathcal{M}$, which we regard as a conformal weight for the sigma model on $\mathcal{M}$. The energy-momentum tensor is calculable in terms of the currents (3.89) and (3.90), and the resulting Virasoro constraint expresses α in terms of h [37],

$$\alpha = \alpha_\pm = -w \cosh \rho_1 \pm \sqrt{w^2 \sinh^2 \rho_1 + \frac{4h}{k}} \,. \tag{3.93}$$

Choosing the branch $\alpha = \alpha_+$, the space-time energy takes the form

$$E = J^3_0 = \frac{k}{2}\left(\cosh \rho_1 \sqrt{\frac{4h}{k} + w^2 \sinh^2 \rho_1} - w \sinh^2 \rho_1\right) \,. \tag{3.94}$$

This expression is valid for both the even and odd winding solutions.

The last ingredient we need for our argument is a precise notion of the size of the string. We define R to be the maximum value of the coordinate $\rho(\sigma, \tau)$. By writing even and odd winding solutions in the matrix form (3.33), it is straightforward to calculate that, for both types of solutions,

$$\cosh R = \cosh \rho_0 \cosh \rho_1 \,. \tag{3.95}$$

In (3.94), we expressed the string energy as a function of ρ_1, the isometry parameter. We now work towards rewriting E as a function of R, in the large R limit.

As $\rho_1 \to \infty$, $\alpha = \alpha_+$ approaches 0 according to

$$\alpha = \frac{\frac{4h}{k} - w^2}{w\cosh\rho_1 + \sqrt{w^2\sinh^2\rho_1 + \frac{4h}{k}}} \sim \frac{1}{w}\left(\frac{4h}{k} - w^2\right)e^{-\rho_1}\,. \tag{3.96}$$

It follows from (3.92) that for odd w, in this limit,

$$\sinh\rho_0 = \frac{\sinh\psi_0}{\sin\frac{\pi\alpha}{2}} \sim \frac{\sinh\psi_0}{\frac{\pi\alpha}{2}} \sim \frac{2w\sinh\psi_0}{\pi(\frac{4h}{k} - w^2)}e^{\rho_1}\,, \tag{3.97}$$

and therefore

$$\cosh R = \cosh\rho_0\cosh\rho_1 \sim \frac{2w\sinh\psi_0}{\pi(\frac{4h}{k} - w^2)}e^{\rho_1}\cosh\rho_1\,, \tag{3.98}$$

so that

$$R \sim 2\rho_1 + \log\left(\frac{2w\sinh\psi_0}{\pi(\frac{4h}{k} - w^2)}\right)\,. \tag{3.99}$$

For even w, as $\rho_1 \to \infty$, $\rho_0 \to \psi_0$, and so

$$\cosh R \sim \cosh\psi_0\cosh\rho_1\,, \tag{3.100}$$

or

$$R \sim \rho_1 + \log\cosh\psi_0\,. \tag{3.101}$$

Substituting (3.99) and (3.101) into (3.94) allows us to determine E as a function of R. We find that, for odd w,

$$E(R) = \frac{4h + kw^2}{4w} - \frac{4h - kw^2}{2\pi kw^2}e^{-R}\sinh\psi_0\,, \tag{3.102}$$

while for even w,

$$E(R) = \frac{4h + kw^2}{4w} - \frac{(4h - kw^2)^2}{4kw^3}e^{-2R}\cosh^2\psi_0\,, \tag{3.103}$$

plus terms respectively of order e^{-4R} and e^{-2R} for even and odd w.

What we learn from this analysis is that, in both the odd and even winding sectors, $E(R)$ has an asymptote at $\frac{4h+kw^2}{4w}$. This asymptote signals the existence of continuous representations. Solutions with energies below the asymptote are bound states—short strings—trapped within a finite radius in AdS_3. By contrast, solutions

with energies above the asymptote are free to escape to the boundary of AdS_3. These are the long strings, which inhabit continuous representations. This interpretation is consistent with the fact that the energy of physical long strings with winding number w is bounded below, in the semiclassical limit of large h and large k, by $\frac{4h+kw^2}{4w}$, the asymptotic value of $E(R)$. We have thus shown that continuous representations of every w exist in the physical string Hilbert space; hence, *a fortiori* such representations exist in the WZW model Hilbert space.

We can take this argument one step further to confirm that the $\psi_0 > 0$ WZW model Hilbert space not only contains continuous representations of every w, but within each winding sector contains representations $\hat{\mathcal{C}}^{\alpha,w}_{j=\frac{1}{2}+is}$ of every s. The Virasoro constraint determines α in terms of s and h. Thus, if s were somehow quantized in the WZW model Hilbert space, the physical long string spectrum at fixed w and h would be quantized as well. As we have seen, though, the physical long string spectrum at fixed w and h is continuous. Thus s must not be quantized in the WZW model Hilbert space; representations with arbitrary $s \in \mathbf{R}$ must actually appear.

The approach of $E(R)$ to its asymptote is different as a function of R and ψ_0 in the even and odd winding sectors. This is consistent with our claim that the ψ_0 dependence of the density of states in the WZW model Hilbert space is different in the odd and even winding long string sectors. An additional piece of evidence for this point comes from an analysis in the spirit of [36] and Appendix D of the divergence structure of the one-loop Euclidean partition function. The divergences in question signal the presence of continuous representations; they originate in the infinite volume factors that appear when long strings are subject to a flat potential. Accordingly, it is sufficient to consider the contribution to the functional integral of the large ρ region. In global coordinates, the WZW action at large ρ takes the form

$$S \sim \int d^2z \left(\partial\rho\bar{\partial}\rho + \frac{1}{4}e^{2\rho}|\bar{\partial}(\theta - it)|^2 + \cdots \right) . \tag{3.104}$$

In the one-loop calculation, the worldsheet is taken to be cylindrical and of Euclidean signature; the target space time is likewise Euclidean. The worldsheet coor-

dinate $z = \sigma + i\tau$ is subject to the periodicity

$$\tau \sim \tau + 2\pi t_W \,, \tag{3.105}$$

with t_W the worldsheet modulus. At finite temperature, the target space coordinates t and θ describe a torus: θ is periodic by nature, and t is periodically identified with period equal to the inverse temperature β; that is,

$$\theta - it \sim \theta - it + 2\pi n + i\beta m \,, \tag{3.106}$$

where m and n are integers.

If ρ is assumed to be fixed at ρ_0, the equations of motion constrain $\theta - it$ to be a harmonic map from the worldsheet to the target space. The general harmonic map from the cylinder to the torus is of the form

$$\theta + it = w\sigma + ib\tau + \theta_0 \,, \tag{3.107}$$

where w, b, and θ_0 are real constants. Matching the periodicities (3.105) and (3.106) of the worldsheet and target space sets $b = \frac{\beta m}{2\pi t_W}$. The partition function thus receives contributions from harmonic maps of the form (3.107), for all integers m. As in Appendix D.2, it is sufficient for our purposes to concentrate on the $m = 1$ sector.

If it is to describe a legitimate open string configuration, the map (3.107) must satisfy the gluing conditions and the Dirichlet condition. A straightforward calculation shows that, in the presence of an AdS_2 brane at $\psi = \psi_0$, the gluing conditions are satisfied if one of two conditions holds:

1. $w = b = \dfrac{\beta}{2\pi t_W}$; or
2. $\theta_0 = 0$ or π, and w is an integer.

Suppose condition 2 is fulfilled. Then the Dirichlet condition $\sin\theta_0 \sinh\rho_0 = \sinh\psi_0$ can be satisfied only if $\psi_0 = 0$. In this case, there is a family of solutions of the form (3.107) with the desired properties, indexed by the continuous parameter ρ_0. The solutions (3.107) are holomorphic—that is, functions of $z = \sigma + i\tau$—if the worldsheet modulus takes the special value

$$t_W = \frac{\beta}{2\pi w} \,. \tag{3.108}$$

As explained in [36], the functional integral suffers a logarithmic divergence at this special value of t_W. The divergence is the hallmark of a continuous representation, whose density of states can be derived by properly regularizing the infinity. We have thus arrived again at a conclusion we reached in Section 3.4: the straight brane Hilbert space contains continuous representations for all values of the winding number.

If $\psi_0 \neq 0$, then harmonic maps satisfying the gluing conditions must fulfill condition 1. In this case, the Dirichlet condition reads

$$\sin\theta_0 \sinh\rho_0 = \sin(w\pi + \theta_0)\sinh\rho_0 = \sinh\psi_0\,. \tag{3.109}$$

If w is not an integer, (3.109) determines θ_0 and ρ_0 uniquely. If w is an odd integer, (3.109) has no solution. If w is an even integer, (3.109) collapses to the single condition $\sin\theta_0 \sinh\rho_0 = \sinh\psi_0$, which has a family of solutions indexed by a single continuous free parameter. Condition 1 trivially implies (3.108); thus the maps (3.107) are holomorphic. The functional integral thus has a divergence at $t_W = \frac{\beta}{2\pi w}$ if w is even, but this divergence is apparently absent if w is odd. Following the logic of the last paragraph, we conclude that the WZW model Hilbert space contains continuous representations in the even winding sectors. On the other hand, this line of reasoning tells us nothing about the odd winding continuous representations. Of course, we have already independently established that continuous representations exist in all winding sectors. This argument points to a difference in the mechanism for generating continuous representations in the even and odd winding sectors, illustrating our claim that the nature of the continuous representations at nonzero ψ_0—and in particular, their density of states—depends significantly on the parity of the winding number.

3.5.3 A two-brane system

An interesting perspective on the Hilbert space in the presence of a curved brane at $\psi = \psi_0$ is obtained by revisiting a device from Section 3.5.1: the introduction of a second brane at $\psi = -\psi_0$. Odd spectral flow maps an open string with both endpoints on the brane at $\psi = \psi_0$ to a string that begins at $\sigma = 0$ on the ψ_0 brane but ends at $\sigma = \pi$ on the $-\psi_0$ brane. The two-brane system thus preserves the full

spectral flow symmetry. The Hilbert space of the enlarged system has the structure

$$\mathcal{H} = \mathcal{H}_{++} \oplus \mathcal{H}_{+-} \oplus \mathcal{H}_{-+} \oplus \mathcal{H}_{--} \,, \tag{3.110}$$

where, for example, $\mathcal{H}_{+-}$ is the Hilbert space of open strings starting on the brane at $\psi = +\psi_0$ and ending on the brane at $\psi = -\psi_0$, and similarly for the other summands. Clearly $\mathcal{H}_{++} \cong \mathcal{H}_{--}$ and $\mathcal{H}_{+-} \cong \mathcal{H}_{-+}$.

Each summand can be further decomposed as the sum of discrete and continuous representations of $\widehat{SL}(2,R)$. As in the single-brane case, the symmetries of the system give clues about how the representations in various sectors of the theory are related. Spectral flow by an even amount is a symmetry of each summand individually, while spectral flow by an odd amount maps $\mathcal{H}_{++} \leftrightarrow \mathcal{H}_{+-}$ and $\mathcal{H}_{--} \leftrightarrow \mathcal{H}_{-+}$. For example, the action of spectral flow with $w = 1$ on the discrete representations of $\mathcal{H}_{++}$ and $\mathcal{H}_{+-}$ is given by

$$\begin{array}{ccccccccccc} \cdots & \hat{\mathcal{D}}^{+,-2}_{++,j} & & \hat{\mathcal{D}}^{+,-1}_{++,j} & & \hat{\mathcal{D}}^{+,0}_{++,j} & & \hat{\mathcal{D}}^{+,1}_{++,j} & & \hat{\mathcal{D}}^{+,2}_{++,j} & \cdots \\ & & \nearrow & & \nearrow & & \nearrow & & \nearrow & & \\ \cdots & \hat{\mathcal{D}}^{+,-2}_{+-,j} & & \hat{\mathcal{D}}^{+,-1}_{+-,j} & & \hat{\mathcal{D}}^{+,0}_{+-,j} & & \hat{\mathcal{D}}^{+,1}_{+-,j} & & \hat{\mathcal{D}}^{+,2}_{+-,j} & \cdots \end{array} \,. \tag{3.111}$$

Extending the reasoning of Section 3.5.2, we can deduce that the ψ_0 dependence of the density of discrete representations in the even (odd) winding sectors of $\mathcal{H}_{++}$ must be the same as the ψ_0 dependence of the density of representations in the odd (even) winding sectors of $\mathcal{H}_{+-}$. A similar statement holds for $\mathcal{H}_{--}$ and $\mathcal{H}_{-+}$, and for the density of states of continuous representations. Within each summand, target space PT symmetry mixes discrete representations with odd and even w, but preserves the parity of w of the continuous representations. We can hence argue further that the ψ_0 dependence of the density of discrete representations is the same for all winding sectors and all summands. By contrast, the ψ_0 dependence of the density of states in the continuous representations is different in the odd winding sectors and the even winding sectors in each summand, and the dependence in $\mathcal{H}_{++}$ is different from the dependence in $\mathcal{H}_{+-}$. One advantage of enlarging our system to include a second brane

is that the entire structure of the continuous sector of the single-brane Hilbert space is encoded in the representations $\hat{\mathcal{C}}^{\alpha,0}_{++,j}$, $\hat{\mathcal{C}}^{\alpha,0}_{+-,j}$ and their properties under spectral flow and the target space PT symmetry.

Just as in the $SU(2)$ WZW model, we may further generalize to a system of AdS_2 branes located at $\psi = \psi_1$ and $\psi = \psi_2$. The discussion is completely analogous to what has already been said. We begin by constructing basic unwound classical solutions stretching from one brane to the other, and employ spectral flow to generate the space of all classical solutions. The basic unwound timelike solutions are again

$$t = \alpha\tau\,, \qquad \theta = \alpha\sigma + \theta_0\,, \qquad \rho = \rho_0\,, \tag{3.112}$$

where $0 \leq \alpha < 1$, and θ_0 and ρ_0 are chosen so as to satisfy the appropriate Dirichlet conditions. The basic spacelike solution is given in matrix form as

$$g = \begin{pmatrix} (1+ab)\exp(\alpha\tau) & a\exp(\alpha\sigma) \\ b\exp(-\alpha\sigma) & \exp(-\alpha\tau) \end{pmatrix}, \tag{3.113}$$

where the integration constants a and b are likewise fixed to satisfy the Dirichlet boundary conditions.

Spectral flow by an even amount w is a symmetry of the system. Short string solutions in odd winding sectors may be constructed by means of the PT symmetry of the target space, as explained in Section 3.5.1. To construct long string solutions belonging to odd winding sectors, we introduce a third AdS_2 brane at $\psi = -\psi_2$, and follow the procedure described in Section 3.5.1 for finding solutions stretching between the ψ_1 and $-\psi_2$ branes. Spectral flow by an odd amount w then gives open string solutions stretching between the ψ_1 and ψ_2 branes.

Again, these classical constructions provide us with a reasonable conjecture for the quantum Hilbert space of the two-brane system: that it contains discrete representations $\hat{\mathcal{D}}^{+,w}_j$ for all integers w and j satisfying $\frac{1}{2} < j < \frac{k-1}{2}$, as well as continuous representations $\hat{\mathcal{C}}^{\alpha,w}_j$ for all integers w, all α in the range $0 \leq \alpha < 1$, and j of the form $j = \frac{1}{2} + is$ for all real s.

3.5.4 The NCOS limit

The WZW Model Action

In the limit $\psi_0 \to \infty$, the AdS_2 brane approaches the boundary of AdS_3. In this limit, the factor of $\cosh^2\psi$ in the metric (3.62) tends to suppress open string fluctuations along the AdS_2 brane. However, the induced electric field on the brane also grows exponentially with ψ_0, balancing the effect of the metric. In fact, as $\psi_0 \to \infty$, the electric field approaches its critial value, and the theory resembles the noncommutative open strings studied in [47, 48]. Let us now make this more precise.

We work in a target space of Euclidean signature. Our first task is to find a system of coordinates that is well adapted to our problem. In the Euclidean AdS_2 coordinates (ψ, ω, t), the AdS_3 metric is

$$ds^2 = d\psi^2 + \cosh^2\psi\,(\cosh^2\omega dt^2 + d\omega^2)\,, \tag{3.114}$$

and the invariant 2-form that describes the NS-NS background takes the form

$$\mathcal{F} = \left(\psi - \psi_0 + \frac{\sinh 2\psi}{2}\right)\cosh\omega\, d\omega \wedge dt\,. \tag{3.115}$$

It proves convenient to replace the AdS_2 coordinates (ω, t) by a complex coordinate γ, defined such that the AdS_2 brane worldvolume is covered by the upper half plane $\mathrm{Im}\gamma \geq 0$. The transformations are

$$\tanh\tau = \frac{|\gamma|^2 - 1}{|\gamma|^2 + 1}\,, \tag{3.116}$$

$$\sinh\omega = -\frac{\mathrm{Re}\,\gamma}{\mathrm{Im}\,\gamma}\,. \tag{3.117}$$

In these coordinates, the metric and 2-form become

$$ds^2 = d\psi^2 + \frac{\cosh^2\psi}{(\mathrm{Im}\,\gamma)^2} d\gamma d\bar{\gamma}\,, \tag{3.118}$$

$$\mathcal{F} = \frac{1}{2}\left(\psi - \psi_0 + \frac{\sinh 2\psi}{2}\right)\frac{d\gamma \wedge d\bar{\gamma}}{(\mathrm{Im}\,\gamma)^2}\,. \tag{3.119}$$

Given these expressions for the metric and the 2-form, the WZW model Lagrangian takes the form

$$\mathcal{L} = \frac{k}{2\pi}\left[2\partial\psi\bar{\partial}\psi + \frac{\cosh^2\psi}{(\mathrm{Im}\,\gamma)^2}\left(\partial\gamma\bar{\partial}\bar{\gamma} + \bar{\partial}\gamma\partial\bar{\gamma}\right) - \left(\psi - \psi_0 + \frac{\sinh 2\psi}{2}\right)\frac{1}{(\mathrm{Im}\,\gamma)^2}(\partial\gamma\bar{\partial}\bar{\gamma} - \bar{\partial}\gamma\partial\bar{\gamma})\right]. \tag{3.120}$$

The worldsheet coordinates are $(z, \bar{z})$, and range over the upper half plane; the worldsheet metric is Euclidean; and the area element is $d^2z \equiv dz\, d\bar{z}$.

To take the limit $\psi_0 \to \infty$, we first redefine $\psi \to \psi - \psi_0$; the new coordinate ψ measures deviations from the brane at ψ_0. The Lagrangian for large ψ_0 is then

$$\mathcal{L} = \frac{k}{\pi}\,\partial\psi\bar{\partial}\psi + \frac{k}{2\pi(\mathrm{Im}\,\gamma)^2}\left[\frac{e^{2(\psi+\psi_0)}}{2}(\bar{\partial}\gamma\partial\bar{\gamma}) + \frac{1}{2}(\partial\gamma\bar{\partial}\bar{\gamma} + \bar{\partial}\gamma\partial\bar{\gamma}) - \psi(\partial\gamma\bar{\partial}\bar{\gamma} - \bar{\partial}\gamma\partial\bar{\gamma})\right]. \tag{3.121}$$

It is useful to introduce Lagrange multipliers β and $\bar{\beta}$, giving

$$\mathcal{L} = \frac{k}{2\pi}\left[2\,\partial\psi\bar{\partial}\psi + \beta\bar{\partial}\gamma + \bar{\beta}\partial\bar{\gamma} - \frac{2(\mathrm{Im}\,\gamma)^2}{e^{2(\psi+\psi_0)}+2}\beta\bar{\beta} + \frac{1}{(\mathrm{Im}\,\gamma)^2}\left(\left(\frac{1}{2} - \psi\right)(\partial\gamma\bar{\partial}\bar{\gamma} - \bar{\partial}\gamma\partial\bar{\gamma})\right)\right]. \tag{3.122}$$

We now redefine $\psi \to \psi/2$ and take the limit $\psi_0 \to \infty$, with the result

$$S = \frac{k}{2\pi}\int d^2z\left(\frac{1}{2}\partial\psi\bar{\partial}\psi + \beta\bar{\partial}\gamma + \bar{\beta}\partial\bar{\gamma} + 2\frac{\psi - 1}{(\gamma - \bar{\gamma})^2}\left(\partial\gamma\bar{\partial}\bar{\gamma} - \bar{\partial}\gamma\partial\bar{\gamma}\right)\right). \tag{3.123}$$

The action (3.123) resembles the action of noncommutative open strings in flat space. The only differences are that the metric in the $(\gamma, \bar{\gamma})$ plane is that of AdS_2, and that there is a coupling to the extra scalar field ψ, which obeys the Dirichlet condition $\psi = 0$ on the boundary.

The Spectrum

Our next goal is to evaluate the Euclidean one-loop thermal partition function exactly and read off the physical string spectrum. As in Appendix D, the partition function may be written as a sum over a complete set of classical solutions and fluctuations about these solutions. Solving the WZW model equations of motion produces classical solutions, given as functions of $(\psi, \gamma, \bar{\gamma})$; the fluctuations about these solutions can then be evaluated by the method of iterative Gaussians [54]. From the resulting

expression for the partition function, we can determine which $\widehat{SL}(2,R)$ representations appear in the WZW model spectrum, as discussed in Appendix D. The result is somewhat unsettling: we find that the Hilbert space contains only the discrete representation $\hat{\mathcal{D}}_j^{w=0}$, for $\frac{1}{2} < j < \frac{k-1}{2}$.

This is clearly wrong: the existence of sectors of the Hilbert space with $w \neq 0$ is guaranteed by the spectral flow symmetry. We understand their absence from the partition function calculation to mean that our set of classical solutions was incomplete. In particular, there seem to be solutions—short and long wound strings—that are not easily expressible in the $(\psi, \gamma, \bar{\gamma})$ coordinates. It would be desirable to find all of the classical solutions and perform a complete computation of the one-loop free energy. Nevertheless, our computation captures part of the physical spectrum. Most important, our result implies that the spectrum contains discrete representations with $\frac{1}{2} < j < \frac{k-1}{2}$, which is a significant fact that cannot be seen at the semiclassical level. These bounds on j are the same as the bounds that come out of the $\psi_0 = 0$ partition function calculation described in Appendix D. This strongly suggests that, for all ψ_0, the spectrum contains discrete representations obeying $\frac{1}{2} < j < \frac{k-1}{2}$.

The one-loop worldsheet is the semi-annulus in the upper half z-plane defined by the identification $z \sim ze^{2\pi t}$, where t is a worldsheet modulus. At finite temperature T, the AdS_3 time coordinate is made periodic with period $1/T$; in the coordinates we are using, this is accomplished by identifying $\gamma \sim \gamma e^{1/T}$. In order that the Lagrangian be single-valued, we must also identify $\beta \sim \beta e^{-1/T}$. These identifications mandate the relations

$$\gamma(ze^{2\pi t}) = e^{n/T}\gamma(z)\,, \qquad \beta(ze^{2\pi t}) = e^{-n/T}\gamma(z)\,, \tag{3.124}$$

for some integer n.

We begin by finding classical solutions for γ and ψ. The equation of motion for β is $\bar{\partial}\gamma = 0$. Classical solutions are of the form

$$\gamma_{cl}(z) = re^{i\theta} z^{\frac{n}{2\pi t T}}\,, \tag{3.125}$$

where $re^{i\theta}$ is a complex constant. The range of the coordinate γ is $\mathrm{Im}\,\gamma \geq 0$. This

necessitates

$$t \geq \frac{|n|}{2\pi T}\,, \tag{3.126}$$

and also determines θ in a manner detailed below.

Let us now expand about the classical solutions, defining fields Γ and B by

$$\gamma = \gamma_{cl}(1+\Gamma)\,, \qquad \beta = \frac{B}{\gamma_{cl}}\,. \tag{3.127}$$

The partition function then involves functional integrals over B and Γ. The $SL(2,R)$-invariant functional measure for these fields is

$$\mathcal{D}\left(\frac{e^{\psi/2}\gamma_{cl}}{2\,\mathrm{Im}\,\gamma_{cl}}\Gamma\right)\mathcal{D}\left(\frac{2e^{-\psi/2}\,\mathrm{Im}\,\gamma_{cl}}{\gamma_{cl}}B\right)\mathcal{D}\left(\frac{e^{\psi/2}\bar{\gamma}_{cl}}{2\,\mathrm{Im}\,\gamma_{cl}}\bar{\Gamma}\right)\mathcal{D}\left(\frac{2e^{-\psi/2}\,\mathrm{Im}\,\gamma_{cl}}{\bar{\gamma}_{cl}}\bar{B}\right)\,. \tag{3.128}$$

Classically, this is equivalent to $\mathcal{D}\Gamma\,\mathcal{D}B\,\mathcal{D}\bar{\Gamma}\,\mathcal{D}\bar{B}$, but quantum mechanically, a chiral anomaly is present, which effectively shifts the Lagrangian by

$$\frac{-2}{\pi}\left[\partial\log\left(\frac{e^{\psi/2}\gamma_{cl}}{2\,\mathrm{Im}\,\gamma_{cl}}\right)\bar{\partial}\log\left(\frac{e^{\psi/2}\bar{\gamma}_{cl}}{2\,\mathrm{Im}\,\bar{\gamma}_{cl}}\right)\right]\,. \tag{3.129}$$

When this term is expanded out and added to (3.123), the result is

$$\mathcal{L} = \frac{k-2}{2\pi}\left(\frac{1}{2}\partial\psi\bar{\partial}\psi + 2\frac{\psi-1}{(\gamma_{cl}-\bar{\gamma}_{cl})^2}\partial\gamma_{cl}\bar{\partial}\bar{\gamma}_{cl}\right) + \frac{k}{2\pi}\left(B\bar{\partial}\Gamma + \bar{B}\partial\bar{\Gamma}\right) + F(\Gamma,\partial\Gamma,\bar{\Gamma},\bar{\partial}\bar{\Gamma})\,, \tag{3.130}$$

where F contains terms from the Taylor expansion of the last term in (3.123). As these terms make no contribution to the partition function, we drop them in what follows. The effect of the chiral anomaly is therefore to shift the prefactor k of the terms in ψ to $k-2$.

Next we separate ψ into its classical and fluctuating parts, defining a new field ϕ by $\psi = \psi_{cl} + \phi$, where ψ_{cl} satisfies the equation of motion

$$\partial\bar{\partial}\psi_{cl} = \frac{2\partial\gamma_{cl}\bar{\partial}\bar{\gamma}_{cl}}{(\gamma_{cl}-\bar{\gamma}_{cl})^2} \tag{3.131}$$

derived from (3.130). One solution is

$$\psi_{cl} = 2\log\mathrm{Im}\,\gamma_{cl} + f(z) + \bar{f}(\bar{z})\,, \tag{3.132}$$

where f is an arbitrary holomorphic function. We can use the freedom of the choice of f to ensure that ψ_{cl} be single-valued and satisfy its Dirichlet boundary condition. Thus we may take

$$\psi_{cl} = \log\left[\frac{\operatorname{Im}\gamma_{cl}}{|\gamma_{cl}|}\right]^2 + c\,, \tag{3.133}$$

where the constant c is adjusted so that $\psi_{cl} = 0$ when $\operatorname{Im} z = 0$. Substituting in the form of γ_{cl} and letting $z = x \in \mathbf{R}^+$, we must have $c = -2\log(\sin\theta)$. Letting $z = -x$, we must have $c = -2\log(\sin(\frac{n}{2Tt} + \theta))$. Consistency then requires $|\sin\theta| = |\sin(\frac{n}{2Tt} + \theta)|$, which is satisfied (for $n \neq 0$) if

$$\theta = \frac{\pi}{2}\left(m - \frac{n}{2\pi Tt}\right)\,, \tag{3.134}$$

for some integer m. Since $\gamma_{cl}(z)$ is constrained to lie in the upper half plane as z ranges over the worldsheet semi-annulus in the upper half z-plane, we must have $0 \leq \arg(\gamma_{cl}(z)) = \theta + \frac{n}{2\pi Tt}\arg(z) \leq \pi$, whenever $0 \leq \arg(z) \leq \pi$. This is possible only if $m = 1$. Thus $\theta = \frac{\pi}{2}(1 - \frac{n}{2\pi Tt})$. In summary, our classical solutions have the form

$$\gamma_{cl} = re^{i\frac{\pi}{2}\left(1-\frac{n}{2\pi Tt}\right)} z^{\frac{n}{2\pi Tt}}\,, \tag{3.135}$$

$$\psi_{cl} = 2\log\left|\frac{\operatorname{Im}\gamma_{cl}}{\gamma_{cl}\cos(\frac{n}{4Tt})}\right|, \tag{3.136}$$

where $t > \frac{|n|}{2\pi T}$ and $r > 0$.

Integration by parts brings the action into the form

$$S = \int d^2z\left[\frac{k-2}{4\pi}\left(\partial\phi\bar\partial\phi + (\psi_{cl} - 2)\partial\bar\partial\psi_{cl}\right) + \frac{k}{2\pi}\left(B\bar\partial\Gamma + \bar B\partial\bar\Gamma\right)\right]. \tag{3.137}$$

The term involving ψ_{cl} can be easily integrated over the worldsheet semi-annulus, giving $(k-2)n^2/8\pi T^2 t$.

Now we evaluate the Euclidean partition function. The partition function breaks up as a sum $\mathcal{Z} = \sum_n \mathcal{Z}_n$ over sectors indexed by the integer n that appears in the classical solutions (3.135) and (3.136). Each $\mathcal{Z}_n$ contains an integral $\int_{|n|/2\pi T}^{\infty} \frac{dt}{t}$ over the worldsheet modulus t; the range of integration is set by (3.126). There is also an integral over the modulus r, but this contributes only a numerical factor. Finally,

we must perform the functional integrals over ϕ, B, Γ, the worldsheet ghosts, and the internal conformal field theory. Upon taking careful account of the boundary conditions for B and Γ, we find that the functional integral of the (B,Γ) system is exactly canceled by the functional determinant coming from the worldsheet ghosts. The remaining functional integral is over the free bosonic field ϕ, which obeys the Dirichlet boundary condition $\phi = 0$. This is a standard functional determinant; the result is $1/|\eta(it)|$. Assembling all the pieces together, we have

$$\mathcal{Z}_n \sim \int_{|n|/2\pi T}^{\infty} \frac{dt}{t} \frac{1}{|\eta(it)|} \exp\left(-\frac{(k-2)n^2}{8\pi T^2 t}\right) q^{h-\frac{c_{int}}{24}} D(h)\,, \tag{3.138}$$

where $q = e^{-2\pi t}$, h indexes the weight in the internal conformal field theory, $D(h)$ is the degeneracy at weight h, and c_{int} is the central charge of the internal conformal field theory.

As in [36] and Appendix D, it is sufficient for our purposes to look at the $n = 1$ sector. The central charges $c_{SL(2,R)}$ of the $SL(2,R)$ conformal field theory and c_{int} of the internal conformal field theory must sum to 26; since $c_{SL(2,R)} = 3 + \frac{6}{k-2}$, we have $c_{int} = 23 - \frac{6}{k-2}$. Substituting this expression into (3.138), and expanding the factors in $1/\eta(it) = e^{2\pi t/24}/\prod_{m=1}^{\infty}(1-e^{-2\pi t m})$ as geometric sums, we may rewrite the integrand as a sum of terms containing exponentials of the form

$$\exp\left(-2\pi t(h+N-1) - \frac{k-2}{8\pi T^2 t} - \frac{\pi t}{2(k-2)}\right)\,, \tag{3.139}$$

where N is an non-negative integer. The dominant contibution to the partition function comes from the saddle point of the exponent,

$$t_s = \frac{k-2}{2\pi T\sqrt{1+4(k-2)(N+h-1)}}\,. \tag{3.140}$$

The lower bound of the t integral forces

$$\frac{1}{2\pi T} < t_s < \infty\,, \tag{3.141}$$

which translates into the bounds

$$0 < N + h - 1 + \frac{1}{4(k-2)} < \frac{k}{4} - \frac{1}{2}\,. \tag{3.142}$$

This is identical to the inequality (79) of [37], with $w = 0$. It was shown in [37] that (3.142) is equivalent to the bounds $\frac{1}{2} < j < \frac{k-1}{2}$ on the $SL(2,R)$ spin. By a chain of reasoning reviewed in Appendix D in the context of the corresponding straight brane calculation, we may conclude that the physical open string spectrum at $\psi_0 = \infty$ contains the unwound discrete representation $\hat{\mathcal{D}}_j^{+,w=0}$, for all j obeying $\frac{1}{2} < j < \frac{k-1}{2}$.

As we remarked above, the appearance of the bounds $\frac{1}{2} < j < \frac{k-1}{2}$ at $\psi_0 = 0$ and at $\psi_0 = \infty$ gives us cause to believe that the same bounds hold for all ψ_0. Nonetheless, this calculation is manifestly incomplete, since it misses the winding sectors. Presumably this is because our choice of coordinates is well suited to describing only a limited subset of the classical solutions. It would be interesting to find the remaining solutions and complete the calculation of the partition sum.

3.6 Discussion

We have studied the spectrum of open strings ending on AdS_2 branes in AdS_3 in an NS-NS background. Perturbative open string theory on an AdS_2 brane is described by the $SL(2,R)$ WZW model, subject to the boundary conditions (3.63) and (3.64), which state that the worldsheet ends on the AdS_2 brane and satisfies Neumann boundary conditions in the directions parallel to the brane. The condition (3.63) also guarantees that the boundary condition preserves one copy of the $SL(2,R)$ current algebra.

Our study of the open string spectrum has been modeled on the treatment of closed strings in AdS_3 in [37]. The basic idea is to begin by studying classical solutions of the WZW model, beginning with the simplest solutions and building up more complicated ones by isometries and spectral flow, and, having compiled a complete catalogue of the classical solutions, to conjecture the form of the quantum Hilbert space. It was shown in [36] that this method leads to a correct proposal for the closed string WZW model Hilbert space.

We have applied this approach to open strings ending on AdS_2 branes. As a warm-up and a useful point of comparison, we first looked at S^2 branes in the $SU(2)$

WZW model. It was known from conformal field theoretic analysis [41] that the Hilbert space of open strings stretched between two S^2 branes at $\psi_0 = \pi n_1/k$ and $\psi_0 = \pi n_2/k$ is the sum of irreducible highest-weight representations of $\widehat{SU}(2)$, whose spin j is bounded as in (3.30). Our analysis of classical string worldsheets precisely reproduced this inequality. The only property of the quantum Hilbert space that could not be seen from our classical analysis was the quantization condition

$$2j + n_1 + n_2 + k \equiv 0 \bmod 2\,. \tag{3.143}$$

We next considered strings ending on AdS_2 branes in AdS_3. We began in Section 3.4 by studying the straight brane located at $\psi_0 = 0$. Analysis of classical solutions led us to conjecture that the Hilbert space of the WZW model in the open string sector is the holomorphic square-root of the closed string Hilbert space. In particular, the spectrum contains both short strings and long strings, and is invariant under spectral flow. We proved this conjecture in Appendix D by exactly evaluating the one-loop open string free energy, as in [36].

The situation of the brane with $\psi_0 > 0$ is more interesting. The boundary condition (3.64) preserves only spectral flow with even w, so it was reasonable to expect differences in the ψ_0 dependence of the spectra in the even and odd winding sectors. We found both short and long classical string solutions in all winding sectors, but also an important difference between the short and long strings. Short string solutions with different winding numbers can be mapped to one another, even when the difference in their winding numbers is odd, by combining spectral flow by an even amount and a PT transformation of the target space. Since both even spectral flow and the PT transformation are symmetries of the full quantum theory, we argued that the ψ_0 dependence of the density of states of the short string solutions must be the same in all winding sectors.

On the other hand, we showed that the ψ_0 dependence of the density of states of long string solutions is different in the odd and even winding sectors. We saw this difference explicitly by computing the energy of odd and even winding *short* strings as a function of the string size. In both cases, the energy rose to an asymptote, signaling

the presence of a continuum above the asymptotic value. The rate of approach to the asymptote differed, though, in the odd and even winding sectors. Further evidence for the different behavior of long strings with odd and even winding number came from an analysis of the divergence structure of the Euclidean partition function.

In the limit $\psi_0 \to \infty$, the induced electric field on the worldvolume of the AdS_2 brane reaches its critical value, producing noncommutative open string theory on AdS_2. In Section 3.5.4, we calculated the worldsheet action for open strings in this limit, and obtained a result similar to that of [55] for noncommutative open strings in flat space [47, 48]. We carried out a partial computation of the one-loop free energy in this limit, using the method of quadratures, as in [54].

Our work has focused exclusively on AdS_2 branes, which preserve one copy of the $SL(2,R)$ current algebra. There are other branes in AdS_3, some of which break the current algebra symmetry entirely [56]. It would be interesting to analyze the open string theory of these branes, as well.

Chapter 4

Boundary States of AdS_2 Branes in AdS_3

4.1 Introduction

In this chapter, we study AdS_2 branes embedded in AdS_3 [57, 52, 58] in the closed string sector by constructing their boundary states. In the previous chapter, the spectrum of the open string ending on the AdS_2 brane was shown to be exactly equal to the holomorphic square root of the spectrum of closed strings in AdS_3 when the brane carries no fundamental string charge. It contains short and long strings, and is invariant under spectral flow. When the brane carries fundamental string charge, we were not able to derive an exact spectrum although we found some qualitative features of the spectrum using semi-classical analysis. One of the purposese of this chapter is to derive an exact open string spectrum in the general case where the D-branes can carry nonzero fundamental string charge and become curved.

A boundary state [59, 60] is a useful concept in studying D-branes. Although the construction in [60] assumes rationality of conformal field theory, it was shown in [61, 62, 63, 64] that the idea can be applied to the non-rational case of the Liouville field theory. More recently the technique developed in the Liouville theory is applied to the AdS_2 branes [66, 67]. In this chapter, we will closely follow the construction in these papers. We will, however, make a different ansatz about one point functions of

closed string operators in a disk worldsheet, which leads to different expressions for the boundary states. We show that the semi-classical limits of these new boundary states reproduce the geometric configurations of the AdS_2 branes.

Given a pair of boundary states, it is straightforward to compute a partition function on an annulus worldsheet. This gives the spectrum of the conformal field theory on a strip where the boundary conditions on the two sides of the strip are specified by the choice of the boundary states. We can also compute an annulus partition function when the target space Euclidean time is periodically identified, adopting a method suggested in [68] . An integral of this partition function over the moduli space of worldsheet then gives the one loop free energy at finite temperature. From this, we can read off the physical spectrum of the open string on the AdS_2 brane. We find that the result agrees with the exact computation in the previous chapter (see [53]) when the brane carries no fundamental string charge.

4.2 One point functions on a disk

The boundary state can be found by computing the one point functions of closed string operators on a disk worldsheet. Here we will derive them for the AdS_2 brane, following the approach in [66, 67].

4.2.1 Review of closed string in AdS_3

In this chapter, we will mostly work in Euclidean AdS_3, which is the three-dimensional hyperbolic space H_3^+ given by one of the two branches of

$$(X^0)^2 - (X^1)^2 - (X^2)^2 - (X_E^3)^2 = R^2, \tag{4.1}$$

embedded in $\mathbf{R}^{1,3}$ with the metric

$$ds^2 = -(dX^0)^2 + (dX^1)^2 + (dX^2)^2 + (dX_E^3)^2, \tag{4.2}$$

where R is the curvature radius of H_3^+. It is related to AdS_3 with the Lorentzian signature metric by the analytic continuation $X^3 \to X_E^3 = -iX^3$. The Euclidean

AdS_3 can also be realized as a right-coset space $SL(2,C)/SU(2)$. Accordingly, the conformal field theory is the $SL(2,C)/SU(2)$ coset model. In the semi-classical approximation, which is applicable when the level $k \sim R^2/\alpha'$ of the $SL(2,C)$ current algebra is large, states in the theory are given by normalizable functions on the target space. The space of such states is decomposed into a sum of principal continuous representations of $SL(2,C)$ with $j = \frac{1}{2} + is$ ($s \in \mathbf{R}_+$). It was shown in [54] that the exact Hilbert space of the coset model at finite value of k consist of the standard representations of $SL(2,C)$ current algebra whose lowest energy states are given by principal continuous representations [54].

Let us introduce a convenient coordinate system (ϕ, γ, $\bar{\gamma}$) on H_3^+. They are related to the embedding coordinates (X^0, X^1, X^2, X_E^3) in (4.1) in the following way:

$$\phi = \log\left(X^0 + X_E^3\right)/R, \tag{4.3}$$

$$\gamma = \frac{X^2 + iX^1}{X^0 + X_E^3},$$

$$\bar{\gamma} = \frac{X^2 - iX^1}{X^0 + X_E^3}.$$

A point in the coset $SL(2,C)/SU(2)$ has its representative as a Hermitian matrix:

$$\begin{pmatrix} \gamma\bar{\gamma}e^{\phi} + e^{-\phi} & -\gamma e^{\phi} \\ -\bar{\gamma}e^{\phi} & e^{\phi} \end{pmatrix}, \tag{4.4}$$

and the metric can be written as

$$ds^2 = R^2\left(d\phi^2 + e^{2\phi}d\gamma d\bar{\gamma}\right). \tag{4.5}$$

In this theory, there exists an important set of primary fields defined by

$$\Phi_j(x,\bar{x};z,\bar{z}) = \frac{1-2j}{\pi}(e^{-\phi} + |\gamma - x|^2 e^{\phi})^{-2j}. \tag{4.6}$$

The labels $x, \bar{x}$ are introduced to keep track of the $SL(2,C)$ quantum numbers.[1] The

[1] In the string theory interpretation discussed in section 3, $(x,\bar{x})$ is identified as the location of the operator in the dual CFT on S^2 on the boundary of H_3^+.

$SL(2,C)$ currents act on it as

$$J^a(z)\Phi_j(x,\bar{x};w,\bar{w}) \sim -\frac{D^a}{z-w}\Phi_j(x,\bar{x};w,\bar{w})\,, \qquad a=\pm\,,3\,, \tag{4.7}$$

where D^a are differential operators with respect to x defined as

$$D^+ = \frac{\partial}{\partial x}, \qquad D^3 = x\frac{\partial}{\partial x} + j, \qquad D^- = x^2\frac{\partial}{\partial x} + 2jx. \tag{4.8}$$

The energy momentum tensor is given by the Sugawara construction, and the world-sheet conformal weights of this operator is

$$\Delta_j = -\frac{j(j-1)}{k-2}. \tag{4.9}$$

When $j = \frac{1}{2} + is$ with $s \in \mathbf{R}$, the operators (4.6) correspond to the normalizable states in the coset model. The operators with the $SL(2,C)$ spin j and $(1-j)$ are not independent but are related to each other by the following reflection symmetry relation,

$$\Phi_j(x,\bar{x};z,\bar{z}) = \mathcal{R}(j)\frac{2j-1}{\pi}\int d^2x'|x-x'|^{-4j}\Phi_{1-j}(x',\bar{x}';z,\bar{z}), \tag{4.10}$$

where

$$\mathcal{R}(j) = \nu^{1-2j}\frac{\Gamma\left(1-\frac{2j-1}{k-2}\right)}{\Gamma\left(1+\frac{2j-1}{k-2}\right)}. \tag{4.11}$$

The two and three point functions of these operators have been computed in [71, 72, 73]. The two point function has the form,

$$\begin{aligned}&\langle\Phi_j(x_1,\bar{x}_1;z_1,\bar{z}_1)\Phi_{j'}(x_2,\bar{x}_2;z_2,\bar{z}_2)\rangle \\ &= \frac{1}{|z_{12}|^{4\Delta_j}}\left[\delta^2(x_1-x_2)\delta(j+j'-1) + \frac{B(j)}{|x_{12}|^{4j}}\delta(j-j')\right].\end{aligned} \tag{4.12}$$

The coefficient $B(j)$ is given by

$$B(j) = \frac{k-2}{\pi}\frac{\nu^{1-2j}}{\gamma\left(\frac{2j-1}{k-2}\right)}, \tag{4.13}$$

where

$$\gamma(x) = \frac{\Gamma(x)}{\Gamma(1-x)}. \tag{4.14}$$

The choice of ν will not play an important role in the discussion of this chapter, except for its behavior in the semi-classical limit

$$\nu \to \pi \quad (k \to \infty). \tag{4.15}$$

It can be deduced by comparing (4.10) with its classical counterpart [65]. In [72], it is set to be

$$\nu = \pi \frac{\Gamma\left(1 - \frac{1}{k-2}\right)}{\Gamma\left(1 + \frac{1}{k-2}\right)}, \tag{4.16}$$

by requiring a certain consistency between the two and three point functions.

The three point function is expressed as

$$\begin{aligned}
&\langle \Phi_{j_1}(x_1, \bar{x}_1; z_1, \bar{z}_1) \Phi_{j_2}(x_2, \bar{x}_2; z_2, \bar{z}_2) \Phi_{j_3}(x_3, \bar{x}_3; z_3, \bar{z}_3) \rangle = \\
&= C(j_1, j_2, j_3) \frac{1}{|z_{12}|^{2(\Delta_1+\Delta_2-\Delta_3)} |z_{23}|^{2(\Delta_2+\Delta_3-\Delta_1)} |z_{31}|^{2(\Delta_3+\Delta_1-\Delta_2)}} \times \\
&\frac{1}{|x_{12}|^{2(j_1+j_2-j_3)} |x_{23}|^{2(j_2+j_3-j_1)} |x_{31}|^{2(j_3+j_1-j_2)}},
\end{aligned} \tag{4.17}$$

with the coefficient $C(j_1, j_2, j_3)$ given by

$$C(j_1, j_2, j_3) = -\frac{G(1-j_1-j_2-j_3) G(j_3-j_1-j_2) G(j_2-j_3-j_1) G(j_1-j_2-j_3)}{2\pi^2 \nu^{j_1+j_2+j_3-1} \gamma\left(\frac{k-1}{k-2}\right) G(-1) G(1-2j_1) G(1-2j_2) G(1-2j_3)} \tag{4.18}$$

where

$$G(j) = (k-2)^{\frac{j(k-1-j)}{2(k-2)}} \Gamma_2(-j \mid 1,\ k-2) \Gamma_2(k-1+j \mid 1,\ k-2). \tag{4.19}$$

and $\Gamma_2(x|1,\omega)$ is the Barnes double Gamma function defined by

$$\begin{aligned}
&\log\left(\Gamma_2(x|1,\omega)\right) \\
&= \lim_{\epsilon \to 0} \frac{\partial}{\partial \epsilon} \left[\sum_{n,m=0}^{\infty} (x+n+m\omega)^{-\epsilon} - \sum_{\substack{n,m=0 \\ (n,m) \neq (0,0)}} (n+m\omega)^{-\epsilon} \right].
\end{aligned} \tag{4.20}$$

4.2.2 Constraints on one-point functions

In this subsection, we will derive functional equations satisfied by one-point functions of closed string operators on a disk with boundary conditions corresponding to AdS_2 branes. We will follow the discussion in [66, 67] closely, except that we use a more general ansatz for the one-point function as we will explain in the next paragraph. Given the one-point functions, we can find boundary states $|B\rangle\rangle$ for the AdS_2 branes. According to [57, 52, 58], AdS_2 branes preserve one half of the current algebra symmetry because of the boundary condition on the currents,

$$J^a(z) = \bar{J}^a(\bar{z}); \quad \text{at } z = \bar{z}, \quad a = 3, +, -. \tag{4.21}$$

In the closed string channel, it is translated into the condition on the boundary states as

$$(J^a_n + \bar{J}^a_{-n})|B\rangle\rangle = 0, \quad a = 3, +, -, \;\; n \in \mathbf{Z}. \tag{4.22}$$

We start with the ansatz that the one-point function is of the form

$$\langle \Phi_j(x, \bar{x}; z, \bar{z})\rangle = \frac{U^+(j)}{|x - \bar{x}|^{2j}|z - \bar{z}|^{2\Delta_j}} \quad \text{for } Im(x) > 0, \tag{4.23}$$

$$\frac{U^-(j)}{|x - \bar{x}|^{2j}|z - \bar{z}|^{2\Delta_j}} \quad \text{for } Im(x) < 0.$$

The z dependence is determined from conformal invariance on the worldsheet and the x dependence is fixed by conformal invariance on the target space. The parameters $(x, \bar{x})$ can be regarded as coordinates on the boundary of Euclidean AdS_3, which is S^2. The AdS_2 brane divides S^2 into half, and the upper half plane covers one patch and the lower half the other. From the point of view of the conformal field theory on the boundary, the AdS_2 introduces a one-dimensional defect on S^2, across which the two different CFT's are glued together [25]. Therefore the one point function $\langle \Phi_j \rangle$ may have a discontinuity across $\mathrm{Im}x = 0$. The expression (4.23) allows this possibility as the coefficients U^+ and U^- can be different.

The reflection symmetry (4.10) implies a relation between U^+ and U^-. Taking the expectation value of (4.10) on both sides, we get

$$\frac{U^{\pm}(j)}{|x - \bar{x}|^{2j}} = \mathcal{R}(j)\frac{2j-1}{\pi}\left(\int_{Imx>0} d^2x' U^+(1-j)\frac{|x - x'|^{-4j}}{|x' - \bar{x}'|^{2(1-j)}} + \right. \tag{4.24}$$

$$+\int_{Imx<0} d^2x' U^-(1-j)\frac{|x-x'|^{-4j}}{|x'-\bar{x}'|^{2(1-j)}}\Bigg)\,,$$

On the left-hand side, we choose U^+ for $\mathrm{Im}x > 0$ and U^- for $\mathrm{Im}x < 0$. Setting $x' = x'_1 + ix'_2$, we can rewrite the above x'-integration as

$$= U^+(1-j)\int_{-\infty}^{\infty} dx'_1 \int_0^{\infty} dx'_2 \frac{\left({x'_1}^2 + (x'_2 - x_2)^2\right)^{-2j}}{|2x'_2|^{2(1-j)}} + \tag{4.25}$$

$$+U^-(1-j)\int_{-\infty}^{\infty} dx'_1 \int_{-\infty}^{0} dx'_2 \frac{\left({x'_1}^2 + (x'_2 - x_2)^2\right)^{-2j}}{|2x'_2|^{2(1-j)}}.$$

By using the Euler integral

$$\int_0^1 dx\, x^{a-1}(1-x)^{b-1} = \frac{\Gamma(a)\Gamma(b)}{\Gamma(a+b)}, \tag{4.26}$$

we see that for the case $x_2 > 0$, the first term vanishes and only the second term contributes. On the other hand, when $x_2 < 0$, the second term vanishes and only the first term contributes. We can summarize the result as

$$U^{\pm}(j) = \mathcal{R}(j)U^{\mp}(1-j). \tag{4.27}$$

Introducing $f^{\pm}(j)$ by

$$U^{\pm}(j) = \Gamma\left(1 - \frac{2j-1}{k-2}\right)\nu^{\frac{1}{2}-j} f^{\pm}(j)\,, \tag{4.28}$$

the reflection relation (4.27) becomes

$$f^{\pm}(j) = f^{\mp}(1-j)\,. \tag{4.29}$$

To determine $f^+(j)$, it is useful to consider the bulk two-point function of Φ_j with a degenerate field. Degenerate fields correspond to those with spin $2j = n+(k-2)m$, where $n, m \in \mathbf{Z}$. A particularly useful one is the degenerate field with $j = -1/2$, which satisfies

$$\partial_x^2 \Phi_{-1/2} = 0. \tag{4.30}$$

It means that there are only two terms in its operator product expansion with Φ_j as

$$\Phi_{-\frac{1}{2}}\Phi_j \sim C_-(j)\Phi_{j-\frac{1}{2}} + C_+(j)\Phi_{j+\frac{1}{2}} + \cdots, \tag{4.31}$$

Here the "$\cdots$" denote the current algebra descendants. To simplify the equations, in this subsection, we are suppressing the dependence on x and z. The coefficients $C_{\pm}(h)$ have been derived in the earlier literature, but let us compute them here for completeness. Let us take a correlation function of $\Phi_{j'}$ with both sides of (4.31). The left hand side gives

$$\langle \Phi_{-\frac{1}{2}} \Phi_j \Phi_{j'} \rangle = C\left(-\frac{1}{2}, j, j'\right). \tag{4.32}$$

Using the expression for the three point function and the identity

$$\lim_{\epsilon \to 0} \frac{G(j_1 - j_2 + \epsilon) G(j_2 - j_1 + \epsilon)}{G(-1) G(1 + 2\epsilon)} = -2\pi(k-2)\gamma\left(\frac{k-1}{k-2}\right)\delta(s_1 - s_2), \tag{4.33}$$

with $j_1 = 1/2 + i s_1, j_2 = 1/2 + i s_2$, we find that (4.32) contains delta functions at $j' = j \pm \frac{1}{2}$. On the other hand, the right-hand side of (4.31) gives

$$\langle \Phi_{-\frac{1}{2}} \Phi_j \Phi_{j'} \rangle \sim \delta\left(j' - j + \frac{1}{2}\right) C_-(j)\, B\left(j - \frac{1}{2}\right) + \delta\left(j' - j - \frac{1}{2}\right) C_+(j) B\left(j + \frac{1}{2}\right) + \cdots. \tag{4.34}$$

Comparing the coefficients of the delta functions, we find

$$\begin{aligned} C_+(j) &= \nu \frac{\gamma\left(-\frac{1}{k-2}\right)}{\gamma\left(-\frac{2}{k-2}\right)} \qquad (4.35) \\ C_-(j) &= \frac{\gamma\left(-\frac{1}{k-2}\right)\gamma\left(\frac{2j-2}{k-2}\right)}{\gamma\left(-\frac{2}{k-2}\right)\gamma\left(\frac{2j-1}{k-2}\right)}. \end{aligned}$$

Given the coefficient $C_{\pm}(j)$ for the operator product expansion of $\Phi_{-\frac{1}{2}}\Phi_j$, one can deduce a functional relation for $U^+(j)$.[2] Consider the following bulk two-point function involving a degenerate field $\Phi_{-1/2}$

$$\langle \Phi_{-\frac{1}{2}}(x; z) \Phi_j(x'; z') \rangle. \tag{4.36}$$

[2]Here we take x to be on the upper half plane. A similar relation for U^- can be derived by considering x in the lower half plane. Since $U^{\pm}$ are related to each other by the reflection relation, it is sufficient to determine conditions on U^+.

Using the operator product expansion derived in the above paragraph, we find

$$\langle \Phi_{-\frac{1}{2}}(x;z)\Phi_j(x';z')\rangle = \frac{|x'-\bar{x}'|^{-1-2j}}{|x-\bar{x}'|^{-2}}\frac{|z'-\bar{z}'|^{-\frac{3u}{2}-2\Delta_j}}{|z-\bar{z}'|^{-3u}}\times \tag{4.37}$$

$$\left(C_+(j)U^+\left(j+\frac{1}{2}\right)\mathcal{F}_+(x,x';z,z')+C_-(j)U^+\left(j-\frac{1}{2}\right)\mathcal{F}_-(x,x';z,z')\right).$$

Here $\mathcal{F}_\pm$ are four-point conformal blocks. According to [71], we have

$$\mathcal{F}_+(x,x';z,z') = \eta^{u(1-j)}(1-\eta)^{-\frac{u}{2}}\Big(\chi F(-u,1-2uj,1-u(2j-1);\eta)+ \tag{4.38}$$

$$+\frac{u\eta}{1+u(1-2j)}F(1-u,1-2uj,2-u(2j-1);\eta)\Big),$$

$$\mathcal{F}_-(x,x';z,z') = \eta^{uj}(1-\eta)^{-\frac{u}{2}}\left(\chi\frac{1}{2j-1}F(2u(j-1),1-u,u(2j-1)+1;\eta)\right. \tag{4.39}$$

$$\left.+F(1-u,-u,u(2j-1);\eta)\Big),\right.$$

where $F(a,b,c;z)$ are the hypergeometric functions ${}_2F_1(a,b,c;z)$,

$$u=\frac{1}{k-2}, \tag{4.40}$$

and χ and η are cross ratios of the target space and the worldsheet coordinates,

$$\chi=\frac{|x-x'|^2}{|x-\bar{x}'|^2},\quad \eta=\frac{|z-z'|^2}{|z-\bar{z}'|^2}. \tag{4.41}$$

It was pointed out in [66] that, when the operator $\Phi_{-\frac{1}{2}}$ approaches the boundary of the worldsheet, it overlaps only with the identity operator and the operator with $j=-1$. This is analogous to the situation in the Liouville theory discussed in [73]. Using this, the two point function $\langle\Phi_{-\frac{1}{2}}\Phi_j\rangle$ can be evaluated as

$$\langle \Phi_{-\frac{1}{2}}(x;z)\Phi_h(x';z')\rangle = \frac{|x'-\bar{x}'|^{-1-2j}}{|x-\bar{x}'|^{-2}}\frac{|z'-\bar{z}'|^{-\frac{3u}{2}-2\Delta_j}}{|z-\bar{z}'|^{-3u}}\times \tag{4.42}$$

$$(B_+(j)\mathcal{G}_+(x,x';z,z')+B_-(j)\mathcal{G}_-(x,x';z,z')),$$

where

$$\mathcal{G}_+(x,x';z,z') = \eta^{uj}(1-\eta)^{\frac{3u}{2}}\Big((1-\chi)F(1+u,2uj,1+2u;1-\eta) - (1-\eta)\frac{2uj}{1+2u}F(1+u,1+2uj,2(1+u);1-\eta)\Big)\,, \tag{4.43}$$

$$\mathcal{G}_-(x,x';z,z') = \eta^{uj}(1-\eta)^{-\frac{u}{2}}\left(\frac{1-\chi}{2}F(2u(j-1),1-u,1-2u;1-\eta)+F(2u(j-1),-u,-2u;1-\eta)\right), \tag{4.44}$$

and u is given by (4.40). The conformal blocks in the two expressions, (4.37) and (4.42), are related to each other as

$$\mathcal{F}_- = \frac{\Gamma(u(2j-1))\Gamma(1+2u)}{\Gamma(2uj)\Gamma(1+u)}\mathcal{G}_- + \frac{\Gamma(u(2j-1))\Gamma(-2u)}{\Gamma(2u(j-1))\Gamma(-u)}\mathcal{G}_+, \tag{4.45}$$

$$\mathcal{F}_+ = \frac{\Gamma(1+u(1-2j))\Gamma(1+2u)}{\Gamma(1+2u(1-j))\Gamma(1+u)}\mathcal{G}_- - \frac{\Gamma(1+u(1-2j))\Gamma(-2u)}{\Gamma(1-2uj)\Gamma(-u)}\mathcal{G}_+. \tag{4.46}$$

(See Appendix E for some useful identities involving the hypergeometric function.) According to [61, 66, 67], B_+ is given by

$$B_+(j) = A_0 U^+(j)\,, \tag{4.47}$$

where A_0 is a constant that depends on the boundary condition and can be interpreted as the fusion coefficient of $\Phi_{-1/2}$ with the boundary unit operator. Likewise, $B_-(j)$ term can be interpreted as the contribution coming from the fusion with $j=-1$ boundary operator. Comparing the terms dependent on $\mathcal{G}_+$ in (4.37) and (4.42), we derive the following functional equation for $U^+(j)$:

$$A_0 U^+(j) = \frac{\Gamma(-2u)}{\Gamma(-u)}\left(C_-(j)U^+\left(j-\frac{1}{2}\right)\frac{\Gamma(u(2j-1))}{\Gamma(2u(j-1))} - C_+(j)U^+\left(j+\frac{1}{2}\right)\frac{\Gamma(1+u(1-2j))}{\Gamma(1-2uj)}\right). \tag{4.48}$$

Substituting the expression for $C_\pm(j)$ given by (4.35), this reduces to

$$A_0\nu^{-1/2}\frac{\Gamma\left(1+\frac{1}{k-2}\right)}{\Gamma\left(1+\frac{2}{k-2}\right)}f^+(j) = f^+\left(j-\frac{1}{2}\right) - f^+\left(j+\frac{1}{2}\right). \tag{4.49}$$

Given $f^+(j)$ satisfying (4.49), we get $f^-(j)$ by using (4.29).

It is convenient to introduce a parameter θ by

$$A_0\nu^{-1/2}\frac{\Gamma\left(1+\frac{1}{k-2}\right)}{\Gamma\left(1+\frac{2}{k-2}\right)} = -2\sinh\theta. \tag{4.50}$$

We can regard θ as parametrizing the boundary condition as A_0 depends on it. In fact, the semi-classical analysis in the next section shows that θ specifies the location of the AdS_2 brane. A general solution to (4.49) and (4.29) is then a linear combination of

$$f^{\pm}(j) = \exp\left[\pm(\theta + i2n\pi)(2j-1)\right] \ , \quad \exp\left[\pm(i\pi(2n+1)-\theta)(2j-1)\right], \tag{4.51}$$

where $n \in \mathbf{Z}$.

4.3 Boundary states for AdS_2 branes

Among the solutions (4.51), we claim that the following one correctly represents the boundary condition for a single AdS_2 brane.

$$f_\theta^{\pm}(j) = Ce^{\pm\theta(2j-1)}, \tag{4.52}$$

where C is a constant independent of j but may depend on θ and k. From now on, we neglect this constant and it will not affect the rest of our discussion. In this section, we will provide evidences for this claim.

Given the $f^{\pm}(j)$ solution (4.52), and therefore the one point function $U^{\pm}(j)$, the boundary state is expressed as

$$|B\rangle\rangle_\theta = \int_{\frac{1}{2}+i\mathbf{R}^+} dj \left(\int_{Imx>0} d^2x \frac{U_\theta^+(1-j)}{|x-\bar{x}|^{2(1-j)}} |j,x,\bar{x}\rangle\rangle_I + \int_{Imx<0} d^2x \frac{U_\theta^-(1-j)}{|x-\bar{x}|^{2(1-j)}} |j,x,\bar{x}\rangle\rangle_I \right), \tag{4.53}$$

where $|j,x,\bar{x}\rangle\rangle_I$ is an Ishibashi state built on the primary state $|j,x,\bar{x}\rangle$. The coefficients are chosen so that the one point functions are correctly reproduced as

$$\langle j,x,\bar{x}|B\rangle\rangle_\theta = \lim_{z\to\infty} |z-\bar{z}|^{2\Delta_j} \langle \Phi_j(x,\bar{x};z,\bar{z})\rangle. \tag{4.54}$$

It can be verified using the two point function (4.12) and the reflection relation (4.27) that the boundary state given by (4.53) satisfies this condition. In the following, we will examine aspects of $|B\rangle\rangle_\theta$.

4.3.1 Semi-classical analysis

Let us first study the semi-classical limit of the boundary state for the solution (4.52). We use the method of [74, 67] to identify the D-brane configuration corresponding to the boundary state. In the semi-classical limit ($k \to \infty$), we can consider a closed string state $|g\rangle$ localized at $g \in H_3^+$. Namely, it is defined so that

$$\langle g|j, x, \bar{x}\rangle = \Phi_j(x, \bar{x}|g). \tag{4.55}$$

The overlap of the localized state $|g\rangle$ with the boundary state $|B\rangle\rangle_\theta$ can then tell us about the configuration of the brane. (An analogous idea has been used in [75] to characterize boundary states for D-branes wrapping on cycles in Calabi-Yau manifolds.) In the limit $k \to \infty$, the overlap $\langle g|B\rangle\rangle_\theta$ is simplified as

$$\begin{aligned}
&\lim_{k\to\infty} \langle g|B\rangle\rangle_\theta \\
&= \int_{\frac{1}{2}+i\mathbf{R}^+} dj \left(\int_{Imx>0} d^2x \frac{f_\theta^+(1-j)}{|x-\bar{x}|^{2(1-j)}} \Phi_j(x, \bar{x}|g) + \int_{Imx<0} d^2x \frac{f_\theta^-(1-j)}{|x-\bar{x}|^{2(1-j)}} \Phi_j(x, \bar{x}|g) \right),
\end{aligned}$$

where we used (4.15). First let us focus on the integral on the upper half plane,

$$\int_{\frac{1}{2}+i\mathbf{R}^+} dj \frac{2j-1}{\pi} \left(\int_{x_2>0} d^2x \frac{f_\theta^+(1-j)}{(2x_2)^{2(1-j)}} \frac{1}{\left[e^\phi(x_1^2+x_2^2-(\gamma+\bar{\gamma})x_1+i(\gamma-\bar{\gamma})x_2+\gamma\bar{\gamma})+e^{-\phi}\right]^{2j}} \right). \tag{4.56}$$

After integrating over x_1 and changing integration variable $x_2' = e^\phi x_2$, we get

$$\int_{\frac{1}{2}+i\mathbf{R}^+} dj \frac{2j-1}{\sqrt{\pi}2^{2-2j}} \frac{\Gamma(2j-\frac{1}{2})}{\Gamma(2j)} f_\theta^+(1-j) \int_0^\infty dx_2' (x_2')^{2j-2} \left[\left(x_2' + \frac{1}{2} i(\gamma-\bar{\gamma}) e^\phi \right)^2 + 1 \right]^{\frac{1}{2}-2j}. \tag{4.57}$$

In terms of AdS_2 coordinates defined in Appendix C, we have

$$\frac{i}{2}(\gamma-\bar{\gamma})e^\phi = -\sinh\psi. \tag{4.58}$$

The x_2'-integral is performed in Appendix E, and the result is

$$\int_{\frac{1}{2}+i\mathbf{R}^+} dj f_\theta^+(1-j)\frac{e^{\psi(2j-1)}}{\cosh\psi} = \int_0^\infty ds \frac{e^{2i(\psi-\theta)s}}{\cosh\psi}, \tag{4.59}$$

where $j = 1/2 + is$. Likewise, we can perform the integral over the lower half plane. Combining the results together, we find that the overlap is given by

$$\lim_{k\to\infty}\langle g|B\rangle\rangle_\theta = \int_0^\infty ds\frac{e^{2i(\psi-\theta)s}}{\cosh\psi} + \int_0^\infty ds\frac{e^{-2i(\psi-\theta)s}}{\cosh\psi} = \int_{-\infty}^\infty ds\frac{e^{2i(\psi-\theta)s}}{\cosh\psi} \tag{4.60}$$

$$= \frac{1}{4\pi\cosh\psi}\delta(\psi-\theta) = \frac{1}{4\pi}\delta(\sinh\psi-\sinh\theta) \tag{4.61}$$

Thus we found that $\langle g|B\rangle\rangle_\theta$ has a support in the two-dimensional subspace at $\psi = \theta$ in AdS_3. We can identify this as the location of the AdS_2 brane.

In this formalism, the insertion of the identity operator should reproduce the Born-Infeld action in the semi-classical regime. Using the reflection symmetry and taking the large k limit in (4.24), we see that

$$\langle 1\rangle_\theta \propto \cosh\theta \int d^2x|x-\bar{x}|^{-2}. \tag{4.62}$$

The Born-Infeld action of AdS_2 branes has been computed by independent methods in [52] to be

$$S_{BI} \propto \cosh\psi \int d\omega dt \cosh\omega. \tag{4.63}$$

If we identify θ with ψ in the semi-classical limit and $\int d^2x|x-\bar{x}|^{-2}$ as the volume divergence associated with the non-compactness of AdS_2 branes, the two expressions agree.

The one point function is given by a linear combination of the solutions (4.51) to the functional equations discussed in the last section. Since we found that $f_\theta^\pm \sim e^{\pm\theta(2j-1)}$ reproduces the correct semi-classical geometry of the AdS_2 brane, the coefficients for all other solutions in (4.51) should vanish in the semi-classical limit $k\to\infty$.

In fact we can make a stronger statement. If we assume the state $|g\rangle$ satisfying (4.55) exists at finite value of k, then the j-integral to compute overlap $\langle g|B\rangle\rangle_\theta$ is finite only for the particular solution, $f_\theta^\pm(j)$. For all other solutions in (4.51), the

integral is divergent for $k > 3$. This suggests that the coefficients in front of the other solutions in (4.51) should vanish identically even for finite k.

4.3.2 Annulus amplitudes

Given the boundary states, the partition function on the annulus worldsheet with the boundary conditions θ_1 and θ_2 on the two boundary of the annulus is computed as exchanges of closed string states between $|B\rangle\rangle_{\theta_1}$ and $|B\rangle\rangle_{\theta_2}$. If we view this in the open string channel, one should be able to express it as a sum over states of open string stretched between the two AdS_2 branes at θ_1 and θ_2. These open string states are normalizable. For the Euclidean AdS_2 branes in Euclidean AdS_3, they belong to principal continuous representations.

We want to compute the following amplitude between two boundary states:

$$
\begin{aligned}
&{}_{\theta_1}\langle\langle B|(q_c^{\frac{1}{2}})^{L_0+\bar{L}_0-\frac{c}{12}}|B\rangle\rangle_{\theta_2} \\
&= \int_{\frac{1}{2}+i\mathbf{R}^+} dj \left(\int_{Imx>0} d^2x \frac{U^+{}_{\theta_1}(j)U^+{}_{\theta_2}(1-j)}{|x-\bar{x}|^2} + \int_{Imx<0} d^2x \frac{U^-{}_{\theta_1}(j)U^-{}_{\theta_2}(1-j)}{|x-\bar{x}|^2} \right) \frac{q_c^{\frac{s^2}{k-2}}}{\eta(q_c)^3} \\
&= \left(\int d^2x |x-\bar{x}|^{-2} \right) \int_0^\infty ds \frac{\cos 2(\theta_1-\theta_2)s}{\sinh \frac{2\pi}{k-2}s} \frac{2\pi}{k-2} s \frac{q_c^{\frac{s^2}{k-2}}}{\eta(q_c)^3}.
\end{aligned}
$$

Using the fact

$$
s\frac{q_c^{\frac{s^2}{k-2}}}{\eta(q_c)^3} = \frac{2\sqrt{2}}{\sqrt{k-2}} \int_0^\infty ds' \sin\left(\frac{4\pi}{k-2}ss'\right) s' \frac{q_o^{\frac{s'^2}{k-2}}}{\eta(q_o)^3} \ , \tag{4.64}
$$

where

$$
q_c = e^{2\pi i\tau_c}, \qquad q_o = e^{2\pi i\tau_o}, \qquad \tau_o = -\frac{1}{\tau_c}, \tag{4.65}
$$

we can go to the open string channel:

$$
= \left(\int d^2x |x-\bar{x}|^{-2} \right) \frac{4\sqrt{2}\pi}{(k-2)^{3/2}} \int_0^\infty ds' \left(\int_0^\infty ds \frac{\cos(2\theta_{12}s)\sin\left(\frac{4\pi}{k-2}ss'\right)}{\sinh\frac{2\pi}{k-2}s} \right) s' \frac{q_o^{\frac{s'^2}{k-2}}}{\eta(q_o)^3}
$$

$$= \left(\int d^2x|x-\bar{x}|^{-2}\right)\frac{\pi}{\sqrt{2}\sqrt{k-2}}\int_0^\infty ds'\frac{2s'\sinh 2\pi s'}{\cosh\left((k-2)\theta_{12}\right)+\cosh\left(2\pi s'\right)}\frac{q_o^{\frac{s'^2}{k-2}}}{\eta(q_o)^3},$$

where $\theta_{12}=\theta_1-\theta_2$. Obviously, the overall factor involving the x-integral is divergent. In the closed string channel, it is the volume divergence coming from the fact that the AdS_2 brane is non-compact. In the open string channel, the divergence can be interpreted as due to the fact that normalizable states are in infinite dimensional principal continuous representations of $SL(2,C)$ and that states in a given representation has the same worldsheet conformal weight.

If we define $\rho(s)$ as states of open string Hilbert space belonging to the principal continuous representation with $j=\frac{1}{2}+is$, the above result shows that it is given by by

$$\rho(s)\propto\frac{s\sinh 2\pi s}{\cosh\left((k-2)\theta_{12}\right)+\cosh\left(2\pi s\right)}\,. \tag{4.66}$$

The spectral density is real and non-negative as it should be. For the case $\theta_1=\theta_2$ (single AdS_2 brane case), θ_1 dependence completely disappears. Note, however, we have neglected the overall constant C in the one point function (4.52), which can be θ-dependent but is independent of s.

The reality and positivity of $\rho(s)$ gives a stringent constraint on the boundary state. One can show that, if $f^{\pm}(j)$ is not given by (4.52) but contains other solutions in (4.51), the spectral density becomes negative at some finite value of s.

4.3.3 Finite temperature partition function calculation

In this subsection, we consider AdS_2 branes in finite-temperature AdS_3 and compute the partition function by using the boundary states we have constructed. For the $\psi=0$ case, we can directly compare the result with that of Appendix A in [53].

Finite-temperature AdS_3 is given by identifying the Euclidean time $t_E=it$ in the target space

$$t_E\sim t_E+\beta\,. \tag{4.67}$$

It induces identification of boundary coordinates as well:

$$|x|\sim|x|e^{\beta}\,. \tag{4.68}$$

As pointed out in [68], the thermal identification induces new sectors of strings winding around the compact time direction. As in [69], given a classical solution $\tilde{g}(\sigma,\tau) = \tilde{g}_+(x^+)\tilde{g}_-(x^-)$, where $x^\pm = -i\tau \pm \sigma$, we can generate new solutions by setting

$$g_+ = e^{\frac{i}{2}w_R x^+ \sigma_2}\tilde{g}_+, \qquad g_- = \tilde{g}_- e^{\frac{i}{2}w_L x^- \sigma_2}, \tag{4.69}$$

where σ_i are the Pauli matrices. If we choose $w_R = -w_L = -iw\beta/2\pi$ with $w \in \mathbf{Z}$, the action generates the following change in the string coordinates,

$$\begin{aligned} t_E &\sim t_E + \frac{w}{2\pi}\sigma, \\ \theta &\sim \theta - \frac{w}{2\pi}\tau, \\ \rho &\sim \rho. \end{aligned} \tag{4.70}$$

The string worldsheet is periodic in $\sigma \to \sigma + 2\pi$, modulo the identification (4.67). This induces the following transformation on the Virasoro generator,

$$L_0 \to L_0 + iw\frac{\beta}{2\pi}J_0^3 + kw^2\frac{\beta^2}{16\pi^2}, \tag{4.71}$$

$$\bar{L}_0 \to \bar{L}_0 - iw\frac{\beta}{2\pi}\bar{J}_0^3 + kw^2\frac{\beta^2}{16\pi^2}.$$

Correspondingly the boundary states include all the winding sectors:

$$|B;\beta\rangle\rangle_\theta = \sum_w |B;\beta\rangle\rangle_{\theta,w}. \tag{4.72}$$

Here $|B;\beta\rangle\rangle_{\theta,w=0}$ is the boundary state given by (4.53), except that the x integral is restricted in the range

$$e^{-\beta} \le |x| \le 1, \tag{4.73}$$

which is the fundamental domain of the identification (4.68). The other states $|B;\beta\rangle\rangle_{\theta,w}$ are given by performing the spectral flow (4.71). The amplitude we want to compute then is

$${}_{\theta_1}\langle\langle B;\beta|(q_c^{\frac{1}{2}})^{L_0+\bar{L}_0-\frac{c}{12}}|B;\beta\rangle\rangle_{\theta_2} = \sum_{w=-\infty}^{\infty} {}_{\theta_1,w}\langle\langle B;\beta|(q_c^{\frac{1}{2}})^{L_0+\bar{L}_0-\frac{c}{12}}|B;\beta\rangle\rangle_{\theta_2,w}. \tag{4.74}$$

The overlap in the w winding sector can be expressed as

$$ {}_{\theta_1,w}\langle\langle B;\beta|(q_c^{\frac{1}{2}})^{L_0+\bar{L}_0-\frac{c}{12}}|B;\beta\rangle\rangle_{\theta_2,w} = q_c^{\frac{k\beta^2}{16\pi^2}w^2}\,{}_{\theta_1,w=0}\langle\langle B;\beta|(q_c^{\frac{1}{2}})^{L_0+\bar{L}_0-\frac{c}{12}}e^{\frac{\beta\tau_c}{2}w(-J_0^3+\bar{J}_0^3)}|B;\beta\rangle\rangle_{\theta_2,w=0}, \tag{4.75} $$

where $\tau_c = it_c$ and $\phi_0 = -\beta\tau_c w/2$. Substituting (4.53) into this, we find that the right-hand side is expressed as an integral over x in the range (4.73). The integration domain is divided into four regions, depending on the signs of Imx and $Ime^{i\phi_0}x$. Combining them together, we find

$$ -2q_c^{\frac{k\beta^2}{16\pi^2}w^2}\int_{\frac{1}{2}+i\mathbf{R}^+}dj\left(\int_{Imx>0,\,Im(xe^{i\phi_0})>0,\,e^{-\beta}<|x|<1}d^2x|x-\bar{x}|^{-2j}|xe^{i\phi_0}-\bar{x}e^{-i\phi_0}|^{-2(1-j)}\right)\times $$

$$ \Big(U_{\theta_1}^+(j)U_{\theta_2}^+(1-j)+U_{\theta_1}^+(j)U_{\theta_2}^-(1-j)+U_{\theta_1}^-(j)U_{\theta_2}^+(1-j)+U_{\theta_1}^-(j)U_{\theta_2}^-(1-j)\Big)\times $$

$$ \sin\phi_0\frac{q_c^{s^2/(k-2)}}{\vartheta_{11}(\frac{\phi_0}{\pi}|it_c)}. $$

The x-integral is performed in Appendix E,

$$ (x\text{-integral}) = \frac{\pi\beta}{|\sin\phi_0|}\delta(s)\,. \tag{4.76} $$

Thus the overlap in the winding number w sector is given by

$$ {}_{\theta_1,w}\langle\langle B,\beta|(q_c^{\frac{1}{2}})^{L_0+\bar{L}_0-\frac{c}{12}}|B,\beta\rangle\rangle_{\theta_2,w} \propto \beta\frac{e^{-\frac{kt_c\beta^2}{8\pi}w^2}}{|\vartheta_{11}(\frac{\beta t_c w}{2\pi}|it_c)|}. \tag{4.77} $$

Altogether we have,

$$ {}_{\theta_1}\langle\langle B|(q_c^{\frac{1}{2}})^{L_0+\bar{L}_0-\frac{c}{12}}|B\rangle\rangle_{\theta_2} \propto \sum_{w=-\infty}^{\infty}\beta\frac{e^{-\frac{kt_c\beta^2}{8\pi}w^2}}{|\vartheta_{11}(\frac{\beta t_c w}{2\pi}|it_c)|}. \tag{4.78} $$

After taking the ghost sector and the internal CFT into account and performing the modular transformation, we recover the partition function computed via the functional integral method in the appendix of [53].

One interesting fact is that the partition function does not depend on θ_1 or θ_2. This is unexpected from the semi-classical analysis performed in [53]. The reason for this is unclear and deserves a closer inspection.

4.4 Discussion

In this chapter, we constructed the boundary states for AdS_2 branes in AdS_3, following [66, 67] but using the different ansatz. The boundary states are expressed as linear combinations of the Ishibashi states as in (4.53), where the one point functions $U_\theta^\pm(j)$ are given by,

$$U^\pm(j) = \Gamma\left(1 - \frac{2j-1}{k-2}\right)\nu^{\frac{1}{2}-j}e^{\pm\theta(2j-1)}, \tag{4.79}$$

modulo factors independent of j. In the semi-classical approximation, the location of the brane is given by $\psi = \theta$ in the AdS_2 coordinates defined in Appendix C.

From the point of view of the boundary conformal field theories, the AdS_2 branes create defects which connect different conformal field theories while preserting at least one Virasoro algebra. Since the boundary states allow study of the AdS_2 branes beyong the supergravity approximation, it would be interesting to use them to explore the correspondence further.

Chapter 5

Summary

The AdS/CFT correspondence states that string theory (M-theory) on an AdS background is equivalent to a conformal field theory defined on the boundary of AdS. Using this correspondence, one ultimately hopes to probe gauge theory computations that greatly simplify on the gravity side and vice versa. Ideally, one would like to better understand physically interesting theories such as QCD ($SU(3)$ gauge theory), whose analysis has been limited to numerical methods. This is because the coupling constant becomes large at low energy scales and perturbative methods fail.

Clearly, string theory on AdS backgrounds is interesting for its own sake. In this thesis, we have explored the properties of Dp-branes, which are p+1 dimensional membranes on which an open string can end, embedded in AdS_3 and AdS_5 backgrounds. For the $AdS_5 \times S^5$ case, ref. [11] explicitly realized the AdS/CFT correspondence by constructing a defect conformal field theory that describes open strings ending on a single D5 brane. A natural generalization would be to study other D-brane setups such as for multiple D-branes. In this thesis, we took a Penrose limit of this setup and ended up with a flat D-brane embedded in PP-Wave background. Following the proposal of [7], we derived a correspondence between open string states and gauge invariant operators of the dual conformal field theory. Furthermore, we have checked that the anomalous dimension of certain near BPS operators matched the light-cone Hamiltonian of excited open-string states. In doing this, a possible problem arose where the chiral primary operators received finite corrections that blow up in the PP-

wave limit. One hopes that this difficulty can be overcome by employing a different renormalization scheme or by considering ratios of correlation functions. Although amplitudes themselves are divergent in the Penrose limit, ratios of amplitudes can be finite. It would be interesting to see if a similar problem also exists in other open string scenarios such as the orbifold model considered in [17].

In Chapters 2 and 3, we investigated AdS_2 branes embedded in $AdS_3 \times S^3 \times M^4$. According to the AdS/CFT correspondence, its dual conformal field theory should be a 1+1 dimensional defect conformal field theory, but the dCFT has not yet been constructed explicitly[1]. During the construction of boundary states for AdS_2 branes, we saw that the defect allowed one-point functions of primary fields to have discontinuous jumps across the boundary. Following [36, 37], we employed semi-classical analysis to propose the spectrum of open strings ending on AdS_2 branes embedded in Lorentzian AdS_3 background. Then, we explicitly checked this proposal by computing the one-loop partition function for the simplest case where the AdS_2 branes contained no fundamental charge. In Chapter 3, boundary states of AdS_2 branes were derived in Euclidean AdS_3 via the $SL(2,C)/SU(2)$ WZW model. One-loop open string amplitude obtained from the boundary states were computed, and it matched the string Hilbert space proposed in Chapter 2. By taking an orbifold of AdS_3, one can obtain the BTZ black hole or the cigar black hole geometry. It would be very interesting to take the orbifold of the D-brane setup considered in Chapters 2 and 3 in hopes of using the D-branes to probe the singularities as in [76]. Lastly, explicit construction of the dual defect conformal field theory analogous to the case of $AdS_5 \times S^5$ is sorely needed.

[1]For a first-step towards this direction, see [52].

Appendix A

Anomalous Dimension Computation

In this appendix, we show that the anomalous dimension for chiral primary operators defined in Chapter 1 of the form $\bar{q}^2 Z^k q^1$ vanish up to order g_{YM}^2. We work in Lorentzian space-time with mostly minus signature. The propagators for the defect conformal field theory defined by equation (4.50) of [11] are

$$\langle X_{V,H}\ X_{V,H}\rangle = \frac{i}{p^2} \to -\frac{1}{2(\vec{p}^2)^{1/2}}, \tag{A.1}$$

$$\langle \lambda_{1\alpha}\bar{\lambda}_{1\beta}\rangle = \frac{-i(\rho^k)_{\alpha\beta}p_k}{p^2}, \tag{A.2}$$

$$\langle \chi^A_{1\alpha}\bar{\chi}^B_{1\beta}\rangle = \frac{-i(\rho^k)_{\alpha\beta}p_k\delta^{AB}}{p^2}, \tag{A.3}$$

$$\langle A_k A_l\rangle = \frac{-ig_{kl}}{p^2}, \tag{A.4}$$

$$\langle q\bar{q}\rangle = \frac{i}{\vec{p}^2}, \tag{A.5}$$

$$\langle \Psi_\alpha\bar{\Psi}_\beta\rangle = \frac{-i(\rho^k)_{\alpha\beta}p_k}{\vec{p}^2}, \tag{A.6}$$

where $\rightarrow$ denotes the effective propagator for pinned operators. In addition, $p = (p^9, \vec{p})$, $k, l = 0, 1, 2$ and ρ^k are three-dimensional gamma matrices such that Majorana spinor indices range over $\alpha, \beta = 1, 2$. Let us first evaluate the self-energy correction at order $O(g_{YM}^2)$ to q. Supersymmetry implies that the divergence should be at most logarithmic and the dimension of q may get renormalized, but not its mass.

A.1 Defect scalar q_i^m

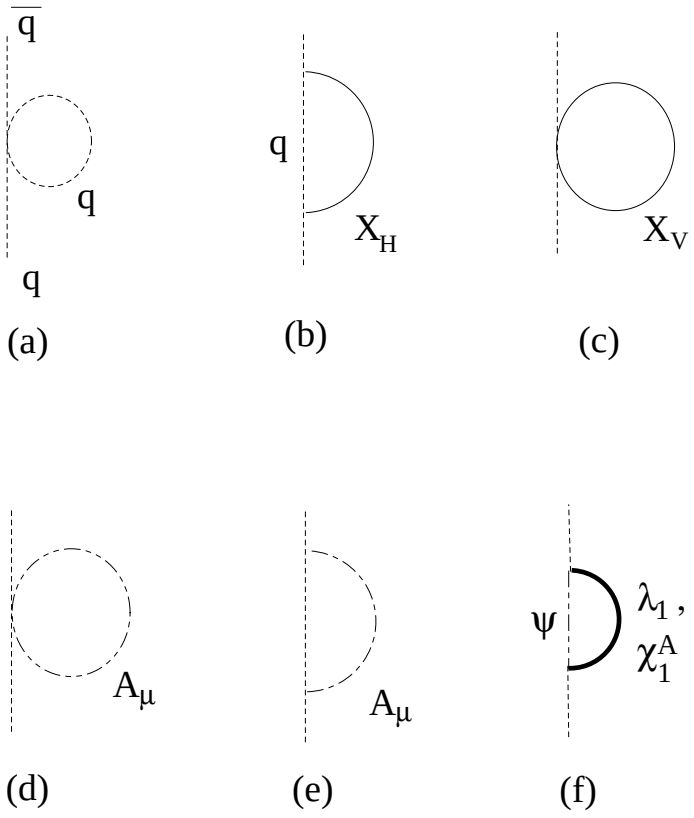

Figure A.1: One-loop self-energy correction to q

In this section, we compute the self-energy contribution to the defect scalar field q_i^m two-point function. Feynman diagram depicted in Figure A.1 (a) has the following

amputated amplitude:

$$i\int\frac{d^3k}{(2\pi)^3}\langle\bar{q}_i^1\frac{-\delta(0)}{2}\left(\bar{q}_k^m\sigma_{mn}^I T_{kl}^a q_l^n\right)^2 q_j^1\rangle = 3\delta(0)\int\frac{d^3k}{(2\pi)^3}(T^aT^a)_{ji}\frac{1}{\vec{k}^2}. \tag{A.7}$$

We follow a paper by Mirabelli and Peskin [77] and reexpress the delta function as

$$\delta(0) = \int\frac{dk^9}{2\pi}e^{ik^90} = \int\frac{dk^9}{2\pi}. \tag{A.8}$$

Using this, the amplitude becomes

$$\int\frac{d^4k}{(2\pi)^4}(T^aT^a)_{ji}3k^2\frac{1}{(\vec{p}-\vec{k})^2k^2}, \tag{A.9}$$

where we shifted $\vec{k}\to\vec{k}-\vec{p}$. All of the Feynman diagrams depicted in figures A.1(a)-(f) have a common factor of the form

$$\int\frac{d^4k}{(2\pi)^4}(T^aT^a)_{ji}\frac{1}{(\vec{p}-\vec{k})^2k^2}\times N_A(\vec{p},k). \tag{A.10}$$

We have already shown that $N_{(a)} = 3k^2$. We use the convention where the incoming momenta have $\partial_\mu\to -ik_\mu$. Straightforward calculation gives

$$N_{(a)} = 3k^2, \tag{A.11}$$

$$N_{(b)} = 3k_9^2, \tag{A.12}$$

$$N_{(c)} = 3(\vec{p}-\vec{k})^2, \tag{A.13}$$

$$N_{(d)} = 3(\vec{p}-\vec{k})^2, \tag{A.14}$$

$$N_{(e)} = -(2\vec{p}-\vec{k})^2, \tag{A.15}$$

$$N_{(f)} = 8\vec{k}\cdot(\vec{p}-\vec{k}). \tag{A.16}$$

Putting all the pieces together, we have

$$(T^aT^a)_{ji}\int\frac{d^4k}{(2\pi)^4}\frac{1}{(\vec{p}-\vec{k})^2k^2}\times 2\vec{p}^2. \tag{A.17}$$

Notice that the quadratic and delta function like divergent pieces all cancelled out. Wick-rotating the integrand by letting $k^0 = ik_E^0$ and including contributions from external legs, the quark q_i^m two-point function at order g_{YM}^2 is given by

$$\frac{-ig_{YM}^2}{\vec{p}^2}(T^aT^a)_{ji}\int\frac{d^3k}{(2\pi)^3}\frac{1}{(\vec{k})^2|\vec{k}|}. \tag{A.18}$$

A.2 $q^1\bar{q}^2$ 2 point function

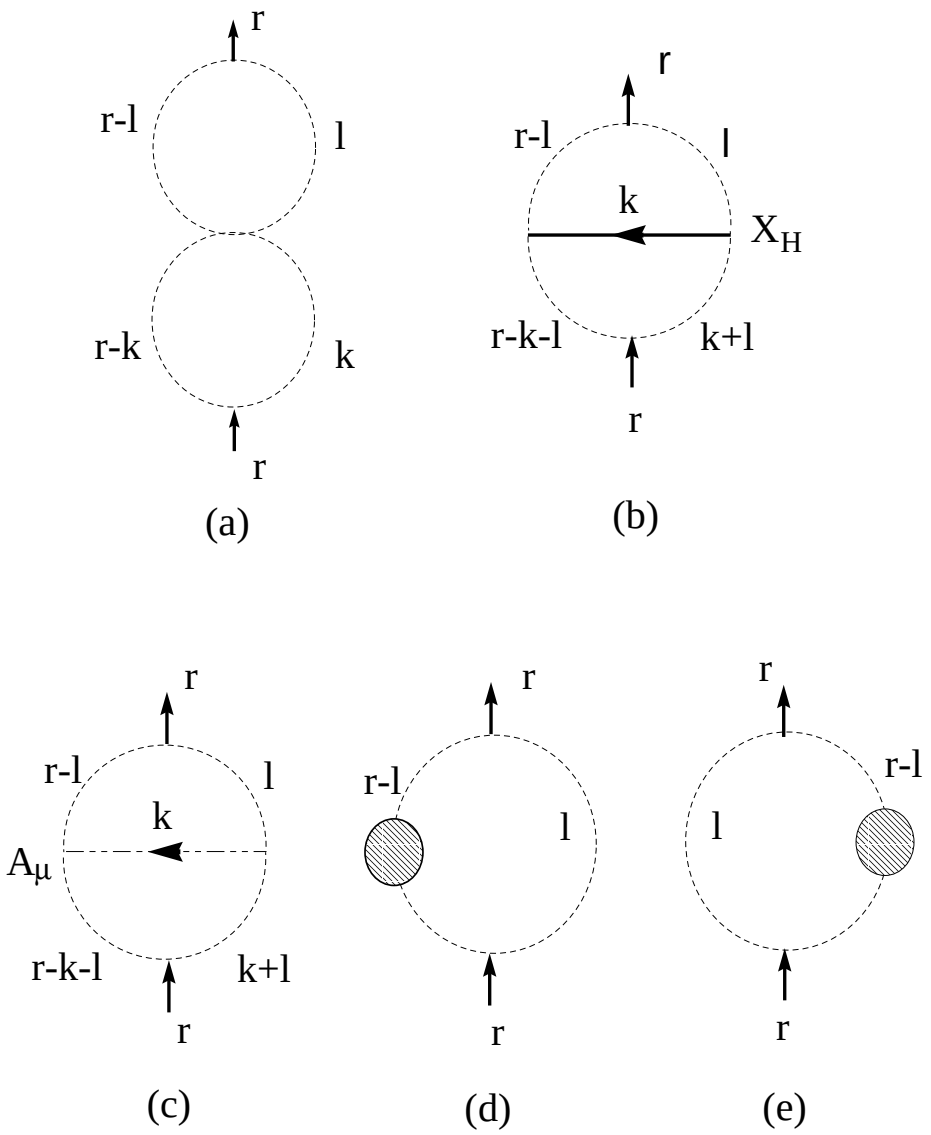

Figure A.2: $O(g^2_{YM})$ self-energy correction to $q^1\bar{q}^2$ 2 point function

The $q^1\bar{q}^2$ composite operator is the simplest CPO discussed in Chapter 1. All non-vanishing Feynman diagrams are summarized in Figure A.2. Other possible diagrams vanish due to the structure of $SU(N)$ algebra. Let us consider those coming from interaction terms. Doing this, we get the following:

For the graph shown in Figure A.2 (a), one gets

$$i\frac{N^2-1}{2}\int\frac{d^4k}{(2\pi)^4}\int\frac{d^3l}{(2\pi)^3}\frac{1}{(\vec{r}-\vec{l})^2\vec{l}^2(\vec{r}-\vec{k})^2\vec{k}^2}. \tag{A.19}$$

For Figure A.2 (b), we get

$$i\frac{N^2-1}{2}\int\frac{d^4k}{(2\pi)^4}\int\frac{d^3l}{(2\pi)^3}\frac{k_9^2}{(\vec{r}-\vec{l})^2\vec{l}^2(\vec{r}-\vec{k}-\vec{l})^2(\vec{k}+\vec{l})^2k^2}. \tag{A.20}$$

For Figure A.2 (c), we get

$$i\frac{N^2-1}{2}\int\frac{d^4k}{(2\pi)^4}\int\frac{d^3l}{(2\pi)^3}\frac{(\vec{k}-2(\vec{r}-\vec{l}))\cdot(\vec{k}+2\vec{l})}{(\vec{r}-\vec{l})^2\vec{l}^2(\vec{r}-\vec{k}-\vec{l})^2(\vec{k}+\vec{l})^2k^2}. \tag{A.21}$$

Simplifying the expression by Wick rotating and integrating over k_9 leads to the following result:

$$-i\frac{N^2-1}{2}\int\frac{d^3k}{(2\pi)^3}\int\frac{d^3l}{(2\pi)^3}\frac{\vec{k}^2+\vec{l}^2-\vec{r}\cdot(\vec{k}+\vec{l})}{(\vec{r}-\vec{l})^2\vec{l}^2(\vec{r}-\vec{k})^2\vec{k}^2|\vec{k}-\vec{l}|}. \tag{A.22}$$

Notice that the above expression is symmetric about $\vec{k}\leftrightarrow\vec{l}$. Now consider the terms coming from quark self-energy.

For Figure A.2 (d), we get

$$-i\frac{N^2-1}{2}\int\frac{d^4k}{(2\pi)^4}\int\frac{d^3l}{(2\pi)^3}\frac{2}{(\vec{r}-\vec{l})^2\vec{l}^2(\vec{r}-\vec{l}-\vec{k})^2k^2}. \tag{A.23}$$

For Figure A.2 (e), we get same result as that of Figure A.2 (d). The entire self-energy contribution after Wick rotation and integrating over k_9 is

$$i\frac{N^2-1}{2}\int\frac{d^3k}{(2\pi)^3}\int\frac{d^3l}{(2\pi)^3}\frac{2}{(\vec{r}-\vec{l})^2\vec{l}^2(\vec{r}-\vec{k})^2|\vec{k}-\vec{l}|}. \tag{A.24}$$

The tree-amplitude of $\langle O^*O\rangle$ is given as

$$\langle O^*(\vec{x})O(0)\rangle=\frac{N}{(4\pi)^2}\frac{1}{\vec{x}^2}. \tag{A.25}$$

At order g_{YM}^2, the logarithmic divergent pieces cancel each other, and the two-point function is given by

$$\langle O^*(\vec{x})O(0)\rangle = \frac{N}{(4\pi)^2\vec{x}^2} + g_{YM}^2\frac{N^2-1}{2}\int\frac{d^3r}{(2\pi)^3}\frac{d^3k}{(2\pi)^3}\frac{d^3l}{(2\pi)^3}\frac{e^{i\vec{r}\cdot\vec{x}}\ \vec{r}\cdot(\vec{k}+\vec{l})}{(\vec{r}-\vec{l})^2\vec{l}^2(\vec{r}-\vec{k})^2\vec{k}^2|\vec{k}-\vec{l}|}. \tag{A.26}$$

For the remaining finite piece, taking $\vec{k}\to\vec{k}/|\vec{r}|, \vec{l}\to\vec{l}/|\vec{r}|$, $\vec{r}\to\vec{r}/|\vec{r}|\equiv\hat{r}$, one can express it as

$$\int\frac{d^3k}{(2\pi)^3}\frac{d^3l}{(2\pi)^3}\frac{\vec{r}\cdot(\vec{k}+\vec{l})}{(\vec{r}-\vec{l})^2\vec{l}^2(\vec{r}-\vec{k})^2\vec{k}^2|\vec{k}-\vec{l}|} = \frac{A}{|\vec{r}|}, \tag{A.27}$$

where A is a positive constant

$$A = \int\frac{d^3k}{(2\pi)^3}\frac{d^3l}{(2\pi)^3}\frac{1}{(\hat{r}-\vec{l})^2\vec{l}^2(\hat{r}-\vec{k})^2\vec{k}^2|\vec{k}-\vec{l}|}. \tag{A.28}$$

The above equality can be easily shown by shifting $\vec{k}\to\hat{r}-\vec{k}$, $\vec{l}\to\hat{r}-\vec{l}$. Finally, we have

$$\langle O^*(\vec{x})O(0)\rangle = \frac{N}{(4\pi)^2}\left(1+\frac{g_{YM}^2(N^2-1)}{N}\frac{A}{4}\right)\frac{1}{\vec{x}^2}. \tag{A.29}$$

A.3 $\bar{q}^1Zq^2$ two-point function

The next simplest chiral primary operator is of the form $\bar{q}Zq$. We divide the computation into two parts.

A.3.1 g_{YM}^2N terms

In this subsection, we focus on amplitudes with color structure that scale as g_{YM}^2N compared to the tree-level amplitude. These come from Feynman diagrams depicted in Figure A.3.

For each of the diagrams depicted in Figures A.3 (a) and (b), the amplitude is obtained to be

$$\frac{N^2-1}{2}\frac{N}{8}\int\frac{d^3k}{(2\pi)^3}\frac{d^3l}{(2\pi)^3}\frac{d^3m}{(2\pi)^3}\frac{1}{\vec{k}^2\vec{l}^2\vec{m}^2[(\vec{r}+\vec{m}-\vec{k})^2]^{\frac{1}{2}}[(\vec{r}+\vec{m}-\vec{l})^2]^{\frac{1}{2}}}. \tag{A.30}$$

For each A.3 (c) and (d), we have

$$\frac{N^2-1}{2}\frac{N}{2}\int \frac{d^4k}{(2\pi)^4}\frac{d^4l}{(2\pi)^4}\frac{d^3m}{(2\pi)^3}\frac{(\vec{k}+\vec{l})\cdot[2(\vec{r}+\vec{m})-(\vec{k}+\vec{l})]}{\vec{k}^2\vec{l}^2\vec{m}^2(r+m-l)^2(k-l)^2(r+m-k)^2}. \tag{A.31}$$

For each A.3 (e) and (f), we have

$$\frac{N^2-1}{2}\frac{N^2-1}{2N}\int \frac{d^3k}{(2\pi)^3}\frac{d^3l}{(2\pi)^3}\frac{d^3m}{(2\pi)^3}\frac{-1}{2\vec{k}^2[\vec{l}^2]^{\frac{1}{2}}\vec{m}^2(\vec{k}-\vec{l})^2[(\vec{r}+\vec{m}-\vec{k})^2]^{\frac{1}{2}}}. \tag{A.32}$$

Lastly, A.3 (g) gives a term of the form

$$\frac{N^2-1}{2}N\int \frac{d^4k}{(2\pi)^4}\frac{d^4l}{(2\pi)^4}\frac{d^3m}{(2\pi)^3}\frac{2}{\vec{k}^2\vec{m}^2l^2(l-(r+m-k))^2(r+m-k)^2.} \tag{A.33}$$

Wick rotating the momenta by taking $k^0 \to ik^0$, etc., keeping only terms that scale as N, and summing all the contributions leads to an expression with a common denominator

$$\frac{N}{4}\frac{1}{\vec{k}^2\vec{l}^2\vec{m}^2|\vec{r}+\vec{m}-\vec{k}||\vec{r}+\vec{m}-\vec{l}||\vec{k}-\vec{l}|\left(|\vec{r}+\vec{m}-\vec{k}|+|\vec{k}-\vec{l}|+|\vec{r}+\vec{m}-\vec{l}|\right)} \tag{A.34}$$

and numerator

$$\begin{aligned}&|\vec{k}-\vec{l}|\left(|\vec{r}+\vec{m}-\vec{k}|+|\vec{k}-\vec{l}|+|\vec{r}+\vec{m}-\vec{l}|\right)+\\&(\vec{k}+\vec{l})\cdot[(\vec{k}+\vec{l})-2(\vec{r}+\vec{m})]+\\&-2|\vec{r}+\vec{m}-\vec{l}|\left(|\vec{r}+\vec{m}-\vec{k}|+|\vec{k}-\vec{l}|+|\vec{r}+\vec{m}-\vec{l}|\right)+\\&-2\vec{l}^2.\end{aligned} \tag{A.35}$$

By noting that the denominator is left invariant under the exchange $\vec{k} \leftrightarrow \vec{l}$, we simplify the above numerator to

$$-2\left((\vec{r}+\vec{m})^2+|\vec{r}+\vec{m}-\vec{k}||\vec{r}+\vec{m}-\vec{l}|\right). \tag{A.36}$$

Finally, the total contribution with a color structure that scales as N compared to the tree-level amplitude can be written as

$$-\frac{N^2-1}{2}\frac{N}{2}\int \frac{d^3k}{(2\pi)^3}\frac{d^3l}{(2\pi)^3}\frac{d^3m}{(2\pi)^3}\times \tag{A.37}$$

$$\frac{(\vec{r}+\vec{m})^2+|\vec{r}+\vec{m}-\vec{k}||\vec{r}+\vec{m}-\vec{l}|}{\vec{k}^2\vec{l}^2\vec{m}^2|\vec{r}+\vec{m}-\vec{k}||\vec{r}+\vec{m}-\vec{l}||\vec{k}-\vec{l}|\left(|\vec{r}+\vec{m}-\vec{k}|+|\vec{k}-\vec{l}|+|\vec{r}+\vec{m}-\vec{l}|\right)}.$$

As before, re-scaling the momenta according to $\vec{r}\to\vec{r}/|\vec{r}|\equiv\hat{r}$, $\vec{k}\to\vec{k}/|\vec{r}|$, $\vec{l}\to\vec{l}/|\vec{r}|$ and $\vec{m}\to\vec{m}/|\vec{r}|$, the above expression can be simplified to

$$-\frac{N^2-1}{2}\frac{N}{2}|\vec{r}|A, \tag{A.38}$$

where A is a finite and non-zero numerical constant

$$A=\int\frac{d^3k}{(2\pi)^3}\frac{d^3l}{(2\pi)^3}\frac{d^3m}{(2\pi)^3}\frac{(\hat{r}+\vec{m})^2+|\hat{r}+\vec{m}-\vec{k}||\hat{r}+\vec{m}-\vec{l}|}{\vec{k}^2\vec{l}^2\vec{m}^2|\hat{r}+\vec{m}-\vec{k}||\hat{r}+\vec{m}-\vec{l}||\vec{k}-\vec{l}|} \tag{A.39}$$

$$\times\frac{1}{\left(|\hat{r}+\vec{m}-\vec{k}|+|\vec{k}-\vec{l}|+|\hat{r}+\vec{m}-\vec{l}|\right)}.$$

Lastly, fourier transforming $|\vec{r}|$ gives

$$\frac{N^2-1}{2}\frac{N}{2}\frac{A}{\pi^2[\vec{x}^2]^2} \tag{A.40}$$

as expected from conformal invariance and the fact that $\Delta_{\bar{q}Zq}=2$.

A.3.2 Other terms

All other contributions to the two-point function are depicted in Figure A.4.

For the Feynman graph shown in Figure A.4 (a), we have

$$\frac{N^2-1}{2}\left(1+\frac{1}{2N}\right)\int\frac{d^4k}{(2\pi)^4}\frac{d^3l}{(2\pi)^3}\frac{d^3m}{(2\pi)^3}\frac{i}{2\vec{k}^2[(\vec{r}-\vec{m})^2]^{\frac{1}{2}}(\vec{m}-\vec{k})^2\vec{l}^2(\vec{m}-\vec{l})^2}. \tag{A.41}$$

Similarly, we have for A.4 (b)

$$\frac{N^2-1}{2}\int\frac{d^4k}{(2\pi)^4}\frac{d^3l}{(2\pi)^3}\frac{d^3m}{(2\pi)^3}\frac{i(k^9)^2}{2\vec{k}^2[(\vec{r}-\vec{m})^2]^{\frac{1}{2}}(\vec{m}-\vec{k})^2\vec{l}^2(\vec{m}-\vec{l})^2(\vec{m}^2-(k^9)^2)}. \tag{A.42}$$

For A.4 (c), we have

$$\frac{N^2-1}{2}\frac{1}{2N}\int\frac{d^4k}{(2\pi)^4}\frac{d^3l}{(2\pi)^3}\frac{d^3m}{(2\pi)^3}\frac{i(k^9-l^9)^2}{2\vec{k}^2[(\vec{r}-\vec{m})^2]^{\frac{1}{2}}(\vec{m}-\vec{k})^2\vec{l}^2(\vec{m}-\vec{l})^2(k-l)^2}. \tag{A.43}$$

For A.4 (d), we have

$$\frac{N^2-1}{2}\frac{1}{2N}\int\frac{d^3k}{(2\pi)^3}\frac{d^3l}{(2\pi)^3}\frac{d^3m}{(2\pi)^3}\frac{(\vec{k}+\vec{l})\cdot\left(2\vec{m}-(\vec{k}+\vec{l})\right)}{4\vec{k}^2[(\vec{r}-\vec{m})^2]^{\frac{1}{2}}(\vec{m}-\vec{k})^2\vec{l}^2(\vec{m}-\vec{l})^2[(\vec{k}-\vec{l})^2]^{\frac{1}{2}}}. \quad \text{(A.44)}$$

Summing over all terms and including contributions that scale as $O(1)$ and $1/N$ compared to the tree-level amplitude from Feynman graphs A.3 (e) and (f) of the last subsection leads to

$$\frac{N^2-1}{2}\int\frac{d^3k}{(2\pi)^3}\frac{d^3l}{(2\pi)^3}\frac{d^3m}{(2\pi)^3}\qquad\left(-\frac{1}{4}\frac{|\vec{m}|}{\vec{k}^2\vec{l}^2(\vec{m}-\vec{k})^2(\vec{m}-\vec{l})^2|\vec{r}-\vec{m}|}+\right. \quad \text{(A.45)}$$

$$\left.+\frac{1}{2N}\frac{1}{4}\frac{2\vec{m}^2}{\vec{k}^2\vec{l}^2(\vec{m}-\vec{k})^2(\vec{m}-\vec{l})^2|\vec{r}-\vec{m}||\vec{k}-\vec{l}|}\right).$$

After rescaling the internal momenta as before and putting all the pieces together, the two-point function becomes

$$\langle\bar{q}^2\bar{Z}q^1(\vec{x})\bar{q}^1Zq^2(0)\rangle=\frac{N^2-1}{2}\frac{1}{[\vec{x}^2]^2}\left(\frac{1}{2(4\pi^2)^2}+\frac{g_{YM}^2}{\pi^2}\left(\frac{N}{2}A+B+\frac{1}{2N}C\right)\right), \quad \text{(A.46)}$$

where A, B, C are finite and non-vanishing constants defined in equations (A.39) and (A.45).

A.4 General case

In this section, we use induction to prove that the anomalous dimension vanishes for all chiral primary operators of the form $\bar{q}^2Z^kq^1$ where k is a nonnegative integer. Let $\{T^a\},\ a=1,\cdots,N^2-1$ denote the generators of Lie algebra of $SU(N)$ in the fundamental representation and $\{v^\alpha\}\ \ \alpha=1,\cdots,N$ be the canonical basis of $\mathbf{C^N}$ in which the fundametal representation lives. For example, $v^1=(1,0,\cdots,0)^T$. Define $N\times N$ matrices $C^{\alpha\beta}\equiv v^\alpha(v^\beta)^T$. Some useful identities of $SU(N)$ Lie algebra are summarized in appendix B. We also need the following set of identities:

$$C^{\alpha\beta}C^{\gamma\delta}=\delta^{\beta\gamma}C^{\alpha\delta},\ \ \sum_\alpha C^{\alpha\alpha}=\mathbf{1_{N\times N}},\ \ \mathrm{Tr}(\mathbf{C}^{\alpha\beta})=\delta^{\alpha\beta}, \quad \text{(A.47)}$$

$$[[C^{\alpha\beta},T^b],T^b]=NC^{\alpha\beta}-\delta^{\alpha\beta}\mathbf{1_{N\times N}}, \quad \text{(A.48)}$$

and

$$\sum_{i=1}^{k} \mathrm{Tr}(A_1 \cdots [A_i, B] \cdots A_k) = 0. \tag{A.49}$$

Consider the two-point function $\langle \bar{q}^2 \bar{Z}^k q^1(x) \bar{q}^1 Z^k q^2(0) \rangle$. We can treat the defect operator $\bar{q}^m Z^k q^n$ as a single trace operator by expressing it as $\mathrm{Tr}(q^n \bar{q}^m Z^k)$. There are 5 classes of Feynman diagrams that give rise to logarithmic divergences:

(A) Z self-energy.

(B) bulk quartic Z interaction and gauge boson exchange between two Z-legs.

(C) bulk-defect quartic interaction and gauge boson exchange between q-leg and Z-leg.

(D) q self-energy.

(E) F_V, $D_9 X_H^I$, and gauge boson exchange between two q-legs.

First of all, as discussed in [78], diagrams of the type (A) give a contribution of the form

$$A(\vec{x}) k N \sum_{\sigma} \mathrm{Tr}(C^{\alpha\beta} T^{a_1} \cdots T^{a_k}) \, \mathrm{Tr}(C^{\beta\alpha} T^{a_{\sigma(1)}} \cdots T^{a_{\sigma(k)}}), \tag{A.50}$$

where $A(\vec{x})$ is a function of x and independent of k and N. In order to derive the contribution from graphs of type (B), consider the bulk quartic Z interaction first. The relevant term in the Lagrangian is

$$-\mathrm{Tr}([Z, \bar{Z}][Z, \bar{Z}]). \tag{A.51}$$

We are interested in

$$-\langle \mathrm{Tr}(q^1 \bar{q}^2 \bar{Z}^k) \, \mathrm{Tr}([Z, \bar{Z}][Z, \bar{Z}]) \, \mathrm{Tr}(q^2 \bar{q}^1 Z^k) \rangle. \tag{A.52}$$

The color structure for the amplitude is given as

$$-\sum_{\sigma} \sum_{i \neq j} \mathrm{Tr}(C^{\alpha\beta} T^{a_1} \cdots T^{a_k}) \, \mathrm{Tr}([T^{a_{\sigma(i)}}, T^b][T^{a_{\sigma(j)}}, T^c]) \, \mathrm{Tr}(C^{\beta\alpha} T^{a_{\sigma(1)}} \cdots T^b \cdots T^c \cdots T^{a_{\sigma(k)}})$$

$$= -\sum_{\sigma} \sum_{i \neq j} \mathrm{Tr}(C^{\alpha\beta} T^{a_1} \cdots T^{a_k}) \, \frac{1}{2} \, i f^{a_{\sigma(i)} bd} \, i f^{a_{\sigma(j)} cd} \, \mathrm{Tr}(C^{\beta\alpha} T^{a_{\sigma(1)}} \cdots T^b \cdots T^c \cdots T^{a_{\sigma(k)}}) \tag{A.53}$$

$$= -\frac{1}{2} \sum_{\sigma} \sum_{i \neq j} \mathrm{Tr}(C^{\alpha\beta} T^{a_1} \cdots T^{a_k}) \, \mathrm{Tr}(C^{\beta\alpha} T^{a_{\sigma(1)}} \cdots (i f^{a_{\sigma(i)} db} T^b) \cdots (i f^{a_{\sigma(j)} dc} T^c) \cdots T^{a_{\sigma(k)}}) \tag{A.54}$$

$$= -\frac{1}{2}\sum_{\sigma}\sum_{i\neq j}\ \mathrm{Tr}(C^{\alpha\beta}T^{a_1}\cdots T^{a_k})\ \mathrm{Tr}(C^{\beta\alpha}T^{a_{\sigma(1)}}\cdots[T^{a_{\sigma(i)}},T^d]\cdots[T^{a_{\sigma(j)}},T^d]\cdots T^{a_{\sigma(k)}}) \quad \text{(A.55)}$$

using the identity given in equation (A.49) we sum over j first, (A.56)

$$= \frac{1}{2}\sum_{\sigma}\sum_{i}\ \mathrm{Tr}(C^{\alpha\beta}T^{a_1}\cdots T^{a_k})\ \Big\{\mathrm{Tr}(C^{\beta\alpha}T^{a_{\sigma(1)}}\cdots[[T^{a_{\sigma(i)}},T^d],T^d]\cdots T^{a_{\sigma(k)}})+ \quad \text{(A.57)}$$

$$+\mathrm{Tr}([C^{\beta\alpha},T^d]T^{a_{\sigma(1)}}\cdots[T^{a_{\sigma(i)}},T^d]\cdots T^{a_{\sigma(k)}})\Big\} \quad \text{(A.58)}$$

using once more the identity given in equation (A.49) to sum over i yields (A.59)

$$= \frac{1}{2}\sum_{\sigma}\ \mathrm{Tr}(C^{\alpha\beta}T^{a_1}\cdots T^{a_k})\ \Big\{kN\mathrm{Tr}(C^{\beta\alpha}T^{a_{\sigma(1)}}\cdots T^{a_{\sigma(k)}})-\mathrm{Tr}([[C^{\beta\alpha},T^d],T^d]T^{a_{\sigma(1)}}\cdots T^{a_{\sigma(k)}})\Big\}$$

$$= \frac{1}{2}kN\sum_{\sigma}\ \mathrm{Tr}(C^{\alpha\beta}T^{a_1}\cdots T^{a_k})\ \mathrm{Tr}(C^{\beta\alpha}T^{a_{\sigma(1)}}\cdots T^{a_{\sigma(k)}}) \quad \text{(A.60)}$$

$$-\frac{1}{2}\sum_{\sigma}\ \mathrm{Tr}(C^{\alpha\beta}T^{a_1}\cdots T^{a_k})\ \mathrm{Tr}([[C^{\beta\alpha},T^d],T^d]T^{a_{\sigma(1)}}\cdots T^{a_{\sigma(k)}}). \quad \text{(A.61)}$$

The gauge boson exchange diagram has exactly the same color structure. Together, (B) gives

$$B(\vec{x})\Big\{kN\sum_{\sigma}\ \mathrm{Tr}(C^{\alpha\beta}T^{a_1}\cdots T^{a_k})\ \mathrm{Tr}(C^{\beta\alpha}T^{a_{\sigma(1)}}\cdots T^{a_{\sigma(k)}}) \quad \text{(A.62)}$$

$$-\sum_{\sigma}\ \mathrm{Tr}(C^{\alpha\beta}T^{a_1}\cdots T^{a_k})\ \mathrm{Tr}([[C^{\beta\alpha},T^d],T^d]T^{a_{\sigma(1)}}\cdots T^{a_{\sigma(k)}})\Big\}, \quad \text{(A.63)}$$

where we have absorbed a numerical factor independent of k and N into the definition of $B(\vec{x})$. For the bulk-defect quartic interaction terms which are of the type (C), the relevant terms in the defect Lagrangian are

$$\mathrm{Tr}(q^1\bar{q}^1[Z,\bar{Z}])-\mathrm{Tr}(q^2\bar{q}^2[Z,\bar{Z}]). \quad \text{(A.64)}$$

The second term simply gives the same result as the first one, and so we just consider the first term here. At g_{YM}^2,

$$\langle\mathrm{Tr}(q^1\bar{q}^2\bar{Z}^k)\ \mathrm{Tr}(q^1\bar{q}^1[Z,\bar{Z}])\ \mathrm{Tr}(q^2\bar{q}^1Z^k)\rangle. \quad \text{(A.65)}$$

Then, the color structure is

$$\sum_{\sigma}\sum_{i}\mathrm{Tr}(C^{\alpha\beta}T^{a_1}\cdots T^{a_k})\ \mathrm{Tr}(C^{\gamma\alpha}[T^{a_{\sigma(i)}},T^b])\ \mathrm{Tr}(C^{\beta\gamma}T^{a_{\sigma(1)}}\cdots T^{a_{\sigma(i-1)}}T^bT^{a_{\sigma(i+1)}}\cdots T^{a_{\sigma(k)}})$$

$$= \sum_\sigma \sum_i \mathrm{Tr}(C^{\alpha\beta} T^{a_1} \cdots T^{a_k})\ \mathrm{Tr}([C^{\gamma\alpha}, T^{a_{\sigma(i)}}] T^b)\ \mathrm{Tr}(T^{a_{\sigma(i+1)}} \cdots T^{a_{\sigma(k)}} C^{\beta\gamma} T^{a_{\sigma(1)}} \cdots T^{a_{\sigma(i-1)}} T^b)$$

$$= \sum_\sigma \sum_i \mathrm{Tr}(C^{\alpha\beta} T^{a_1} \cdots T^{a_k})\ \Big\{ \frac{1}{2} \mathrm{Tr}(C^{\beta\gamma} T^{a_{\sigma(1)}} \cdots [C^{\gamma\alpha}, T^{a_{\sigma(i)}}] \cdots T^{a_{\sigma(k)}}) \tag{A.66}$$

$$- \frac{1}{2N} \mathrm{Tr}([C^{\gamma\alpha}, T^{a_{\sigma(i)}}])\ \mathrm{Tr}(T^{a_{\sigma(i+1)}} \cdots T^{a_{\sigma(k)}} C^{\beta\gamma} T^{a_{\sigma(1)}} \cdots T^{a_{\sigma(i-1)}}) \Big\} \tag{A.67}$$

where the second term vanishes, (A.68)

$$= \frac{1}{2} \sum_\sigma \mathrm{Tr}(C^{\alpha\beta} T^{a_1} \cdots T^{a_k})\ \sum_i \mathrm{Tr}(C^{\beta\gamma} T^{a_{\sigma(1)}} \cdots [C^{\gamma\alpha}, T^{a_{\sigma(i)}}] \cdots T^{a_{\sigma(k)}}) \tag{A.69}$$

using the identity given in equation (A.49), (A.70)

$$= -\frac{1}{2} \sum_\sigma \mathrm{Tr}(C^{\alpha\beta} T^{a_1} \cdots T^{a_k})\ \mathrm{Tr}([C^{\gamma\alpha}, C^{\beta\gamma}] T^{a_{\sigma(1)}} \cdots T^{a_{\sigma(k)}}). \tag{A.71}$$

(A.72)

The gauge boson exchange part of (C) has the following color structure:

$$\langle \mathrm{Tr}(q^1 \bar{q}^2 \bar{Z}^k)\ \mathrm{Tr}(q^1 \bar{q}^1 A_\mu)\ \mathrm{Tr}(\bar{Z}[A_\mu, Z])\ \mathrm{Tr}(q^2 \bar{q}^1 Z^k) \rangle \tag{A.73}$$

$$\to \sum_\sigma \sum_i \mathrm{Tr}(C^{\alpha\beta} T^{a_1} \cdots T^{a_k})\ \mathrm{Tr}(C^{\gamma\alpha} T^b)\ \mathrm{Tr}(T^c [T^b, T^{a_{\sigma(i)}}])$$

$$\times \mathrm{Tr}(C^{\beta\gamma} T^{a_{\sigma(1)}} \cdots T^{a_{\sigma(i-1)}} T^c T^{a_{\sigma(i+1)}} \cdots T^{a_{\sigma(k)}})$$

$$= \sum_\sigma \sum_i \mathrm{Tr}(C^{\alpha\beta} T^{a_1} \cdots T^{a_k})\ \mathrm{Tr}(C^{\gamma\alpha} T^b)\ \mathrm{Tr}([T^{a_{\sigma(i)}}, T^c] T^b)$$

$$\times \mathrm{Tr}(C^{\beta\gamma} T^{a_{\sigma(1)}} \cdots T^{a_{\sigma(i-1)}} T^c T^{a_{\sigma(i+1)}} \cdots T^{a_{\sigma(k)}})$$

$$= \frac{1}{2} \sum_\sigma \sum_i \mathrm{Tr}(C^{\alpha\beta} T^{a_1} \cdots T^{a_k})\ \mathrm{Tr}(C^{\gamma\alpha} [T^{a_{\sigma(i)}}, T^c])\ \mathrm{Tr}(C^{\beta\gamma} T^{a_{\sigma(1)}} \cdots T^{a_{\sigma(i-1)}} T^c T^{a_{\sigma(i+1)}} \cdots T^{a_{\sigma(k)}})$$

$$= \frac{1}{2} \sum_\sigma \sum_i \mathrm{Tr}(C^{\alpha\beta} T^{a_1} \cdots T^{a_k})\ \mathrm{Tr}([C^{\gamma\alpha}, T^{a_{\sigma(i)}}] T^c)\ \mathrm{Tr}(C^{\beta\gamma} T^{a_{\sigma(1)}} \cdots T^{a_{\sigma(i-1)}} T^c T^{a_{\sigma(i+1)}} \cdots T^{a_{\sigma(k)}})$$

$$= \frac{1}{4} \sum_\sigma \sum_i \mathrm{Tr}(C^{\alpha\beta} T^{a_1} \cdots T^{a_k})\ \mathrm{Tr}(C^{\beta\gamma} T^{a_{\sigma(1)}} \cdots T^{a_{\sigma(i-1)}} [C^{\gamma\alpha}, T^{a_{\sigma(i)}}] T^{a_{\sigma(i+1)}} \cdots T^{a_{\sigma(k)}})$$

$$= -\frac{1}{4} \sum_\sigma \mathrm{Tr}(C^{\alpha\beta} T^{a_1} \cdots T^{a_k})\ \mathrm{Tr}([C^{\gamma\alpha}, C^{\beta\gamma}] T^{a_{\sigma(1)}} \cdots T^{a_{\sigma(k)}}).$$

The result is the same as the bulk-defect quartic interaction up to a numerical factor. Together, (C) contributes with

$$C(\vec{x})\sum_{\sigma}\mathrm{Tr}(C^{\alpha\beta}T^{a_1}\cdots T^{a_k})\ \mathrm{Tr}([C^{\gamma\alpha},C^{\beta\gamma}]T^{a_{\sigma(1)}}\cdots T^{a_{\sigma(k)}}) \tag{A.74}$$

Now consider the terms coming from Feynman graphs of type (D). There are many diagrams in this group but all of them have the same color structure. In the following, we compute the gauge boson loop diagram to obtain

$$\begin{aligned}
&\langle \mathrm{Tr}(q^1\bar{q}^2\bar{Z}^k)\ \mathrm{Tr}(q^1\bar{q}^1A_\mu)\ \mathrm{Tr}(q^1\bar{q}^1A_\mu)\ \mathrm{Tr}(q^2\bar{q}^1Z^k)\rangle \qquad (A.75)\\
\to\ &\sum_{\sigma}\mathrm{Tr}(C^{\alpha\beta}T^{a_1}\cdots T^{a_k})\ \underbrace{\mathrm{Tr}(C^{\rho\alpha}T^b)\ \mathrm{Tr}(C^{\gamma\rho}T^b)}_{\frac{1}{2}\mathrm{Tr}(C^{\rho\alpha}C^{\gamma\rho})-\frac{1}{2N}\mathrm{Tr}(C^{\rho\alpha})\mathrm{Tr}(C^{\gamma\rho})}\ \mathrm{Tr}(C^{\beta\gamma}T^{a_{\sigma(1)}}\cdots T^{a_{\sigma(k)}})\\
=\ &\frac{N^2-1}{2N}\sum_{\sigma}\mathrm{Tr}(C^{\alpha\beta}T^{a_1}\cdots T^{a_k})\ \mathrm{Tr}(C^{\beta\alpha}T^{a_{\sigma(1)}}\cdots T^{a_{\sigma(k)}})
\end{aligned}$$

Together, (D) gives a contribution of the form

$$D(\vec{x})\frac{N^2-1}{N}\sum_{\sigma}\mathrm{Tr}(C^{\alpha\beta}T^{a_1}\cdots T^{a_k})\ \mathrm{Tr}(C^{\beta\alpha}T^{a_{\sigma(1)}}\cdots T^{a_{\sigma(k)}}) \tag{A.76}$$

Lastly, let us compute the color structure of (E). Again three diagrams give the same structure. For instance, the gauge boson exchange diagram gives

$$\begin{aligned}
&\langle \mathrm{Tr}(q^1\bar{q}^2\bar{Z}^k)\ \mathrm{Tr}(q^2\bar{q}^2A_\mu)\ \mathrm{Tr}(q^1\bar{q}^1A_\mu)\ \mathrm{Tr}(q^2\bar{q}^1Z^k)\rangle \qquad (A.77)\\
\to\ &\sum_{\sigma}\mathrm{Tr}(C^{\alpha\beta}T^{a_1}\cdots T^{a_k})\ \underbrace{\mathrm{Tr}(C^{\beta\gamma}T^b)\ \mathrm{Tr}(C^{\rho\alpha}T^b)}_{\frac{1}{2}\mathrm{Tr}(C^{\beta\gamma}C^{\rho\alpha})-\frac{1}{2N}\mathrm{Tr}(C^{\beta\gamma})\mathrm{Tr}(C^{\rho\alpha})}\ \mathrm{Tr}(C^{\gamma\rho}T^{a_{\sigma(1)}}\cdots T^{a_{\sigma(k)}})\\
=\ &\frac{1}{2}\sum_{\sigma}\mathrm{Tr}(T^{a_1}\cdots T^{a_k})\ \mathrm{Tr}(T^{a_{\sigma(1)}}\cdots T^{a_{\sigma(k)}})-\frac{1}{2N}\mathrm{Tr}(C^{\alpha\beta}T^{a_1}\cdots T^{a_k})\ \mathrm{Tr}(C^{\beta\alpha}T^{a_{\sigma(1)}}\cdots T^{a_{\sigma(k)}}).
\end{aligned}$$

Hence, Feynman graphs of type (E) give a contribution of the form

$$\begin{aligned}
E(\vec{x})\Big\{&\sum_{\sigma}\mathrm{Tr}(T^{a_1}\cdots T^{a_k})\ \mathrm{Tr}(T^{a_{\sigma(1)}}\cdots T^{a_{\sigma(k)}}) \qquad (A.78)\\
&-\frac{1}{N}\sum_{\sigma}\mathrm{Tr}(C^{\alpha\beta}T^{a_1}\cdots T^{a_k})\ \mathrm{Tr}(C^{\beta\alpha}T^{a_{\sigma(1)}}\cdots T^{a_{\sigma(k)}})\Big\}.
\end{aligned}$$

Putting all the results together and thanks to the following identity:

$$[[C^{\beta\alpha},T^d],T^d]=NC^{\beta\alpha}-\delta^{\alpha\beta}\mathbf{1}_{\mathbf{N}\times\mathbf{N}}=-[\mathbf{C}^{\gamma\alpha},\mathbf{C}^{\beta\gamma}], \tag{A.79}$$

we can express the result in terms of only two types of color structure given by

$$\mathcal{B}(k,N) = \sum_{\sigma} \mathrm{Tr}(T^{a_1}\cdots T^{a_k})\ \mathrm{Tr}(T^{a_{\sigma(1)}}\cdots T^{a_{\sigma(k)}}), \tag{A.80}$$

$$\mathcal{D}(k,N) = \sum_{\sigma} \mathrm{Tr}(C^{\alpha\beta}T^{a_1}\cdots T^{a_k})\ \mathrm{Tr}(C^{\beta\alpha}T^{a_{\sigma(1)}}\cdots T^{a_{\sigma(k)}}). \tag{A.81}$$

Altogether, we have

$$\begin{aligned}&\Big[kN(A(\vec{x})+B(\vec{x}))+N(D(\vec{x})-B(\vec{x})-C(\vec{x}))-\frac{1}{N}(D(\vec{x})+E(\vec{x}))\Big] \\ &\times\mathcal{D}(k,N)+[B(\vec{x})+C(\vec{x})+E(\vec{x})]\mathcal{B}(k,N).\end{aligned} \tag{A.82}$$

Notice that the functions $A(\vec{x}), B(\vec{x}), C(\vec{x}), D(\vec{x}), E(\vec{x})$ are independent of both k and N and we can evaluate them for any convenient value of k and N.
As argued in [78],

$$A(\vec{x})+B(\vec{x})=0. \tag{A.83}$$

When $k=1$, we have $\mathcal{B}(1,N)=0$ and the amplitude simplifies to

$$\Big[N(D(\vec{x})-B(\vec{x})-C(\vec{x}))-\frac{1}{N}(D(\vec{x})+E(\vec{x}))\Big]\mathcal{D}(k,N) \tag{A.84}$$

From the result obtained in the previous section, we know the logarithmic pieces cancel for all N and conclude that

$$D(\vec{x})-B(\vec{x})-C(\vec{x})=finite, \quad D(\vec{x})+E(\vec{x})=finite. \tag{A.85}$$

These equations together imply that

$$B(\vec{x})+C(\vec{x})+E(\vec{x})=finite. \tag{A.86}$$

Therefore, logarithmically diverging terms in Eq. (A.82) cancel out for any value of k and N, and the dimension of pinned operators of the form $\bar{q}^2Z^kq^1$ are not renormalized. This gives a convincing support that these operators are indeed chiral primaries of the defect conformal field theory. In this section, we have ignored some Feynman diagrams such as figure A.4 (b) because they are finite. Unlike the CPO's of the usual $\mathcal{N}=4$ SYM gauge theory, the CPO's of the defect conformal field theory considered in this appendix are renormalized and receive a finite contribution. As

mentioned in the discussion of Chapter 1, this may ruin the specific PP-wave/dCFT duality we have constructed since the amplitude blows up in the Penrose limit. It would be highly interesting if this shortfall can be overcome by employing a different renormalization scheme or by comparing ratios of amplitudes instead.

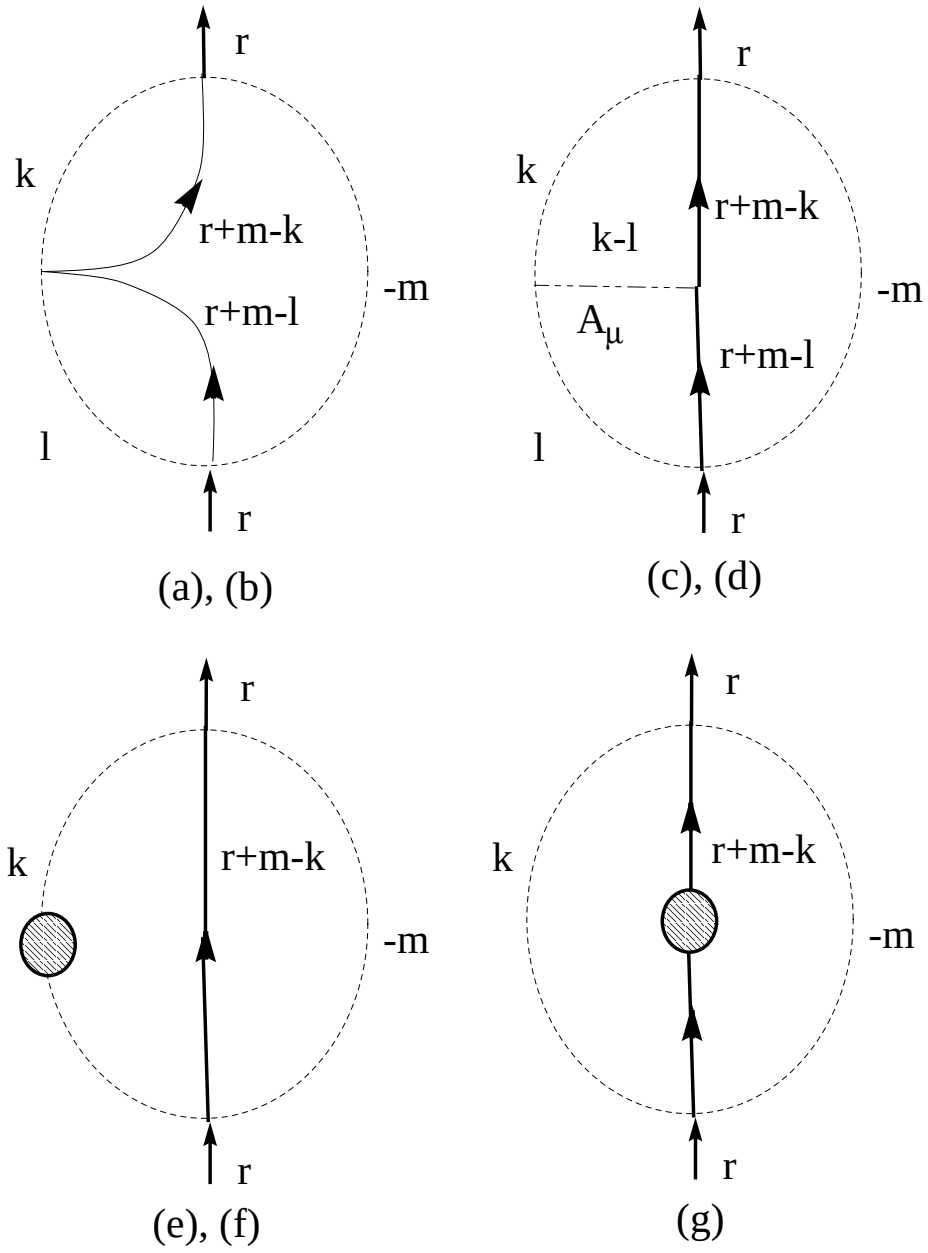

Figure A.3: $O(g_{YM}^2)$ self-energy correction to $\bar{q}^1 Z q^2$ 2 point function which scales as N compared to the free part.

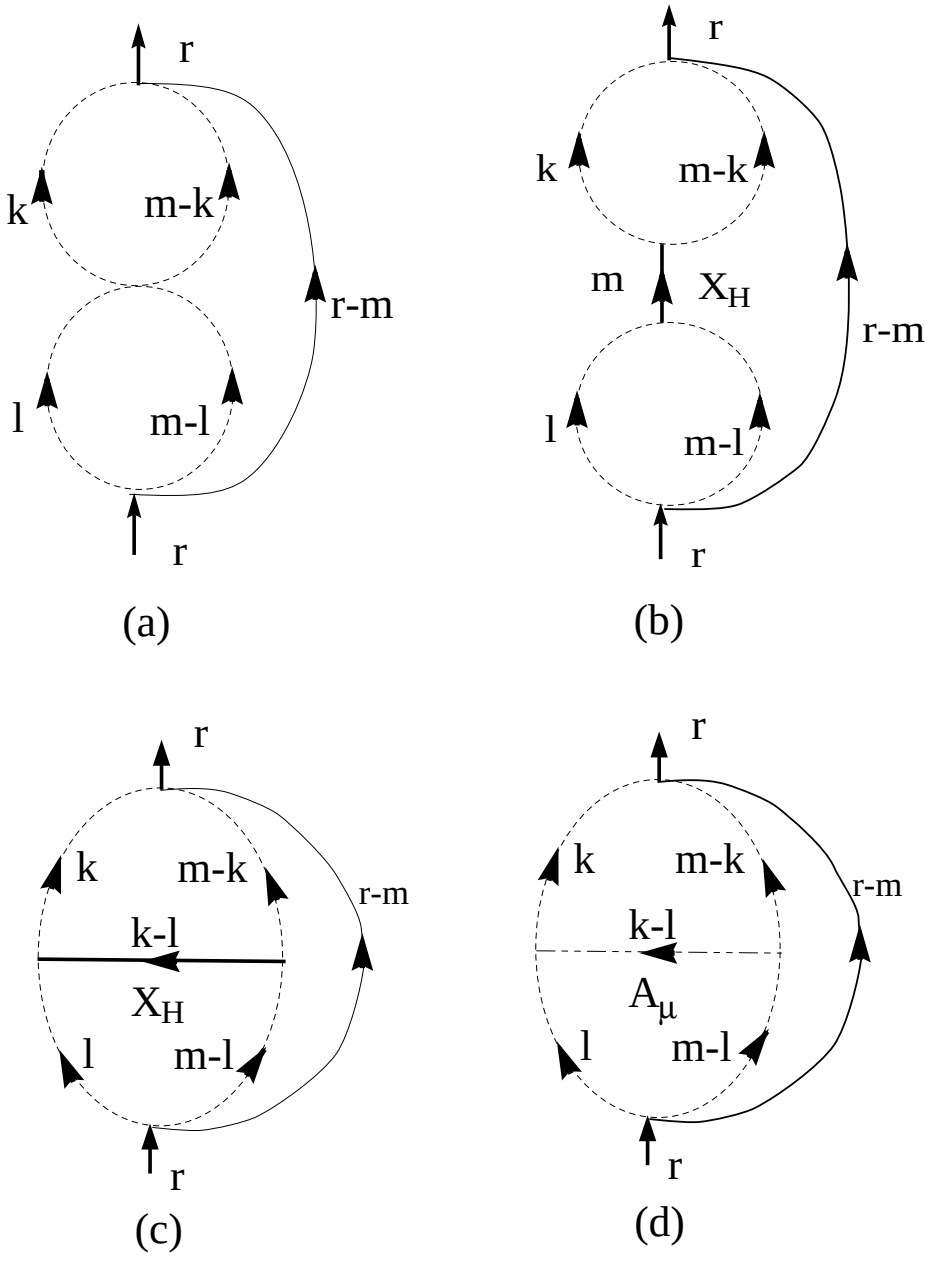

Figure A.4: Other $O(g_{YM}^2)$ self-energy corrections to $\bar{q}^1 Z q^2$ 2 point function.

Appendix B

Useful Formulae for dCFT

For fundamental representation of SU(N) t^a such that $[t^a, t^b] = if^{abc}t^c$, we have

$$\mathrm{Tr}[t^a, t^b] = \frac{1}{2}\delta^{ab}, \quad t^a t^a = \frac{N^2-1}{2N}\mathbf{1}, \tag{B.1}$$

$$f^{acd}f^{bcd} = N\delta^{ab}, \quad f^{abc}t^b t^c = \frac{N}{2}it^a, \tag{B.2}$$

$$(t^a)_{ij}(t^a)_{kl} = \frac{1}{2}\left(\delta_{il}\delta_{kj} - \frac{1}{N}\delta_{ij}\delta_{kl}\right). \tag{B.3}$$

Some d-dimensional integrals in **Minkowski** space are given by

$$\int \frac{d^d l}{(2\pi)^d}\frac{1}{(l^2-\Delta)^n} = \frac{(-1)^n i}{(4\pi)^{d/2}}\frac{\Gamma(n-\frac{d}{2})}{\Gamma(n)}\left(\frac{1}{\Delta}\right)^{n-\frac{d}{2}}, \tag{B.4}$$

$$\int \frac{d^d l}{(2\pi)^d}\frac{l^2}{(l^2-\Delta)^{n-1}} = \frac{(-1)^n i}{(4\pi)^{d/2}}\frac{d}{2}\frac{\Gamma(n-\frac{d}{2}-1)}{\Gamma(n)}\left(\frac{1}{\Delta}\right)^{n-\frac{d}{2}-1}. \tag{B.5}$$

Other useful integrals are

$$\int \frac{dx}{2\pi}\frac{1}{(a^2+(x+c)^2)(b^2+x^2)} = \frac{|a|+|b|}{2|a||b|\left[(|a|+|b|)^2+c^2\right]}, \tag{B.6}$$

$$\int \frac{dxdy}{(2\pi)^2}\frac{1}{(x^2+a^2)(y^2+b^2)[(x-y)^2+c^2]} = \frac{1}{4|a||b||c|\left(|a|+|b|+|c|\right)}, \tag{B.7}$$

$$\int \frac{dxdy}{(2\pi)^2}\frac{(x-y)^2}{(x^2+a^2)(y^2+b^2)[(x-y)^2+c^2]} = \frac{|a|+|b|}{4|a||b|\left(|a|+|b|+|c|\right)}. \tag{B.8}$$

Appendix C

Coordinate Systems for AdS_3

The space AdS_3 is defined as the hyperboloid

$$(X^0)^2 - (X^1)^2 - (X^2)^2 + (X^3)^2 = R^2\,, \tag{C.1}$$

embedded in $\mathbf{R}^{2,2}$. The metric

$$ds^2 = -(dX^0)^2 + (dX^1)^2 + (dX^2)^2 - (dX^3)^2 \tag{C.2}$$

on $\mathbf{R}^{2,2}$ induces a metric of constant negative curvature on AdS_3. The quantity R that appears in (C.1) is the *anti-de Sitter radius*; for convenience, we set $R = 1$. In addition, to avoid closed timelike curves, we work not with the hyperboloid (C.1) itself, but with its universal cover.

The two coordinate systems we use most extensively are *global coordinates* and *AdS_2 coordinates*. The global coordinates (ρ, θ, τ) are defined by

$$X^0 + iX^3 = \cosh\rho\, e^{it}\,, \qquad X^1 + iX^2 = -\sinh\rho\, e^{-i\theta}\,. \tag{C.3}$$

The range of the radial coordinate ρ is $0 \le \rho < \infty$; the angular coordinate θ ranges over $0 \le \theta < 2\pi$; and the global time coordinate t may be any real number. The AdS_3 metric in global coordinates is

$$ds^2 = -\cosh^2\rho\, dt^2 + d\rho^2 + \sinh^2\rho\, d\theta^2\,. \tag{C.4}$$

The AdS_2 coordinates (ψ, ω, t) are particularly well adapted to the AdS_2 branes we consider in Sections 3.4 and 3.5. They are defined by

$$X^1 = \cosh\psi \sinh\omega\,, \qquad X^2 = \sinh\psi\,, \qquad X^0 + iX^3 = \cosh\psi\cosh\omega\, e^{it}\,. \tag{C.5}$$

All three AdS_2 coordinates range over the entire real line. In this parametrization, the fixed ψ slices have the geometry of AdS_2. The AdS_3 metric in AdS_2 coordinates takes the form

$$ds^2 = d\psi^2 + \cosh^2\psi\,(-\cosh^2\omega\,dt^2 + d\omega^2)\,; \tag{C.6}$$

the quantity in parentheses is the metric of the AdS_2 subspace at fixed ψ. The transformation between global and AdS_2 coordinates is

$$\sinh\psi = \sin\theta\sinh\rho\,, \qquad \cosh\psi\sinh\omega = -\cos\theta\sinh\rho\,. \tag{C.7}$$

The global time t is the same in both coordinate systems.

The space AdS_3 is the group manifold of the group $SL(2,R)$. A point in AdS_3 is given by the $SL(2,R)$ matrix

$$g = \begin{pmatrix} X^0 + X^1 & X^2 + X^3 \\ X^2 - X^3 & X^0 - X^1 \end{pmatrix}. \tag{C.8}$$

In the global coordinate system,

$$g = \begin{pmatrix} \cos t\cosh\rho - \cos\theta\sinh\rho & \sin t\cosh\rho + \sin\theta\sinh\rho \\ -\sin t\cosh\rho + \sin\theta\sinh\rho & \cos t\cosh\rho + \cos\theta\sinh\rho \end{pmatrix}. \tag{C.9}$$

Appendix D

A Partition Function Calculation of the Open String Spectrum

In this appendix, we explicitly verify the proposal presented in Section 3.4.2 for the open-string spectrum. First, in Section D.1, we compute the worldsheet one-loop partition function $\mathcal{Z}$ for open string theory on Euclidean AdS_3 at finite temperature $1/\beta$. The partition function is proportional to the single-particle contribution to the space-time free energy, $\mathcal{Z} = -\beta F$. The free energy, in turn, can be written as

$$F = \frac{1}{\beta} \sum_{s \in \mathcal{H}} \log \left(1 - e^{-\beta E_s}\right) , \tag{D.1}$$

where the sum is over states s in the physical Hilbert space $\mathcal{H}$ of single-string states, and E_s is the energy of the state s.[1] By writing $\mathcal{Z}$ in the right form, we can thus read off the spectrum of open strings in (Lorentzian) AdS_3. We show in Section D.2 that the spectrum breaks up into a sum over discrete states and an integral over a continuum, with energies agreeing with the expressions found in Section 3.4. Moreover, we compute the density of states of the continuum.

Our calculation is patterned on the one done in [36] for closed strings in AdS_3. Especially in Section D.1, we emphasize here those features that are novel in the open string case; the reader seeking greater detail is directed to [36] and the references

[1] We work at zero chemical potential.

therein.

One point is worth clarifying at the outset. Though the free energy whose form we undertake to calculate receives contributions only from states in the physical Hilbert space of the string, our calculation is sufficient to confirm our proposal for the spectrum of the WZW model. The physical Hilbert space is the tensor product of a Hilbert space of AdS_3 excitations and a Hilbert space associated with the "internal" manifold $\mathcal{M}$. For our purposes, we can take the spectrum of the internal conformal field theory to be arbitrary. One of the physical state conditions is $L_0 + h = 1$, where L_0 is the zeroth Virasoro generator of the AdS_3 conformal field theory, and h is a conformal weight in the conformal field theory on $\mathcal{M}$. This condition can be seen as parametrizing the spectrum of L_0 in the WZW model. The remaining physical state conditions, $L_n + L_n^{\mathcal{M}} = 0$, with $n \geq 1$, relate the Virasoro generators in the AdS_3 and internal conformal field theories. They can be solved within the tensor product of an irreducible representation of $\widehat{SL}(2,R)$ with some subspace of the internal conformal field theory state space. Therefore, given the physical string spectrum in AdS_3, it is possible to deduce how the Hilbert space of the WZW model is decomposed into a sum of irreducible representations of $\widehat{SL}(2,R)$. This is why the one-loop free energy computation below, though it is carried out in the physical string Hilbert space, is nonetheless relevant to the spectrum of the WZW model.

D.1 The one-loop partition function

Our first business is to write the WZW action for Euclidean AdS_3 at finite temperature and the boundary conditions appropriate to a flat AdS_2 brane. We define the coordinates $(v, \bar{v}, \phi)$ on Euclidean AdS_3 by

$$v = \sinh\rho\, e^{i\theta}\,, \tag{D.2}$$

$$\bar{v} = \sinh\rho\, e^{-i\theta}\,, \tag{D.3}$$

$$\phi = t - \log\cosh\rho\,, \tag{D.4}$$

where (ρ, θ, t) are global coordinates. The metric in these coordinates is [54]

$$ds^2 = k\left(d\phi^2 + (dv + v d\phi)(d\bar{v} + \bar{v} d\phi)\right) , \tag{D.5}$$

where k is the square of the anti-de Sitter radius, and is identified with the level of the WZW model. Euclidean AdS_3 is the coset manifold $SL(2,C)/SU(2)$; in the coordinates (D.2), a general element is written as

$$g = \begin{pmatrix} e^{\phi}(1 + |v|^2) & v \\ \bar{v} & e^{-\phi} \end{pmatrix} . \tag{D.6}$$

Thermal AdS_3 is given by the identification

$$t \sim t + \beta \, , \tag{D.7}$$

where β is the inverse temperature. In the coordinates (D.2), this translates to

$$\phi \sim \phi + \beta \, . \tag{D.8}$$

The WZW action in the coordinates (D.2) is[2]

$$S = \frac{k}{\pi} \int d^2 z \left(\partial\phi \, \bar{\partial}\phi + (\partial\bar{v} + \partial\phi \, \bar{v})(\bar{\partial} v + \bar{\partial}\phi \, v)\right) . \tag{D.9}$$

Throughout this calculation, we take the worldsheet to be Euclidean. In addition, we alternate between real (σ, τ) and complex conjugate $(z, \bar{z})$ worldsheet coordinates. The relation between the two sets is

$$z = \sigma + i\tau \, , \qquad \partial \equiv \frac{\partial}{\partial z} \, . \tag{D.10}$$

and similarly for $\bar{z}$ and $\bar{\partial}$.

[2]The action given here differs from the WZW model Lagrangian given in Section 3.5.4 by boundary terms that can be ignored only if the straight brane boundary condition (D.11) holds. If the AdS_2 brane is curved, these terms must be included. The action then becomes considerably more complicated, and loses some of the special properties that make possible the partition function calculation described below.

In the coordinates (D.2), the boundary conditions suitable for open strings ending on a straight AdS_2 brane are

$$v_2 = 0\,, \tag{D.11}$$

$$\partial_\sigma v_1 = 0\,, \tag{D.12}$$

$$\partial_\sigma \phi = 0\,, \tag{D.13}$$

where v_1 and v_2 are, respectively, the real and imaginary parts of v.

The one-loop open string partition function is obtained by considering worldsheets with the topology of a cylinder. As usual, $0 \leq \sigma \leq \pi$. The worldsheet is made cylindrical by imposing the periodicity

$$\tau \sim \tau + 2\pi t\,. \tag{D.14}$$

Here (and henceforth) t is simply a modulus, and is not to be confused with the global time coordinate. The space-time periodicity $\phi \sim \phi + \beta$ of thermal AdS_3 implies

$$\phi(\sigma, \tau + 2\pi t) = \phi(\sigma, \tau) + \beta n\,, \tag{D.15}$$

for some integer n. If we define

$$u_n = \frac{n\tau}{4\pi t} \tag{D.16}$$

and

$$\hat{\phi} = \phi - 2\beta u_n\,, \tag{D.17}$$

then $\hat{\phi}$ is periodic in τ, *i.e.*, $\hat{\phi}(\tau + 2\pi t) = \hat{\phi}(\tau)$. The WZW action may be written in terms of $\hat{\phi}$ as

$$S = \frac{k\beta^2 n^2}{8\pi t} + \frac{k}{\pi}\int d^2z \left(|\partial\hat{\phi}|^2 + |(\partial - iu_n + \partial\hat{\phi})\bar{v}|^2\right)\,. \tag{D.18}$$

The partition function for Euclidean AdS_3 is

$$\mathcal{Z}_n(\beta) \equiv \int \mathcal{D}\hat{\phi}\,\mathcal{D}v\,\mathcal{D}\bar{v}\,e^{-S}\,, \tag{D.19}$$

summed over n. The rest of this section is devoted to evaluating the functional integrals in (D.19).

The second term in parentheses in (D.18) couples ϕ, v, and $\bar{v}$. The field $\hat{\phi}$ can be disentangled from v and $\bar{v}$ using a standard chiral gauge transformation and the chiral anomaly formulae familiar from the closed string calculation. This procedure is valid in the open string case as well, since the string boundary conditions are left invariant by the chiral transformation. The partition function then factorizes into a functional integral over $\hat{\phi}$ and a functional integral over v and $\bar{v}$, multiplied by the constant $e^{-k\beta^2 n^2/8\pi t}$ coming from the constant term in the action. The $\hat{\phi}$ functional integral is standard [79], and, up to normalization, yields

$$\mathcal{Z}_{\hat{\phi}} = \frac{\beta(k-2)^{1/2}}{t^{1/2}|\eta(it)|}\,, \tag{D.20}$$

where η is the Dedekind eta function. The remaining functional integral may be written as

$$\mathcal{Z}_v = \int \mathcal{D}v\,\mathcal{D}\bar{v}e^{-S_v}\,, \tag{D.21}$$

where

$$S_v = \frac{k}{\pi}\int d^2z|(\partial - iu_n)\bar{v}|^2. \tag{D.22}$$

Integrating S_v by parts gives

$$S_v = -\frac{k}{\pi}\left(\int_\Sigma d^2z\,\bar{v}\,(\partial + iu_n)\,(\bar{\partial} + iu_n)\,v + \int_{\partial\Sigma} d\bar{z}\,v_1\,\partial_\sigma v_2 - u_n\int_{\partial\Sigma} d\bar{z}\,v_1 v_1\right)\,, \tag{D.23}$$

where Σ denotes the worldsheet cylinder. Note that the two boundary terms are pure imaginary.

Let us work on the bulk term in (D.23). We begin by expanding v_1 and v_2 in a complete basis of functions. The boundary conditions (D.11) and (D.12) dictate the expansions

$$v_1(\sigma,\tau) = \sum_{M\geq 0, N\in\mathbf{Z}} a_{MN}\frac{1}{\pi\sqrt{2t}}\cos\,M\sigma\,\psi_N(\tau/t)\,, \tag{D.24}$$

$$v_2(\sigma,\tau) = \sum_{M> 0, N\in\mathbf{Z}} b_{MN}\frac{1}{\pi\sqrt{2t}}\sin\,M\sigma\,\psi_N(\tau/t)\,, \tag{D.25}$$

where a_{MN} and b_{MN} are real-valued coefficients, and ψ_N is defined to be $\cos(N\tau/t)$

for $N \geq 0$ and $\sin(N\tau/t)$ for $N < 0$. It follows that

$$v = v_1 + iv_2 = \sum_{M,N\in\mathbf{Z}} v_{MN} \frac{1}{\pi\sqrt{2t}} e^{iM\sigma} \psi_N(\tau/t)\,, \tag{D.26}$$

where

$$a_{MN} = (v_{MN} + v_{-MN})/2\,, \tag{D.27}$$

$$b_{MN} = (v_{MN} - v_{-MN})/2\,. \tag{D.28}$$

The advantage of this rewriting is that $e^{iM\sigma}\psi_N(\tau/t)$ is an eigenfunction of the operator $\Delta_v = -\frac{k}{\pi}(\partial + iu_n)(\bar{\partial} + iu_n)$ that appears in the bulk term of (D.23), with eigenvalue $\lambda_{MN} = -\left((M + \hat{u}_n)^2 + (N/t)^2\right)$. If we substitute the expansion (D.26) of v into (D.23), then, expressing S_v in terms of the worldsheet coordinates (σ, τ), we can immediately integrate over τ, to obtain

$$\begin{aligned} S_v &= \frac{1}{\pi}\int_0^\pi d\sigma \sum_{M',M,N\in\mathbf{Z}} v_{M'N}\, v_{MN}\, \lambda_{MN} \left[\cos M'\sigma\, \cos M\sigma + \sin M'\sigma\, \sin M\sigma \right. \\ &\quad \left. + i\,(\cos M'\sigma\, \sin M\sigma - \sin M'\sigma\, \cos M\sigma)\right] + \text{boundary terms}\,, \end{aligned} \tag{D.29}$$

up to a normalization factor. Since S_v is positive-definite, v_{MN} and λ_{MN} are real constants, and the boundary terms are pure imaginary, the imaginary part of the bulk term must cancel with the boundary terms. We are then left with

$$\begin{aligned} S_v &= \frac{1}{2}\sum_{M',M,N\in\mathbf{Z}} v_{MN}\, v_{MN}\, \lambda_{MN}\, (\delta_{M',M} + \delta_{M',-M} + \delta_{M',M} - \delta_{M',-M}) \\ &= \sum_{M,N\in\mathbf{Z}} v_{MN}\, v_{M,N}\, \lambda_{M,N}\,. \end{aligned} \tag{D.30}$$

The functional integral is a product of Gaussians, and may be evaluated by standard methods. Up to a constant,

$$\mathcal{Z}_v = \prod_{M,N\in\mathbf{Z}} \frac{1}{\sqrt{(M + 2u_n)^2 + (N/t)^2}}\,, \tag{D.31}$$

which may be zeta-function regularized [80] to give

$$\mathcal{Z}_v^{-1} = \left| e^{-4\pi u_n^2 t} \frac{\vartheta_1(-2itu_n, it)}{\eta(it)} \right|\,, \tag{D.32}$$

where ϑ_1 is a Jacobi theta function.

We have now obtained expressions for all of the factors entering into $\mathcal{Z}_n(\beta;t)$. The overall normalization of $\mathcal{Z}_n$ is fixed in the usual way, by examining the infrared limit. Putting everything together, we obtain

$$\begin{aligned}\mathcal{Z}_n(\beta;t) &= \frac{1}{4\pi\sqrt{2t}}\frac{\beta(k-2)^{1/2}e^{-k\beta^2n^2/8\pi t}e^{4\pi u_n^2 t}}{|\vartheta_1(-2itu_n,it)|} \\ &= \frac{1}{4\pi\sqrt{2t}}\frac{\beta(k-2)^{1/2}}{\sinh(\beta n/2)}\frac{e^{-(k-2)\beta^2n^2/8\pi t}\ e^{\pi t/4}}{[\prod_{m=1}^{\infty}(1-e^{-2\pi tm})(1-e^{-2\pi tm}e^{\beta n})(1-e^{-2\pi tm}e^{-\beta n})]}\,.\end{aligned} \tag{D.33}$$

The partition function we have calculated is that of a conformal field theory with Euclidean AdS_3 as its target space, but our physical open string theory contains more: we must incorporate the contributions of the (b,c) ghosts as well as those of the "internal" conformal field theory. In addition, we must integrate over the worldsheet modulus t. When this is done, the partition function becomes

$$\begin{aligned}\mathcal{Z}(\beta) &= \frac{\beta(k-2)^{1/2}}{4\sqrt{2}\pi}\sum_{m=1}^{\infty}\int_0^{\infty}\frac{dt}{t^{3/2}}e^{2\pi t(1-\frac{1}{4(k-2)})}\sum_h D(h)e^{-2\pi th}\frac{e^{-(k-2)\beta^2m^2/8\pi t}}{\sinh(\beta m/2)}\times \\ &\quad \prod_{n=1}^{\infty}\left|\frac{1-e^{-2\pi tn}}{(1-e^{-2\pi tn+\beta m})(1-e^{-2\pi tn-\beta m})}\right|\,.\end{aligned} \tag{D.34}$$

Here h indexes the weight in the internal conformal field theory, and $D(h)$ is the degeneracy at weight h.

D.2 The spectrum

Having calculated the partition function (D.34), we now massage it into a form from which we can read off the spectrum. We noted at the beginning of this appendix that the partition function $\mathcal{Z}$ is proportional to the the free energy

$$F = \frac{1}{\beta}\sum_{s\in\mathcal{H}}\log\left(1-e^{-\beta E_s}\right) = \sum_{m=1}^{\infty}\sum_{s\in\mathcal{H}}\frac{1}{m\beta}e^{-m\beta E_s}\,. \tag{D.35}$$

The partition function is likewise a sum over m of a function of $m\beta$. It suffices, then, to compare the $m = 1$ terms of the two expressions. In this section, we verify that E_s, extracted from the identification

$$\sum_{s\in\mathcal{H}} \frac{1}{\beta} e^{-\beta E_s} = \frac{\beta(k-2)^{1/2}}{4\sqrt{2}\pi} \int_0^\infty \frac{dt}{t^{3/2}} e^{2\pi t(1-\frac{1}{4(k-2)})} \sum_h D(h) e^{-2\pi t h} \frac{e^{-(k-2)\beta^2 x f/8\pi t}}{\sinh(\beta/2)} \times$$

$$\prod_{n=1}^{\infty} \left| \frac{1-e^{-2\pi t n}}{(1-e^{-2\pi t n+\beta})(1-e^{-2\pi t n-\beta})} \right|, \tag{D.36}$$

agrees with the string spectrum proposed in Section 3.4.

To aid us in carrying out the t integral, let us introduce a new variable c, defined by

$$e^{-(k-2)\beta^2/8\pi t} = -\frac{8\pi i}{\beta} \left(\frac{2t}{k-2}\right)^{3/2} \int_{-\infty}^{\infty} dc\ c\ e^{-\frac{8\pi t}{k-2}c^2 + 2i\beta c}. \tag{D.37}$$

As explained in [36], the right-hand side of (D.34) can be expressed as a summation of terms of the form

$$\frac{-4i}{\beta(k-2)} \int_{-\infty}^{\infty} dc\ c \int_{\frac{\beta}{2\pi(w+1)}}^{\frac{\beta}{2\pi w}} dt$$

$$\times \exp\left[-\beta\left(q+w+\frac{1}{2}\right) + 2ic\beta - 2\pi t\left(h + N_w + \frac{4c^2+\frac{1}{4}}{k-2} - \frac{w(w+1)}{2} - 1\right)\right]$$

$$= \frac{-2i}{\pi\beta} \int_{-\infty}^{\infty} dc\ c\ \frac{\exp\left[2ic\beta - \beta(q+w+\frac{1}{2})\right]}{-2\pi(h+N_w+\frac{4c^2+\frac{1}{4}}{k-2} - \frac{w(w+1)}{2} - 1)}$$

$$\times \left\{ -\exp\left[-\frac{\beta}{w}\left(h + N_w - 1 + \frac{4c^2+\frac{1}{4}}{k-2} - \frac{w(w+1)}{2}\right)\right]\right.$$

$$\left. + \exp\left[-\frac{\beta}{w+1}\left(h + N_w - 1 + \frac{4c^2+\frac{1}{4}}{k-2} - \frac{w(w+1)}{2}\right)\right]\right\} \tag{D.38}$$

where w ranges over non-negative integers. We can complete the square of the exponent in the first term (the fourth line) of (D.38) by letting $c = s + \frac{i}{4}(k-2)w$. Let us think of the c integral as an integration over a contour (as it happens, the real line) in the complex plane. We may then shift the contour of integration in the first term

of (D.38) to $c = s + \frac{i}{4}(k-2)w$, and the contour of integration in the second term to $c = s + \frac{i}{4}(k-2)(w+1)$, where s in both cases runs over the real line. In doing so, the contour of integration crosses some poles in the integrand, and the integral picks up the residues of these poles. The residues of the poles from the first term are partially cancelled by the residues of the poles from the second. The net result of the contour shift is to pick up only the poles in the range

$$\frac{(k-2)}{4}w < \text{Im } c < \frac{(k-2)}{4}(w+1)\,. \tag{D.39}$$

Their residues are

$$\frac{1}{\beta}\ \exp\left[-\beta q - \beta\left(\frac{1}{2} + w + \sqrt{\frac{1}{4} + (k-2)(N_w + h - 1 - \frac{1}{2}w(w+1))}\right)\right]\,. \tag{D.40}$$

The coefficient of $-\beta$ in the exponent is supposed to be the energy of a typical state in the discrete spectrum. Considerations similar to those given in [37] for closed strings show that (3.70) (with the minus sign chosen) indeed takes the form (D.40) after the physical state conditions are imposed. Our partition function calculation thus reproduces the discrete spectrum of open strings in the physical Hilbert space.

We now turn our attention to the s integration. It is convenient to rearrange the sum in (D.38) by redefining $w \to w-1$ in the second term and by deforming the contours in both terms to $c = s + \frac{i}{4}(k-2)w$. The result is

$$\begin{aligned}
&\frac{1}{2\pi i\beta}\int_{-\infty}^{\infty} ds\ \left(\frac{4s}{(k-2)w} + i\right) \\
&\times\left\{\frac{\exp\left[-\beta q - \beta\left(\frac{kw}{4} + \frac{1}{w}\left(\frac{4s^2+\frac{1}{4}}{k-2} + N_{w-1} + h - 1\right)\right)\right]}{\frac{1}{4} + is - \frac{kw}{8} + \frac{1}{2w}\left(N_{w-1} + h - 1 + \frac{4s^2+\frac{1}{4}}{k-2}\right)}\right. \\
&\left.-\frac{\exp\left[-\beta q - \beta\left(\frac{kw}{4} + \frac{1}{w}\left(\frac{4s^2+\frac{1}{4}}{k-2} + N_w + h - 1\right)\right)\right]}{-\frac{1}{4} + is - \frac{kw}{8} + \frac{1}{2w}\left(N_w + h - 1 + \frac{4s^2+\frac{1}{4}}{k-2}\right)}\right\}\,.
\end{aligned} \tag{D.41}$$

Let us consider the third line of (D.41). It can be shown [36] that summing over

terms of this type yields

$$\frac{1}{2\pi i\beta}\int_{-\infty}^{\infty} ds\,\left(i+\frac{4s}{(k-2)w}\right)\left(2\,\log\epsilon+\left(i+\frac{4s}{w(k-2)}\right)^{-1}\frac{d}{ds}\log\Gamma\left(\frac{1}{2}-2is-\tilde{M}\right)\right)e^{-\beta f(s)}\,, \tag{D.42}$$

where

$$\tilde{M}=\frac{1}{w}\left(\frac{4s^2+\frac{1}{4}}{k-2}+\tilde{N}+h-1\right)-\frac{kw}{4}\,, \tag{D.43}$$

$$f(s)=\frac{kw}{4}+\frac{1}{w}\left(\frac{4s^2+\frac{1}{4}}{k-2}+\tilde{N}+h-1\right)\,, \tag{D.44}$$

$\tilde{N}=qw+N_w$, and ϵ is a cutoff introduced to regularize a divergence that arises in the sum. Similarly, summing over terms in the form of the second line of (D.41) gives

$$\frac{1}{2\pi i\beta}\int_{-\infty}^{\infty} ds\,\left(i+\frac{4s}{(k-2)w}\right)\left(2\log\epsilon-\left(i+\frac{4s}{w(k-2)}\right)^{-1}\frac{d}{ds}\log\Gamma(\frac{1}{2}+2is+\tilde{M})\right)e^{-\beta f(s)}. \tag{D.45}$$

Combining these results and making the change of variables $s\rightarrow\frac{s}{2}$, we find that (D.41) can be written in the form

$$\frac{2}{\beta}\int_0^{\infty} ds\;\rho(s)\exp\left[-\beta E(s)\right]\,, \tag{D.46}$$

where

$$\rho(s)=\frac{1}{2\pi}2\log\epsilon+\frac{1}{2\pi i}\frac{1}{2}\frac{d}{ds}\log\left(\frac{\Gamma(\frac{1}{2}-is+\tilde{m})\Gamma(\frac{1}{2}-is-\tilde{m})}{\Gamma(\frac{1}{2}+is+\tilde{m})\Gamma(\frac{1}{2}+is-\tilde{m})}\right)\,, \tag{D.47}$$

$$E(s) \;=\; \frac{kw}{4}+\frac{1}{w}\left(\frac{s^2+\frac{1}{4}}{k-2}+\tilde{N}+h-1\right)\,, \tag{D.48}$$

$$\tilde{m} \;=\; \frac{1}{w}(\frac{s^2+\frac{1}{4}}{k-2}+\tilde{N}+h-1)-\frac{kw}{4}\,. \tag{D.49}$$

Here $\rho(s)$ and $E(s)$ are the density of states and energy of the long strings. The expression (D.48) is exactly what we would find if we imposed the physical state conditions on the form (3.70) given in Section 3.4.1 for the long string energy.

Thus, by analyzing the partition function, we have reproduced our conjecture for the spectrum of the straight brane. The result is summarized by writing the free energy summand $f(\beta)$ as

$$f(\beta) = \frac{1}{\beta} \sum D(h, \tilde{N}, w) \left[\sum_q e^{-\beta E(q)} + \int ds\, \rho(s) e^{-\beta E(s)} \right] , \tag{D.50}$$

where $E(q)$, $E(s)$, and $\rho(s)$ are the discrete state energy, the continuum state energy, and the continuum density of states.

Appendix E

Some Useful Integrals and Formulae for Chapter 3

E.1 y-integral

The integral we want to compute is

$$\int_{Imy>0,\, Im(ye^{i\phi_0})>0,\, e^{-\beta}<|y|<1} d^2y|y-\bar{y}|^{-2j}|ye^{i\phi_0}-\bar{y}e^{-i\phi_0}|^{-2(1-j)}. \tag{E.1}$$

Use polar coordinates such that $y = re^{i\theta}$. Then, we get

$$= \left(\int_{e^{-\beta}}^{1}\frac{dr}{r}\right)\int_0^{\pi-\phi_0} d\theta|\sin\theta\sin(\theta+\phi_0)|^{-1}\exp\left(2is\ln\left|\frac{\sin(\theta+\phi_0)}{\sin\theta}\right|\right). \tag{E.2}$$

The r integral is just β. Denote the remaining θ integral as $g(s)$ and consider its Fourier transformation:

$$\tilde{g}(\tilde{s}) = \int_{-\infty}^{\infty} ds e^{is\tilde{s}}g(s) \tag{E.3}$$

$$= \int_0^{\pi-\phi_0} d\theta|\sin\theta\sin(\theta+\phi_0)|^{-1}\int_{-\infty}^{\infty} ds\exp\left[is\left(\tilde{s}+2\ln\left|\frac{\sin(\theta+\phi_0)}{\sin\theta}\right|\right)\right] \tag{E.4}$$

$$= 2\pi\int_0^{\pi-\phi_0} d\theta|\sin\theta\sin(\theta+\phi_0)|^{-1}\delta\left(\tilde{s}+2\ln\left|\frac{\sin(\theta+\phi_0)}{\sin\theta}\right|\right) \tag{E.5}$$

$$= \frac{\pi}{|\sin\phi_0|}. \tag{E.6}$$

Inverting the transform gives

$$g(s) = \int_{-\infty}^{\infty} \frac{d\tilde{s}}{2\pi} e^{-is\tilde{s}} \frac{\pi}{|\sin\phi_0|} \tag{E.7}$$

$$= \frac{\pi}{|\sin\phi_0|}\delta(s)\,. \tag{E.8}$$

Therefore, we get

$$(\text{y-integral}) = \frac{\pi\beta}{|\sin\phi_0|}\delta(s)\,. \tag{E.9}$$

E.2 Integral in the localized graviton calculation

According to p. 344 Eq. 7 of Gradshteyn/Ryzhik, we have

$$\int_0^\infty dx \frac{x^n}{(ax^2+2bx+c)^{n+3/2}} = \frac{n!}{(2n+1)!!\sqrt{c}\,(\sqrt{ac}+b)^{n+1}}\,, \tag{E.10}$$

where $a \geq 0, c > 0, b > -\sqrt{ac}$. We want to integrate

$$\int_0^\infty dx_2' \;\; (x_2')^{2j-2}\,(x_2'^2 - 2\sinh\psi x_2' + \cosh^2\psi)^{\frac{1}{2}-2j}\,. \tag{E.11}$$

Using $n = 2j-2$, $a = 1$, $c = \cosh^2\psi$ and $b = -\sinh\psi$, we see the restrictions are clearly satisfied for all values of $\psi \in \mathbf{R}$. Using the fact that $\Gamma\left(\frac{1}{2}+n\right) = \frac{\sqrt{\pi}}{2^n}(2n-1)!!$, we have

$$\int_0^\infty dx_2' \;(x_2')^{2j-2}\,(x_2'^2 - 2\sinh\psi x_2' + \cosh^2\psi)^{\frac{1}{2}-2j} = \frac{2^{2-2j}\Gamma(2j-1)\sqrt{\pi}e^{\psi(2j-1)}}{\Gamma\left(2j-\frac{1}{2}\right)\cosh\psi}. \tag{E.12}$$

E.3 Useful relations

We list some useful formulae involving the hypergeometric function and the gamma function. The hypergeometric function, ${}_2F_1(\alpha,\beta,\gamma;z)$, enjoys following useful identities:

$${}_2F_1(\alpha,\beta,\gamma;z) = (1-z)^{\gamma-\alpha-\beta}\,{}_2F_1(\gamma-\alpha,\gamma-\beta,\gamma;z). \tag{E.13}$$

The Gauss recursion formulae are given by

$$\gamma\,{}_2F_1(\alpha,\beta,\gamma;z)+(\beta-\gamma)\,{}_2F_1(\alpha+1,\beta,\gamma+1;z)- \tag{E.14}$$
$$\beta(1-z)\,{}_2F_1(\alpha+1,\beta+1,\gamma+1;z)=0,$$
$$\gamma\,{}_2F_1(\alpha,\beta,\gamma;z)-\gamma\,{}_2F_1(\alpha+1,\beta,\gamma;z)+\beta z\,{}_2F_1(\alpha+1,\beta+1,\gamma+1;z)=0, \tag{E.15}$$
$$\gamma\,{}_2F_1(\alpha,\beta,\gamma;z)-(\gamma-\beta)\,{}_2F_1(\alpha,\beta,\gamma+1;z)-\beta\,{}_2F_1(\alpha,\beta+1,\gamma+1;z)=0. \tag{E.16}$$

Under $z\to 1-z$, we have

$${}_2F_1(\alpha,\beta,\gamma;1-z)=\frac{\Gamma(\gamma)\Gamma(\gamma-\alpha-\beta)}{\Gamma(\gamma-\alpha)\Gamma(\gamma-\beta)}{}_2F_1(\alpha,\beta,1-\gamma+\alpha+\beta;z)+ \tag{E.17}$$
$$z^{\gamma-\alpha-\beta}\frac{\Gamma(\gamma)\Gamma(\alpha+\beta-\gamma)}{\Gamma(\alpha)\Gamma(\beta)}{}_2F_1(\gamma-\alpha,\gamma-\beta,1+\gamma-\alpha-\beta;z).$$

Lastly, under $z\to 1/z$, we get

$${}_2F_1(\alpha,\beta,\gamma;z)=\frac{\Gamma(\gamma)\Gamma(\beta-\alpha)}{\Gamma(\beta)\Gamma(\gamma-\alpha)}\left(-\frac{1}{z}\right)^{\alpha}{}_2F_1\left(\alpha,1+\alpha-\gamma,1+\alpha-\beta;\frac{1}{z}\right)+ \tag{E.18}$$
$$\frac{\Gamma(\gamma)\Gamma(\alpha-\beta)}{\Gamma(\alpha)\Gamma(\gamma-\beta)}\left(-\frac{1}{z}\right)^{\beta}{}_2F_1\left(\beta,1+\beta-\gamma,1+\beta-\alpha;\frac{1}{z}\right).$$

We list some useful identities involving the gamma, $\Gamma(z)$, function:

$$\Gamma(1+z)=z\Gamma(z), \tag{E.19}$$
$$\Gamma\left(\frac{1}{2}\right)=\sqrt{\pi}, \tag{E.20}$$
$$\Gamma(1-z)\Gamma(z)=\frac{\pi}{\sin(\pi z)}, \tag{E.21}$$
$$\Gamma(1+ix)\Gamma(1-ix)=\frac{\pi x}{\sinh(\pi x)},\qquad x\in\mathbf{R} \tag{E.22}$$
$$\Gamma(2z)=\frac{2^{2z-1}}{\sqrt{\pi}}\Gamma(z)\Gamma\left(z+\frac{1}{2}\right). \tag{E.23}$$

Bibliography

[1] G. 't Hooft, "A Planar Diagram Theory for Strong Interactions," *Nucl. Phys.* **B72** (1974) 461.

[2] O. Aharony, S. S. Gubser, J. Maldacena, H. Ooguri, and Y. Oz, "Large N field theories, string theory and gravity," *Phys. Rept.* **323** (2000) 183, `hep-th/9905111`.

[3] E. Witten, "Anti-de Sitter Space and Holography," *Adv. Theor. Math. Phys.* **2** (1998) 253, `hep-th/9802150`.

[4] S. S. Gubser, I. R. Klebanov, and A. M. Polyakov, "Gauge Theory Correlators from Non-critical String Theory," *Phys. Lett. B* **428** (1998) 105, `hep-th/9802109`.

[5] R. R. Metsaev, "Type IIB Green-Schwarz Superstring in Plane Wave Ramond-Ramond Background," *Nucl. Phys. B* **625** (2002) 70–96, `hep-th/0112044`.

[6] R. Metsaev and A. Tseytlin, "Exactly Solvable Model of Superstring in Ramond-Ramond Plane Wave Background," *Phys. Rev.* **D65** (2002) 126004, `hep-th/0202109`.

[7] D. Berenstein, J. Maldacena, and H. Nastase, "Strings in Flat Space and PP Waves from $\mathcal{N} = 4$ Super Yang Mills," `hep-th/0202021`.

[8] J. Maldacena, "The Large N Limit of Superconformal Field Theories and Supergravity," *Adv. Theor. Math. Phys.* **2** (1998) 231, `hep-th/9711200`.

[9] A. Karch and L. Randall, "Locally Localized Gravity," *JHEP* **0105** (2001) 008, hep-th/0011156.

[10] A. Karch and L. Randall, "Open and Closed String Interpretation of SUSY CFT's on Branes with Boundaries," *JHEP* **0106** (2001) 063, hep-th/0105132.

[11] O. DeWolfe, D. Freedman, and H. Ooguri, "Holography and Defect Conformal Field Theories," *Phys. Rev.* **D66** (2002) 025009, hep-th/0111135.

[12] J. Maldacena, "Black Holes in String Theory," hep-th/9607235.

[13] A. Sen, "Tachyon Condensation on the Brane Antibrane System," *JHEP* **9808** (1998) 012, hep-th/9805170.

[14] J. Erdmenger, Z. Guralnik, and I. Kirsch, "Four-dimensional Superconformal Theories with Interacting Boundaries or Defects," *Phys. Rev.* **D66** (2002) 025020, hep-th/0203020.

[15] M. Blau, J. Figueroa-O'Farrill, and G. Papadopoulos, "Penrose Limits, Supergravity and Brane Dynamics," *Class. Quant. Grav.* **19** (2002) 4753, hep-th/0202111.

[16] R. Penrose, "Any Spacetime Has a Plane Wave As a Limit," *Differential geometry and relativity, Reidel, Dordrecht* (1976) 271–275.

[17] D. Berenstein, E. Gava, J. Maldacena, K. Narain, and H. Nastase, "Open Strings On Plane Waves and Their Yang-Mills Duals," hep-th/0203249.

[18] A. Dabholkar and S. Parvizi, "Dp Branes in PP-wave Background," *Nucl. Phys.* **B641** (2002) 223-234, hep-th/0203231.

[19] K. Skenderis, M. Taylor, "An Overview of Branes in the Plane Wave Background," http://arXiv.org/abs/hep-th/0301221

[20] P. Lee, J. w. Park, "Open Strings in PP-Wave Background from Defect Conformal Field Theory," *Phys. Rev.* **D67** (2003) 026002, hep-th/0203257.

[21] P. Lee, H. Ooguri, and J. w. Park, "Boundary States for AdS_2 Branes in AdS_3," *Nucl. Phys.* **B632** (2002) 283-302, `hep-th/0112188`.

[22] B. Ponsot, V. Schomerus, and J. Teschner, "Branes in the Euclidean AdS_3," *JHEP* **0202** (2002) 016, `hep-th/0112198`.

[23] N. D. Lambert and P. C. West, "D-Branes in the Green-Schwarz Formalism," *Phys. Lett.* **B459** (1999) 515-521, `hep-th/9905031`.

[24] S. R. Das, C. Gomez, and S.-J. Rey, "Penrose Limit, Spontaneous Symmetry Breaking and Holography in PP-wave Background," *Phys. Rev.* **D66** (2002) 046002, `hep-th/0203164`.

[25] C. Bachas, J. de Boer, R. Dijkgraaf, and H. Ooguri, "Permeable Conformal Walls and Holography," *JHEP* **0206** (2002) 027, `hep-th/0111210`.

[26] A. M. Polyakov, "Quantum Geometry of Bosonic Strings," *Phys. Lett.* **B103** (1981) 207–210.

[27] J.-L. Gervais and A. Neveu, "The Dual Spectrum in Polyakov's Quantization. 1.," *Nucl. Phys.* **B199** (1982) 59.

[28] J.-L. Gervais and A. Neveu, "Dual String Spectrum in Polyakov's Quantization. 2. Mode Separation," *Nucl. Phys.* **B209** (1982) 125.

[29] V. G. Knizhnik, A. M. Polyakov, and A. B. Zamolodchikov, "Fractal Structure of 2d Quantum Gravity," *Mod. Phys. Lett.* **A3** (1988) 819.

[30] E. Witten, "(2+1)-Dimensional Gravity as an Exactly Soluble System," *Nucl. Phys.* **B311** (1988) 46.

[31] E. Witten, "On String Theory and Black Holes," *Phys. Rev.* **D44** (1991) 314–324.

[32] C. G. Callan, J. A. Harvey, and A. Strominger, "Supersymmetric String Solitons," `hep-th/9112030`.

[33] S. Mukhi and C. Vafa, "Two-Dimensional Black Hole as a Topological Coset Model of $c = 1$ String Theory," *Nucl. Phys.* **B407** (1993) 667–705, hep-th/9301083.

[34] D. Ghoshal and C. Vafa, "$c = 1$ String as the Topological Theory of the Conifold," *Nucl. Phys.* **B453** (1995) 121–128, hep-th/9506122.

[35] H. Ooguri and C. Vafa, "Two-Dimensional Black Hole and Singularities of CY Manifolds," *Nucl. Phys.* **B463** (1996) 55–72, hep-th/9511164.

[36] J. Maldacena, H. Ooguri, and J. Son, "Strings in AdS_3 and the $SL(2, R)$ WZW Model. Part 2: Euclidean Black Hole," hep-th/0005183.

[37] J. Maldacena and H. Ooguri, "Strings in AdS_3 and the $SL(2, R)$ WZW Model. Part 1: The Spectrum," *J. Math. Phys.* **42** (2001) 2929-2960, hep-th/0001053.

[38] C. Klimcík and P. Severa, "Open Strings and D-Branes in WZNW Models," *Nucl. Phys.* **B488** (1997) 653–676, hep-th/9609112.

[39] M. Kato and T. Okada, "D-Branes on Group Manifolds," *Nucl. Phys.* **B499** (1997) 583–595, hep-th/9612148.

[40] A. Y. Alekseev and V. Schomerus, "D-Branes in the WZW Model," *Phys. Rev.* **D60** (1999) 061901, hep-th/9812193.

[41] A. Y. Alekseev, A. Recknagel, and V. Schomerus, "Non-Commutative World-Volume Geometries: Branes on $SU(2)$ and Fuzzy Spheres," *JHEP* **09** (1999) 023, hep-th/9908040.

[42] G. Felder, J. Fröhlich, J. Fuchs, and C. Schweigert, "The Geometry of WZW Branes," *J. Geom. Phys.* **34** (2000) 162–190, hep-th/9909030.

[43] S. Stanciu, "D-Branes in Group Manifolds," *JHEP* **01** (2000) 025, hep-th/9909163.

[44] C. Bachas, M. Douglas, and C. Schweigert, "Flux Stabilization of D-Branes," *JHEP* **05** (2000) 048, hep-th/0003037.

[45] J. Pawelczyk, "$SU(2)$ WZW D-Branes and Their Noncommutative Geometry from DBI Action," *JHEP* **08** (2000) 006, hep-th/0003057.

[46] A. Y. Alekseev, A. Recknagel, and V. Schomerus, "Brane Dynamics in Background Fluxes and Non-Commutative Geometry," *JHEP* **05** (2000) 010, hep-th/0003187.

[47] R. Gopakumar, J. Maldacena, S. Minwalla, and A. Strominger, "S-Duality and Noncommutative Gauge Theory," *JHEP* **06** (2000) 036, hep-th/0005048.

[48] N. Seiberg, L. Susskind, and N. Toumbas, "Strings in Background Electric Field, Space/Time Noncommutativity and a New Noncritical String Theory," *JHEP* **06** (2000) 021, hep-th/0005040.

[49] P. M. Petropoulos and S. Ribault, "Some Remarks on Anti-de Sitter D-Branes," *JHEP* **0107** (2001) 036, hep-th/0105252.

[50] A. Giveon, D. Kutasov, and A. Schwimmer, "Comments on D-branes in AdS_3," *Nucl. Phys.* **B615** (2001) 133-168, hep-th/0106005.

[51] S. Stanciu, "D-Branes in an AdS_3 Background," *JHEP* **09** (1999) 028, hep-th/9901122.

[52] C. Bachas and M. Petropoulos, "Anti-de-Sitter D-Branes," *JHEP* **02** (2001) 025, hep-th/0012234.

[53] P. Lee, H. Ooguri, J. w. Park, and J. Tannenhauser, "Open Strings on AdS_2 Branes," *Nucl. Phys.* **B610** (2001) 3–48, http://arXiv.org/abs/hep-th/0106129.

[54] K. Gawędzki, "Noncompact WZW Conformal Field Theories," hep-th/9110076.

[55] J. Gomis and H. Ooguri, "Non-Relativistic Closed String Theory," *J. Math. Phys.* **42** (2001) 3127-3151, hep-th/0009181.

[56] J. Maldacena, G. Moore, and N. Seiberg, "Geometrical Interpretation of D-Branes in Gauged WZW Models," *JHEP* **0107** (2001) 046, hep-th/0105038.

[57] S. Stanciu, "D-branes in an AdS_3 Background," *JHEP* **09** (1999) 028, http://arXiv.org/abs/hep-th/9901122.

[58] P. M. Petropoulos and S. Ribault, "Some Remarks on Anti-de-Sitter D-branes," *JHEP* **07** (2001) 036, http://arXiv.org/abs/hep-th/0105252.

[59] N. Ishibashi, "The Boundary and Crosscap States in Conformal Field Theories," *Mod. Phys. Lett.* **A4** (1989) 251.

[60] J. L. Cardy, "Boundary Conditions, Fusion Rules and the Verlinde Formula," *Nucl. Phys.* **B324** (1989) 581.

[61] V. Fateev, A. B. Zamolodchikov, and A. B. Zamolodchikov, "Boundary Liouville Field Theory. I: Boundary State and Boundary Two-Point Function," http://arXiv.org/abs/hep-th/0001012.

[62] A. B. Zamolodchikov and A. B. Zamolodchikov, "Liouville Field Theory on a Pseudosphere," http://arXiv.org/abs/hep-th/0101152.

[63] J. Teschner, "Remarks on Liouville Theory with Boundary," http://arXiv.org/abs/hep-th/0009138.

[64] B. Ponsot and J. Teschner, "Boundary Liouville Field Theory: Boundary Three Point Function," *Nucl. Phys.* **B622** (2002) 309-327, http://arXiv.org/abs/hep-th/0110244.

[65] J. Teschner, "The Mini-Superspace Limit of the $SL(2,C)/SU(2)$ WZNW Model," *Nucl. Phys.* **B546** (1999) 369–389, http://arXiv.org/abs/hep-th/9712258.

[66] A. Giveon, D. Kutasov, and A. Schwimmer, "Comments on D-branes in AdS_3," *Nucl. Phys.* **B615** (2001) 133–168, http://arXiv.org/abs/hep-th/0106005.

[67] A. Parnachev and D. A. Sahakyan, "Some Remarks on D-Branes in AdS_3," *JHEP* **10** (2001) 022, http://arXiv.org/abs/hep-th/0109150.

[68] A. Rajaraman and M. Rozali, "Boundary States for D-Branes in AdS_3," *Phys. Rev.* **D66** (2002) 026006, http://arXiv.org/abs/hep-th/0108001.

[69] J. Maldacena and H. Ooguri, "Strings in AdS_3 and $SL(2,R)$ WZW model. I: Spectrum," *J. Math. Phys.* **42** (2001) 2929–2960, http://arXiv.org/abs/hep-th/0001053.

[70] J. Maldacena, H. Ooguri, and J. Son, "Strings in AdS_3 and the $SL(2,R)$ WZW Model. II: Euclidean Black Hole," *J. Math. Phys.* **42** (2001) 2961–2977, http://arXiv.org/abs/hep-th/0005183.

[71] J. Teschner, "On Structure Constants and Fusion Rules in the $SL(2,C)/SU(2)$ WZNW Model," *Nucl. Phys.* **B546** (1999) 390–422, http://arXiv.org/abs/hep-th/9712256.

[72] J. Teschner, "Operator Product Expansion and Factorization in the H_3^+ WZNW Model," *Nucl. Phys.* **B571** (2000) 555–582, http://arXiv.org/abs/hep-th/9906215.

[73] V. Fateev, A. Zamolodchikov, and Al. Zamolodchikov *unpublished notes.*

[74] J. Maldacena, G. W. Moore, and N. Seiberg, "Geometric Interpretation of D-Branes in Gauged WZW Models," *JHEP* **07** (2001) 046, http://arXiv.org/abs/hep-th/0105038.

[75] H. Ooguri, Y. Oz, and Z. Yin, "D-Branes on Calabi-Yau Spaces and Their Mirrors," *Nucl. Phys.* **B477** (1996) 407–430, http://arXiv.org/abs/hep-th/9606112.

[76] M. R. Douglas, D. Kabat, P. Pouliot, and S. H. Shenker, "D-Branes and Short Distances in String Theory," *Nucl. Phys.* **B485** (1997) 85–127, hep-th/9608024.

[77] E. A. Mirabelli and M. Peskin, "Transmission of Supersymmetry Breaking from a Four-Dimensional Boundary," *Phys. Rev. D* (1997) `hep-th/9712214`.

[78] E. D'Hoker, D. Z. Freedman, and W. Skiba, "Field Theory Tests for Correlators in the AdS/CFT Correspondence," *Phys. Rev.* **D59** (1999) 045008, `hep-th/9807098`.

[79] J. Polchinski, *String Theory*, vol. 1. Cambridge Univ. Press, Cambridge, 1998.

[80] D. B. Ray and I. M. Singer, "Analytic Torsion for Complex Manifolds," *Ann. Math.* **98** (1973) 154.